



Transportation Consortium of South-Central States

*Solving Emerging Transportation Resiliency, Sustainability, and Economic Challenges through the Use of Innovative Materials and Construction Methods: From Research to Implementation*

# Field Implementation and Monitoring of an Ultra-High Performance Concrete Bridge Deck Overlay

---

Project No. 19CNMS01

Lead University: New Mexico State University

**Final Report**  
**December 2021**

### **Disclaimer**

The contents of this report reflect the views of the authors, who are responsible for the facts and the accuracy of the information presented herein. This document is disseminated in the interest of information exchange. The report is funded, partially or entirely, by a grant from the U.S. Department of Transportation's University Transportation Centers Program. However, the U.S. Government assumes no liability for the contents or use thereof.

### **Acknowledgments**

The authors would like to acknowledge the support and direction of the Project Review Committee that included Dr. Paul Barr of Utah State University, Ken Wylie of Wood Plc, and Kathy Crowell of the New Mexico Department of Transportation.

## TECHNICAL DOCUMENTATION PAGE

<b>1. Project No.</b> 19CNMS01	<b>2. Government Accession No.</b>	<b>3. Recipient's Catalog No.</b>	
<b>4. Title and Subtitle</b>  Field Implementation and Monitoring of an Ultra-High Performance Concrete Bridge Deck Overlay		<b>5. Report Date</b> Dec. 2021	
<b>7. Author(s)</b> PI: Craig M. Newtonson <a href="https://orcid.org/0000-0002-2140-9759">https://orcid.org/0000-0002-2140-9759</a> Co-PI: Brad D. Weldon <a href="https://orcid.org/0000-0001-7196-8690">https://orcid.org/0000-0001-7196-8690</a> GRA: William K. Toledo <a href="https://orcid.org/0000-0002-3436-5118">https://orcid.org/0000-0002-3436-5118</a> GRA: Andres Alvarez <a href="https://orcid.org/0000-0003-0917-8588">https://orcid.org/0000-0003-0917-8588</a> GRA: Mark P. Manning <a href="https://orcid.org/0000-0003-4862-7606">https://orcid.org/0000-0003-4862-7606</a>		<b>6. Performing Organization Code</b>	
<b>9. Performing Organization Name and Address</b> Transportation Consortium of South-Central States (Tran-SET) University Transportation Center for Region 6 3319 Patrick F. Taylor Hall, Louisiana State University Baton Rouge, LA 70803		<b>8. Performing Organization Report No.</b>	
<b>12. Sponsoring Agency Name and Address</b> United States of America Department of Transportation Research and Innovative Technology Administration		<b>10. Work Unit No. (TRAIS)</b>	
		<b>11. Contract or Grant No.</b> 69A3551747106	
		<b>13. Type of Report and Period Covered</b> Final Research Report August 2019 – December 2021	
		<b>14. Sponsoring Agency Code</b>	
<b>15. Supplementary Notes</b> Report uploaded and accessible at: <a href="http://transet.lsu.edu/">Tran-SET's website (http://transet.lsu.edu/)</a>			
<b>16. Abstract</b> This project focused on field implementation of an ultra-high performance concrete (UHPC) overlay during rehabilitation of an existing concrete bridge (No. 7032) deck in Socorro, New Mexico, USA. Bridge 7032 is a two-lane bridge that is approximately 300 ft. (91.4 m) long and 54 ft. (16.5 m) in width. Rehabilitation of bridge 7032 included removal of deteriorated concrete from the existing deck, installation of a high-performance deck (HPD) leveling course, and installation of a 1 in. (25 mm) UHPC overlay. An UHPC mixture with a 19.5 ksi (134 MPa) compressive strength developed in previous research was selected for this project. This mixture was revised at the beginning of the project, highlighting the need for robust mixtures that can accommodate constituent material substitutions. Prior to placement of the UHPC overlay, the HPD substrate was ceramic bead blasted to remove surface paste and partially expose fine aggregate, thoroughly cleaned, and maintained saturated for 24 hours prior to UHPC placement. The non-proprietary UHPC overlay was successfully placed in four sections between April 10, 2021 and April 27, 2021. During construction of the UHPC overlay, a total of 105 batches were placed. The average direct tensile bond strength of the UHPC overlaid bridge deck was 239 psi (1.65 MPa), which is conservative since several of the tests had fractures that occurred at the epoxy-UHPC interface. Strain gauges and thermocouples were used to monitor the UHPC overlay and existing deck through initial, early-age, and longer-term monitoring programs. Temperature and strain monitoring showed that daily and multi-day strain trends coincided well with daily temperature trends. Major observations during this field implementation project were that four small areas of possible delamination were identified using non-destructive testing, the bond strength was good since the 239 psi (1.65 MPa) average was conservative, preliminary monitoring results were consistent with expectations based on temperature measurements and restraint provided by the concrete superstructure, and relative strains from the monitoring data are being used for detailed analysis of the bridge and overlay behaviors for an ongoing NMDOT project that runs for another two years.			
<b>17. Key Words</b> Overlay, Bridge Deck, Concrete , UHPC, Rehabilitation, Implementation		<b>18. Distribution Statement</b> No restrictions.	
<b>19. Security Classif. (of this report)</b> Unclassified	<b>20. Security Classif. (of this page)</b> Unclassified	<b>21. No. of Pages</b> 110	<b>22. Price</b>

# SI\* (MODERN METRIC) CONVERSION FACTORS

## APPROXIMATE CONVERSIONS TO SI UNITS

Symbol	When You Know	Multiply By	To Find	Symbol
<b>LENGTH</b>				
in	inches	25.4	millimeters	mm
ft	feet	0.305	meters	m
yd	yards	0.914	meters	m
mi	miles	1.61	kilometers	km
<b>AREA</b>				
in <sup>2</sup>	square inches	645.2	square millimeters	mm <sup>2</sup>
ft <sup>2</sup>	square feet	0.093	square meters	m <sup>2</sup>
yd <sup>2</sup>	square yard	0.836	square meters	m <sup>2</sup>
ac	acres	0.405	hectares	ha
mi <sup>2</sup>	square miles	2.59	square kilometers	km <sup>2</sup>
<b>VOLUME</b>				
fl oz	fluid ounces	29.57	milliliters	mL
gal	gallons	3.785	liters	L
ft <sup>3</sup>	cubic feet	0.028	cubic meters	m <sup>3</sup>
yd <sup>3</sup>	cubic yards	0.765	cubic meters	m <sup>3</sup>
NOTE: volumes greater than 1000 L shall be shown in m <sup>3</sup>				
<b>MASS</b>				
oz	ounces	28.35	grams	g
lb	pounds	0.454	kilograms	kg
T	short tons (2000 lb)	0.907	megagrams (or "metric ton")	Mg (or "t")
<b>TEMPERATURE (exact degrees)</b>				
°F	Fahrenheit	5 (F-32)/9 or (F-32)/1.8	Celsius	°C
<b>ILLUMINATION</b>				
fc	foot-candles	10.76	lux	lx
fl	foot-Lamberts	3.426	candela/m <sup>2</sup>	cd/m <sup>2</sup>
<b>FORCE and PRESSURE or STRESS</b>				
lbf	poundforce	4.45	newtons	N
lbf/in <sup>2</sup>	poundforce per square inch	6.89	kilopascals	kPa
<b>APPROXIMATE CONVERSIONS FROM SI UNITS</b>				
Symbol	When You Know	Multiply By	To Find	Symbol
<b>LENGTH</b>				
mm	millimeters	0.039	inches	in
m	meters	3.28	feet	ft
m	meters	1.09	yards	yd
km	kilometers	0.621	miles	mi
<b>AREA</b>				
mm <sup>2</sup>	square millimeters	0.0016	square inches	in <sup>2</sup>
m <sup>2</sup>	square meters	10.764	square feet	ft <sup>2</sup>
m <sup>2</sup>	square meters	1.195	square yards	yd <sup>2</sup>
ha	hectares	2.47	acres	ac
km <sup>2</sup>	square kilometers	0.386	square miles	mi <sup>2</sup>
<b>VOLUME</b>				
mL	milliliters	0.034	fluid ounces	fl oz
L	liters	0.264	gallons	gal
m <sup>3</sup>	cubic meters	35.314	cubic feet	ft <sup>3</sup>
m <sup>3</sup>	cubic meters	1.307	cubic yards	yd <sup>3</sup>
<b>MASS</b>				
g	grams	0.035	ounces	oz
kg	kilograms	2.202	pounds	lb
Mg (or "t")	megagrams (or "metric ton")	1.103	short tons (2000 lb)	T
<b>TEMPERATURE (exact degrees)</b>				
°C	Celsius	1.8C+32	Fahrenheit	°F
<b>ILLUMINATION</b>				
lx	lux	0.0929	foot-candles	fc
cd/m <sup>2</sup>	candela/m <sup>2</sup>	0.2919	foot-Lamberts	fl
<b>FORCE and PRESSURE or STRESS</b>				
N	newtons	0.225	poundforce	lbf
kPa	kilopascals	0.145	poundforce per square inch	lbf/in <sup>2</sup>

# TABLE OF CONTENTS

TABLE OF CONTENTS.....	iv
LIST OF TABLES .....	vii
LIST OF FIGURES .....	viii
ACRONYMS, ABBREVIATIONS, AND SYMBOLS .....	xiii
EXECUTIVE SUMMARY .....	xiv
1. INTRODUCTION .....	1
1.1. Background.....	1
2. OBJECTIVE .....	3
3. LITERATURE REVIEW .....	4
3.1. Ultra-High Performance Concrete .....	4
3.2. Non-Proprietary UHPC Developed at NMSU .....	4
3.2.1. Non-Proprietary UHPC Mixture Proportions .....	4
3.2.2. Selection of UHPC Mixture Proportions .....	5
3.3. UHPC Overlay Compared to Common Overlay Materials .....	6
3.4. UHPC as an Overlay Material .....	6
3.4.1. Quantifying Bonding between UHPC and NSC.....	6
3.4.2. UHPC Overlay Projects .....	7
3.5. Assessment of Non-Proprietary UHPC as an Overlay Material at NMSU .....	7
3.5.1. Bond Strength Testing .....	7
3.5.2. Shrinkage and Coefficient of Thermal Expansion.....	8
3.5.3. Slab Testing .....	8
3.5.4. Full-Scale Channel Girder Testing .....	8
3.6. UHPC Bond Performance with Delay in Cold Joint Formation.....	9
3.7. Factors That Influence Bond Strength .....	9
3.8. Surface Preparation.....	10
3.9. Bonding Agents .....	10
3.10. Stresses at the Bonded Interface .....	11
3.10.1. Mechanical Stresses at the Bonded Interface.....	11
3.10.2. Thermal Compatibility .....	11
3.10.3. Shrinkage Compatibility .....	12

4. METHODOLOGY .....	13
4.1. Bridge Description and Location .....	13
4.2. Condition Assessment of Existing Deck.....	14
4.3. Design .....	14
4.3.1. Removal of Deteriorated Concrete .....	14
4.3.2. Design of Bridge Rehabilitation .....	15
4.4. Mixture Proportions .....	16
4.4.1. Proposed UHPC Mixture Proportions .....	16
4.4.2. Buy America (49 U.S. Code § 5323 [j]) Enforcement.....	17
4.4.3. Selection of the New Steel Fibers.....	17
4.5. UHPC Overlay Mock-Up Placements .....	18
4.5.1. Mock-Up Placement 1 (May 29, 2020) .....	18
4.5.2. Mock-Up Placement 2 (June 24, 2020) .....	18
4.5.3. Mock-Up Placement 3 (July 7, 2020).....	18
4.5.4. Mock-up Placement 4 (April 5, 2021) .....	19
4.6. Test Methods.....	21
4.6.1. Slump Flow Test.....	21
4.6.2. Compressive Strength Test .....	22
4.6.3. Flexural Strength Test.....	23
4.6.4. Direct Tension Pull-off Tests.....	23
4.6.4.1. Direct Tension Pull-off Tests for Mock-up Placement 3.....	23
4.6.4.2. Direct Tension Pull-off Test for Mock-up Placement 4 .....	25
4.7. HPD Installation.....	26
4.8. UHPC Production Placement.....	27
4.8.1. Substrate Surface Preparation .....	27
4.8.2. Material Preparation and UHPC Mixing .....	28
4.8.3. UHPC Placement .....	28
4.8.4. Data Collection during Construction of UHPC Overlay .....	29
4.8.4.1. Weather Conditions .....	29
4.8.4.2. Construction Sequence.....	29
4.8.4.3. Substrate Surface Conditions.....	29
4.8.4.4. UHPC Quality Assurance Testing .....	29
4.9. Instrumentation on Bridge 7032 .....	30
4.10. Initial, Early-age, and Longer-term Monitoring Programs .....	37
4.10.1. Initial Monitoring Program .....	37
4.10.2. Early-age Monitoring Program .....	37
4.10.2.1. Overlay-Substrate Bond Assessment.....	37
4.10.2.1.1. Hammer Sounding and Chain Drag.....	37
4.10.2.1.2. Ground Penetrating Radar.....	38
4.10.2.1.3. Infrared Thermal Imaging.....	38

4.10.2.1.4. Direct Tension Pull-Off Testing .....	38
4.10.2.2. Strain and Temperature Monitoring.....	39
4.10.3. Longer-term Monitoring Program .....	40
5. FINDINGS .....	41
5.1. Mock-up Placement Direct Tension Test Results.....	41
5.1.1. Direct Tension Pull-off Test Results for Mock-up Placement 3.....	41
5.1.2. Direct Tension Pull-off Test Results for Mock-up Placement 4.....	42
5.2. Data Collection During Construction of UHPC Overlay .....	42
5.2.1. Weather Conditions .....	42
5.2.2. Substrate Surface Conditions.....	43
5.2.3. Construction Sequence.....	43
5.2.3.1. Placement.....	43
5.2.3.2. Vibrating and screeding the overlay material. ....	44
5.2.3.3. Curing .....	45
5.2.3.4. Construction joints.....	46
5.2.4. UHPC Temperature and Workability Data.....	47
5.2.5. UHPC Strength Data.....	50
5.3. Initial Monitoring.....	51
5.3.1. Westbound HPD Placement.....	52
5.3.2. Eastbound HPD Placement.....	60
5.4. Early-age Monitoring.....	67
5.4.1. Overlay-substrate Bond Assessment.....	67
5.4.1.1. Hammer Sounding and Chain Drag.....	67
5.4.1.2. GPR.....	70
5.4.1.3. Infrared Thermal Imaging.....	70
5.4.1.4. Direct Tension Pull-off Test Results for UHPC Overlaid Bridge .....	71
5.4.2. Eastbound Early-age Monitoring.....	74
5.4.3. Westbound Early-age Monitoring.....	82
5.5. Longer-term Monitoring .....	91
CONCLUSIONS.....	106
REFERENCES .....	107
APPENDIX.....	111

## LIST OF TABLES

Table 1. Mixture proportions for UHPC.....	4
Table 2. UHPC Mixture proportions for 1.5% by volume fibers. ....	17
Table 3. ASF-GEL Minimum Cure Time Based on Substrate Temperature.....	39
Table 4. Direct tension pull-off test results for mock-up placement 3. ....	41
Table 5. Direct tension pull-off test results from fourth mock-up placement. ....	42
Table 6. Temperature and workability measurements from all batches. ....	47
Table 7. Production Placement – compressive and flexural strength results.....	51
Table 8. Direct tension pull-off test results from bridge 7032.....	72

## LIST OF FIGURES

Figure 1. Compressive strength of non-proprietary UHCP developed at NMSU. ....	5
Figure 2. Steel fibers used for UHPC fiber reinforcement. ....	5
Figure 3. Material cost per m2 of different overlaying material alternatives (2). ....	6
Figure 4. Slant-shear and direct tension test setups (1). ....	8
Figure 5. UHPC overlaid girder flexural testing setup (1).....	9
Figure 6. a) Top view of bridge 7032, b) plan view of bridge 7032, and c) bottom of multicell box girder superstructure. ....	13
Figure 7. Bridge 7032 concrete deck with two lanes separated by a median. ....	14
Figure 8. Transverse cracks observed on the concrete bridge deck.....	14
Figure 9. Condition of deck on southbound lane after removal of deteriorated concrete. ....	15
Figure 10. Replacement of the expansion joint seal. ....	15
Figure 11. Concrete barrier railing.....	16
Figure 12. Raised median after placement of UHPC overlay.....	16
Figure 13. Compressive strength curve of UHPC. ....	17
Figure 14. Horizontal shaft mixers. ....	19
Figure 15. Mock-up placement 4 – a) UHPC placement and b) UHPC screeding.....	20
Figure 16. Mock-up placement 4 – UHPC finish. ....	20
Figure 17. Mock-up placement 4 – UHPC overlay cracking.....	21
Figure 18. a) Slump and b) spread measurements. ....	22
Figure 19. UHPC cube sample at failure under compression test. ....	22
Figure 20. UHPC prismatic sample at failure during flexural test. ....	23
Figure 21. a) Core drilling and b) pull-off test setup. ....	24
Figure 22. Direct tension pull-off locations on the mock-up placement 3 slab.....	25
Figure 23. Direct tension pull-off test locations on mock-up placement 4 slab. ....	26
Figure 24. Tine rake used to texture the HPD surface.....	27
Figure 25. Ceramic bead blaster. ....	28
Figure 26. Production placement 1 – UHPC overlay cracking.....	29
Figure 27. Bridge 7032 before and after first deck section removal. ....	30
Figure 28. External sensor installation inside box girder cells. ....	30
Figure 29. Embedded sensor installation in HPD. ....	31
Figure 30. Embedded sensor installation in UHPC overlay. ....	31
Figure 31. Data-logger box setup.....	32
Figure 32. Sensors used on bridge 7032. ....	32
Figure 33. a) Plan view, b) west end plan view, and c) strain gauge direction layout. ....	34
Figure 34. a) Cross-section and b) profile strain gauge layout. ....	36
Figure 35. a) GPR system and b) GPR system in use (56).....	38
Figure 36. Direct tension pull-off test on bridge 7032 - a) core sawing, b) epoxying of steel platens, and c) test set up. ....	39
Figure 37. a) Substrate surface texture and b) substrate surface moisture condition during placement. ....	43
Figure 38. Concrete buggy delivering UHPC.....	44
Figure 39. Construction workers spreading UHPC with shovels prior to screeding. ....	44

Figure 40. a) Handheld concrete vibrator and b) vibrating screed. ....	45
Figure 41. Application of curing compound after screeding. ....	46
Figure 42. UHPC overlay covered with plastic sheeting. ....	46
Figure 43. Images of construction joint blocking. ....	47
Figure 44. Longitudinal and transverse strain during HPD placement 1 (westbound lane) – bay 1 – position 1. ....	53
Figure 45. Longitudinal and transverse strain during HPD placement 1 (westbound lane) – bay 1 – position 2. ....	53
Figure 46. Longitudinal and transverse strain during HPD placement 1 (westbound lane) – bay 1 – position 3. ....	54
Figure 47. Longitudinal and transverse strain during HPD placement 1 (westbound lane) – bay 2 – position 1. ....	54
Figure 48. Longitudinal and transverse strain during HPD placement 1 (westbound lane) – bay 2 – position 2. ....	55
Figure 49. Longitudinal and transverse strain during HPD placement 1 (westbound lane) – bay 2 – position 3. ....	55
Figure 50. Longitudinal and transverse strain during HPD placement 1 (westbound lane) – bay 3 – position 1. ....	56
Figure 51. Longitudinal and transverse strain during HPD placement 1 (westbound lane) – bay 3 – position 2. ....	56
Figure 52. Longitudinal and transverse strain during HPD placement 1 (westbound lane) – bay 3 – position 3. ....	57
Figure 53. Longitudinal and transverse strain during HPD placement 1 (westbound lane) – bay 3 – position 4. ....	57
Figure 54. Longitudinal and transverse strain during HPD placement 1 (westbound lane) – bay 3 – position 5. ....	58
Figure 55. Temperature during HPD placement 1 (westbound lane) – bay 1. ....	58
Figure 56. Temperature during HPD placement 1 (westbound lane) – bay 2. ....	59
Figure 57. Temperature during HPD placement 1 (westbound lane) – bay 3. ....	59
Figure 58. Longitudinal and transverse strain during HPD placement 1 (eastbound lane) – bay 1 – position 1. ....	60
Figure 59. Longitudinal and transverse strain during HPD placement 1 (eastbound lane) – bay 1 – position 2. ....	60
Figure 60. Longitudinal and transverse strain during HPD placement 1 (eastbound lane) – bay 1 – position 3. ....	61
Figure 61. Longitudinal and transverse strain during HPD placement 1 (eastbound lane) – bay 2 – position 1. ....	62
Figure 62. Longitudinal and transverse strain during HPD placement 1 (eastbound lane) – bay 2 – position 2. ....	62
Figure 63. Longitudinal and transverse strain during HPD placement 1 (eastbound lane) – bay 2 – position 3. ....	63
Figure 64. Longitudinal and transverse strain during HPD placement 1 (eastbound lane) – bay 3 – position 1. ....	63

Figure 65. Longitudinal and transverse strain during HPD placement 1 (eastbound lane) – bay 3 – position 2.....	64
Figure 66. Longitudinal and transverse strain during HPD placement 1 (eastbound lane) – bay 3 – position 3.....	64
Figure 67. Longitudinal and transverse strain during HPD placement 1 (eastbound lane) – bay 3 – position 3.....	65
Figure 68. Longitudinal and transverse strain during HPD placement 1 (eastbound lane) – bay 3 – position 5.....	65
Figure 69. Temperature during HPD placement 2 (eastbound lane) – Bay 1.....	66
Figure 70. Temperature during HPD placement 2 (eastbound lane) – bay 2. ....	66
Figure 71. Temperature during HPD placement 2 (eastbound lane) – bay 3. ....	67
Figure 72. Delaminated areas on bridge after UHPC placement.....	69
Figure 73. Photograph and color-coded infrared thermal image at the first potential delamination.....	70
Figure 74. Infrared thermal imaging on fourth potential delamination. ....	71
Figure 75. Direct tension pull-off test locations on bridge 7032. ....	73
Figure 76. Core sample with substrate that lacks roughness. ....	74
Figure 77. UHPC/epoxy failure. ....	74
Figure 78. Early-age longitudinal and transverse strain in eastbound lane - bay 1 – position 1. ....	75
Figure 79. Early-age longitudinal and transverse strain in eastbound lane - bay 1 – position 1. ....	75
Figure 80. Early-age longitudinal and transverse strain in eastbound lane - bay 1 – position 1. ....	76
Figure 81. Early-age longitudinal and transverse strain in eastbound lane - bay 2 – position 1. ....	76
Figure 82. Early-age longitudinal and transverse strain in eastbound lane - bay 2 – position 2. ....	77
Figure 83. Early-age longitudinal and transverse strain in eastbound lane - bay 2 – position 3. ....	77
Figure 84. Early-age longitudinal and transverse strain in eastbound lane - bay 3 – position 1. ....	78
Figure 85. Early-age longitudinal and transverse strain in eastbound lane - bay 3 – position 2. ....	78
Figure 86. Early-age longitudinal and transverse strain in eastbound lane - bay 3 – position 3. ....	79
Figure 87. Early-age longitudinal and transverse strain in eastbound lane - bay 3 – position 4. ....	79
Figure 88. Early-age longitudinal and transverse strain in eastbound lane - bay 3 – position 5. ....	80
Figure 89. Temperature during UHPC Production Placements 1 and 2 (eastbound lane) – bay 1.....	80
Figure 90. Temperature during UHPC Production Placements 1 and 2 (eastbound lane) – bay 2.....	81

Figure 91. Temperature during UHPC production placements 1 and 2 (eastbound lane) – bay 3.....	81
Figure 92. Early-age longitudinal and transverse strain in westbound lane - bay 1 – position 1. ....	83
Figure 93. Early-age longitudinal and transverse strain in westbound lane - bay 1 – position 2. ....	84
Figure 94. Early-age longitudinal and transverse strain in westbound lane - bay 1 – position 3. ....	84
Figure 95. Early-age longitudinal and transverse strain in westbound lane - bay 2 – position 1. ....	85
Figure 96. Early-age longitudinal and transverse strain in westbound lane - bay 2 – position 2. ....	85
Figure 97. Early-age longitudinal and transverse strain in westbound lane - bay 2 – position 3. ....	86
Figure 98. Early-age longitudinal and transverse strain in westbound lane - bay 3 – position 1. ....	86
Figure 99. Early-age longitudinal and transverse strain in westbound lane - bay 3 – position 2. ....	87
Figure 100. Early-age longitudinal and transverse strain in westbound lane - bay 3 – position 3.....	87
Figure 101. Early-age longitudinal and transverse strain in westbound lane - bay 3 – position 4.....	88
Figure 102. Early-age longitudinal and transverse strain in westbound lane - bay 3 – position 5.....	88
Figure 103. Temperature during UHPC Production Placements 3 and 4 (westbound lane) – bay 1.....	89
Figure 104. Temperature during UHPC Production Placements 3 and 4 (westbound lane) – bay 2.....	89
Figure 105. Temperature during UHPC Production Placements 3 and 4 (westbound lane) – bay 3.....	90
Figure 106. Longer-term longitudinal and transverse strain in eastbound lane - bay 1 – position 1.....	92
Figure 107. Longer-term longitudinal and transverse strain in eastbound lane - bay 1 – position 2.....	92
Figure 108. Longer-term longitudinal and transverse strain in eastbound lane - bay 1 – position 3.....	93
Figure 109. Longer-term longitudinal and transverse strain in eastbound lane - bay 2 – position 1.....	93
Figure 110. Longer-term longitudinal and transverse strain in eastbound lane - bay 2 – position 2.....	94
Figure 111. Longer-term longitudinal and transverse strain in eastbound lane - bay 2 – position 3.....	94
Figure 112. Longer-term longitudinal and transverse strain in eastbound lane - bay 3 – position 1.....	95

Figure 113. Longer-term longitudinal and transverse strain in eastbound lane - bay 3 – position 2.....	95
Figure 114. Longer-term longitudinal and transverse strain in eastbound lane - bay 3 – position 3.....	96
Figure 115. Longer-term longitudinal and transverse strain in eastbound lane - bay 3 – position 4.....	96
Figure 116. Longer-term longitudinal and transverse strain in eastbound lane - bay 3 – position 5.....	97
Figure 117. Temperature during UHPC Production Placements 1 and 2 (eastbound lane) – bay 1.....	97
Figure 118. Temperature during UHPC Production Placements 1 and 2 (eastbound lane) – Bay 2.....	98
Figure 119. Temperature during UHPC Production Placements 1 and 2 (eastbound lane) – bay 3.....	98
Figure 120. Longer-term longitudinal and transverse strain in westbound lane - bay 1 – position 1.....	99
Figure 121. Longer-term longitudinal and transverse strain in westbound lane - bay 1 – position 2.....	99
Figure 122. Longer-term longitudinal and transverse strain in westbound lane - bay 1 – position 3.....	100
Figure 123. Longer-term longitudinal and transverse strain in westbound lane - bay 2 – position 1.....	100
Figure 124. Longer-term longitudinal and transverse strain in westbound lane - bay 2 – position 2.....	101
Figure 125. Longer-term longitudinal and transverse strain in westbound lane - bay 2 – position 3.....	101
Figure 126. Longer-term longitudinal and transverse strain in westbound lane - bay 3 – position 1.....	102
Figure 127. Longer-term longitudinal and transverse strain in westbound lane - bay 3 – position 2.....	102
Figure 128. Longer-term longitudinal and transverse strain in westbound lane - bay 3 – position 3.....	103
Figure 129. Longer-term longitudinal and transverse strain in westbound lane - bay 3 – position 4.....	103
Figure 130. Longer-term longitudinal and transverse strain in westbound lane - bay 3 – position 4.....	104
Figure 131. Temperature during UHPC Production Placements 3 and 4 (westbound lane) – bay 1.....	104
Figure 132. Temperature during UHPC Production Placements 3 and 4 (westbound lane) – bay 2.....	105
Figure 133. Temperature during UHPC Production Placements 3 and 4 (westbound lane) – bay 3.....	105

## **ACRONYMS, ABBREVIATIONS, AND SYMBOLS**

ACI	American Concrete Institute
ASTM	American Society for Testing Materials
BS	British Standard
CFS	Concrete Fiber Solutions
GPR	Ground penetrating radar
HPC	High-performance concrete
HPD	High-performance deck
HRWRA	High range water reducing admixture
LMC	Latex-modified concrete
LSC	Low-slump concrete
LVDT	Linear variable displacement transducer
NMDOT	New Mexico Department of Transportation
NMSU	New Mexico State University
NSC	Normal strength concrete
PBC	Polymer-based concrete
SCM	Supplementary cementitious material
Tran-SET	Transportation Consortium of South-Central States
TxDOT	Texas Department of Transportation
UHPC	Ultra-high performance concrete

## **EXECUTIVE SUMMARY**

The purpose of this project was to collaborate with the New Mexico Department of Transportation (NMDOT) on the field implementation of a non-proprietary ultra-high performance concrete (UHPC) overlay during the rehabilitation of an existing concrete bridge deck in Socorro, New Mexico, USA.

This implementation project built on a prior Tran-SET project (Project 17CNMS01) that was funded during 2017-2018 to assess the feasibility of using of a locally produced, non-proprietary UHPC as a concrete bridge deck overlay. To assess the non-proprietary UHPC, several small-scale laboratory tests were conducted that investigated bond strength and a large-scale test was performed on a full-scale, pre-stressed channel girder with a 1 in. (25 mm) UHPC overlay subjected to flexural loading. Results from that project indicated that the non-proprietary UHPC has the potential to serve as an overlay material as long as proper measures are used to prepare the substrate surface and ensure high quality bond with the existing deck.

Bridge 7032 off Exit 150 in Socorro, New Mexico is the bridge that was overlaid with a non-proprietary UHPC. The bridge is a two-lane bridge with a center median and is approximately 300 ft. (91.4 m) in length and 54 ft. (16.5 m) in width. This bridge is a four-span, multi-cell box girder bridge with three intermediate supports provided by column bents (integral caps) containing six cylindrical columns. To rehabilitate bridge 7032, construction included removal of deteriorated concrete from the existing deck, installation of a high-performance deck (HPD) levelling course to re-establish the original elevation of the concrete deck, and installation of a 1 in. (25 mm) UHPC overlay.

As the project was being let, the Buy America requirement was enforced for purchasing steel products. Since the proposed UHPC mixture proportions included steel fibers produced in China, alternative steel fibers produced in the US needed to be selected. An UHPC mixture with a 19.5 ksi (134 MPa) compressive strength developed in previous research was selected that used steel fibers produced in the US.

To prepare for construction, mock-up placements were conducted that allowed NMSU to transfer technology to NMDOT personnel and contractors regarding the mixing, handling, placement, and finishing of the UHPC overlay material. The mock-up placements were conducted at A1 Quality Ready Mix located in Socorro, NM. Mock placement bond tests revealed the importance of maintaining saturated conditions for 24 hours prior to overlay placement and providing a visibly moist substrate surface during placement of the overlay to achieve adequate bond between the overlay and substrate concrete materials. To achieve adequate bond (greater than 150 psi [1.0 MPa]), the substrate should also have a surface texture that removes surface paste and exposes some aggregate. Prior to placement of the UHPC overlay on bridge 7032, the HPD substrate was ceramic bead blasted to remove surface paste and partially expose fine aggregate. After the surface was textured, the deck was thoroughly cleaned of any debris and the deck was maintained saturated for 24 hours prior to UHPC overlay placement. The deck appeared moist at installation of the UHPC overlay.

The non-proprietary UHPC overlay was successfully placed between April 10, 2021 and April 27, 2021. During construction of the UHPC overlay, a total of 105 batches were placed on

bridge 7032 (53 batches on the eastbound lane and 52 batches on the westbound lane). Production Placements 1 and 2 (eastbound lane) started from the west end of the bridge, and Production Placements 3 and 4 (westbound lane) started from the east end of the bridge. The first placement experienced visible cracking because the UHPC overlay was not covered under plastic sheets and burlap as soon as surface finishing was completed. Therefore, curing procedures were modified for Production Placements 2 through 4. The revised curing procedures required application of curing compound immediately after screeding and finishing were completed, and then coverage with plastic sheets as soon as possible after the curing compound was applied. The revised curing practices resulted in no significant cracking being observed for the remaining production placements.

Monitoring of the UHPC overlay included initial, early-age, and longer-term monitoring plans to assess the quality of the overlay-substrate bond and monitor the structural behavior of the superstructure such as thermal and shrinkage effects. The bridge deck was instrumented with external strain gauges and thermocouples placed on the ceiling of the cells in the multi-cell box girders, strain gauges and thermocouples attached to the reinforcing steel in the HPD leveling course, and embedded strain gauges and thermocouples in the UHPC overlay. The initial monitoring program used the embedded strain gauge sensors and thermocouples to monitor shrinkage and internal temperature of HPD prior to placement of the UHPC overlay. Early-age monitoring consisted of bond assessment tests, as well as strain and temperature monitoring of the first 28 days after placing the non-proprietary UHPC overlay. The longer-term monitoring of the overlay included strain and temperature monitoring from an overlay age of 28 days to December 15, 2021.

From the data collected for initial monitoring, the daily temperature cycle was easily observed in the strain results, and relative strain changes for sensors in the HPD and box girder cells provide the combined effects of HPD shrinkage and thermal effects in both the HPD and original superstructure concrete. After placement of the UHPC overlay, bond assessment tests were conducted after overlaying bridge 7032. The average direct tensile bond strength, calculated from nine pull-off tests performed at intact locations on the overlaid deck, was 239 psi (1.65 MPa). This average is conservative since four of the tests had fractures that occurred at the epoxy-UHPC interface. Based on thermal effects observed for daily cycles during early-age monitoring, the strain response of unrestrained UHPC can be as large as 1000  $\mu$ strain. Measured strain responses were generally 200 to 250  $\mu$ strain, which is attributed to restraint provided by the concrete superstructure (substrate). Early-age monitoring also showed that multi-day strain trends coincided well with daily temperature trends. The early-age monitoring data are being analyzed in detail for an ongoing NMDOT project that continues for another two years. The longer-term monitoring data contained periods where gauges spiked out of range or experienced excessive drift. Relative strains occurring during windows of time that do not contain such anomalies are being used for detailed analysis of the bridge and overlay behaviors for the ongoing NMDOT project.

Conclusions drawn from this field implementation project included: 1) robust or additional UHPC mixture proportions should be available to accommodate a potential lack of availability of a constituent material, 2) compressive strength gain of field cast specimens were hindered

due to improper field curing, 3) it is important to plan multiple mock placements requiring the contractor to demonstrate the ability to perform all procedures required for the project, 4) cracking on the UHPC surface was observed when curing compound and plastic sheeting were not applied as soon as possible to the finished overlay surface, 5) four small areas of possible delamination were identified using non-destructive testing, 6) the average direct tensile strength from nine pull-off tests performed at intact locations was 239 psi (1.65 MPa), 7) early-age monitoring results were consistent with expectations based on temperature measurements and restraint provided by the concrete superstructure, and 8) relative strains from portions of the longer-term monitoring data that do not contain periods of spiking data or excessive drift are being used for detailed analysis of the bridge and overlay behaviors for an ongoing NMDOT project that runs for another two years.

# 1. INTRODUCTION

The project discussed in this report covers the field implementation of a locally produced ultra-high performance concrete (UHPC) overlay to a concrete bridge deck in Socorro, NM. A 2017-2018 research project at New Mexico State University (NMSU), that was funded by the Transportation Consortium of South-Central States (Tran-SET), demonstrated that UHPC produced with local materials was able to achieve adequate bond strength with substrate concrete when used as an overlay material in the laboratory (1). Consequently, the New Mexico Department of Transportation (NMDOT) implemented the UHPC overlay technology by specifying UHPC as the overlay material for the bridge in Socorro. The current project includes developing and initiating a long-term monitoring program to assess the performance of the UHPC overlay.

## 1.1. Background

Concrete bridge decks are exposed to a wide range of environmental and mechanical distress and are critical bridge elements that are intended to provide a comfortable and safe riding surface as well as protect structural elements beneath them. According to 2016 United States National Bridge Inventory data, 23.9% of US bridges have concrete bridge decks in “Satisfactory” condition and only 10 out of 43 transportation agencies anticipate that their bridge deck overlays last more than 25 years (2).

High bridge deck maintenance costs have led agencies to consider more durable materials for bridge deck overlays. Materials currently available for overlay applications include asphalt concrete, high-performance concrete, low-slump concrete, latex-modified concrete, and polymer-modified concrete. However, each of these materials has drawbacks such as high cost, inadequate service life expectancy, or limited availability.

Most transportation agencies in the US avoid asphalt concrete overlays because water and chlorides can get trapped beneath the waterproofing membrane during installation (3). Through the 1980s, latex-modified concrete and low-slump dense concrete were commonly used as overlay materials with claims that these materials could extend service life of decks by 30 to 50 years (4). However, some agencies raised chloride permeability concerns with low-slump dense concrete and questioned the ability of that material to adequately protect the deck reinforcing steel (5). Additionally, latex-modified concrete overlays have been documented as often needing patch repairs within five years (6).

During the 1990s, polyester polymer concrete became a popular overlay material for transportation agencies because it is nearly impermeable, can be used at thickness as small as 0.75 inches (19 mm), and can be opened to traffic in as little as two to four hours (7). In New Mexico, polyester polymer concrete is being used for all bridge deck overlays less than 3 inches (75 mm) thick. However, personnel from the Bridge Design Bureau of the NMDOT have indicated that polyester polymer concrete overlays have two perceived drawbacks: the materials costs for polyester polymer concrete overlays seems high in comparison to portland cement concrete overlays and rehabilitation of polyester polymer concrete overlays is often necessary after about eight years.

Recent research has demonstrated that ultra-high performance concrete (UHPC) may have the ability to increase service lives of bridge deck overlays and reduce maintenance costs (1, 2, 8-10). This technology may also extend the service life of the underlying concrete deck. Research at New Mexico State University (NMSU) has shown that UHPC produced with local materials has excellent durability, and materials costs can be decreased by 30 to 70% compared to proprietary UHPC mixtures (11-13). Although there is a small reduction in compressive strength of UHPC when using local materials compared to strengths obtained with commercial UHPC mixtures, the reduced cost of the material can improve sustainability of UHPC usage.

## **2. OBJECTIVE**

The overall objective of this study was to assist NMDOT with the field implementation of a non-proprietary UHPC overlay technology. The non-proprietary UHPC was specified as the overlay material for a bridge deck rehabilitation project for a bridge in Socorro, NM, USA. To facilitate the transfer of the technology during field implementation, the research team worked closely with NMDOT through the planning, preparation, and construction phases of the construction project. Aspects of the project that required guidance from the research team included batching, mixing, and placement, and curing methods for the UHPC overlay material as well as surface preparation requirements for the substrate concrete.

Another objective for this project was to develop and implement short and long-term monitoring programs to assess the performance of the UHPC overlay and monitor the structural behavior of the bridge superstructure. The short and long-term plans for monitoring and assessing the UHPC overlay included test methods and instrumentation to assess the quality of the overlay substrate bond, the magnitude of shrinkage that occurs in the UHPC overlay, and monitor the combined shrinkage and thermal movements of the overlaid deck.

### 3. LITERATURE REVIEW

#### 3.1. Ultra-High Performance Concrete

UHPC is a novel class of concrete exhibiting exceptional mechanical and durability properties. These properties include compressive strength greater than 17,000 psi (120 MPa) (14), high ductility when fiber reinforced, and excellent resistance to frost damage, alkali-silica-reaction, and abrasion (15-17). UHPC's properties are achieved through careful selection of its constituent materials to ensure optimized gradation and maximized packing density as well as detailed preparation methods to properly mix and cure UHPC elements (18-20). UHPC's excellent properties make it an attractive material for use as a concrete repair material (21).

Previous UHPC research at New Mexico State University (NMSU) has shown that UHPC produced with local materials and locally available supplementary cementitious materials (SCMs), such as silica fume and class F fly ash, exhibits mechanical and durability properties that are comparable to proprietary UHPC mixtures (15, 18, 22). Incorporation of locally available materials can reduce materials cost up to 70% compared to proprietary UHPC (12, 23).

#### 3.2. Non-Proprietary UHPC Developed at NMSU

UHPC's exceptional mechanical and durability properties make it an attractive candidate for use as a repair material. The most significant drawbacks of UHPC is that it has limited commercial availability, commercially available proprietary UHPC products are often expensive, and proprietary UHPC products often need to be shipped long distances. Previous research at NMSU developed an UHPC using local materials. This non-proprietary UHPC has been assessed for use in a number of repair applications including shear key rehabilitation and as a bridge deck overlay (1, 24-26).

##### 3.2.1. Non-Proprietary UHPC Mixture Proportions

Table 1 presents the mixture proportions for one of the UHPC mixtures developed in the NMSU research (1). The UHPC mixture consisted of Type I/II portland cement, silica fume, fly ash, high-range water reducing admixture (HRWRA), water, and 1.5% by volume of 0.5 in. (13 mm) steel fibers. The sand, cement, and fly ash were obtained from local sources while the silica fume, steel fibers, and HRWRA were acquired from regional suppliers.

Table 1. Mixture proportions for UHPC.

Constituents	Unit	Unit/yd <sup>3</sup> [m <sup>3</sup> ]
Cement	lb. [kg]	1377 [817]
Silica Fume	lb. [kg]	172 [102]
Fly Ash	lb. [kg]	172 [102]
Sand	lb. [kg]	1702 [1010]
Fibers <sup>1</sup>	lb. [kg]	201 [119]
HRWRA	gal. [L]	9.09 [45]
Water	lb. [kg]	258 [153]

<sup>1</sup> - Mixture contains 1.5% by volume of steel fibers.

### 3.2.2. Selection of UHPC Mixture Proportions

In a laboratory study to assess the ability of locally produced UHPC to serve as a bridge deck overlay material, it was stated that a mixture with adequate workability for overlay applications that produces the desired compressive strength (17,000 psi [117.2 MPa]) under field conditions needed to be developed. Therefore, testing of several UHPC mixtures to assess workability and compressive strength was conducted. Twenty percent of the total cementitious materials was comprised of silica fume and fly ash. The use of fly ash helps to reduce the cost of UHPC by replacing portions of the silica fume and cement, which are higher cost materials (1).

UHPC mixtures were proportioned by varying an individual constituent so that its effect on the properties of a mixture could be studied. After investigating the workability and strengths of the mixtures, one mixture was selected as the best candidate for overlay applications that provided adequate workability and met the minimum 28-day compressive strength requirement of 17,000 psi (117.2 MPa) (14). The compressive strength gain curve of this non-proprietary UHPC is shown in Figure 1. This mixture used 0.5 in. (13 mm) steel fibers as shown in Figure 2 to fill 1.5% of the UHPC volume. Tayeh et al. (27) reported that the performance of UHPC greatly depends on the properties of the fiber reinforcement.

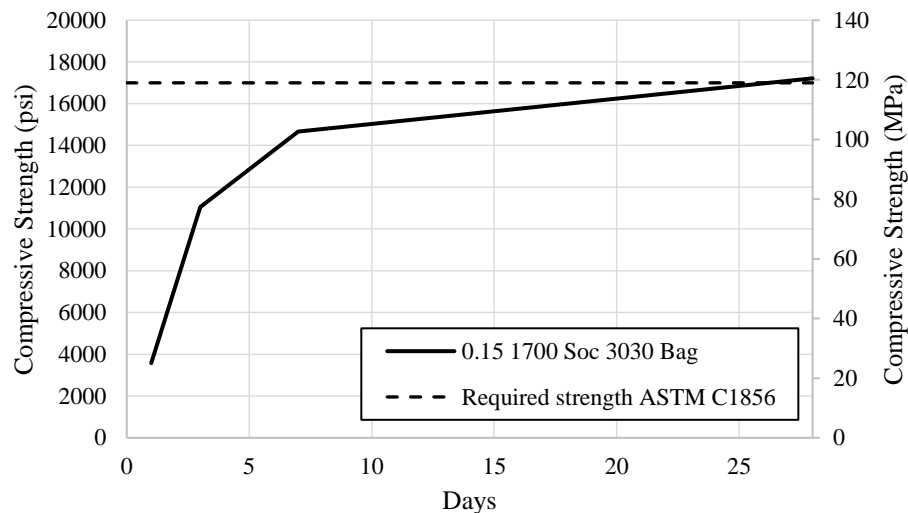


Figure 1. Compressive strength of non-proprietary UHCP developed at NMSU.



Figure 2. Steel fibers used for UHPC fiber reinforcement.

### 3.3. UHPC Overlay Compared to Common Overlay Materials

Bridge deck overlays are a common rehabilitation option to extend the life of concrete bridge decks. Common overlay materials include high-performance concrete (HPC), low-slump concrete (LSC), latex-modified concrete (LMC), and polymer-based concrete (PBC). However, each of these alternatives has drawbacks such as cost, service life expectancy, or availability. Figure 3 shows a cost comparison in US dollars of these overlay alternatives. It should be noted that the cost of local UHPC in Figure 3 includes only materials cost while the other alternatives include construction costs (2). Guidelines for selection of bridge deck overlays, sealers, and treatments approximated bridge deck replacement to cost \$43 - \$53 per square foot (\$462-\$570 per square meter) in 2009 (3).

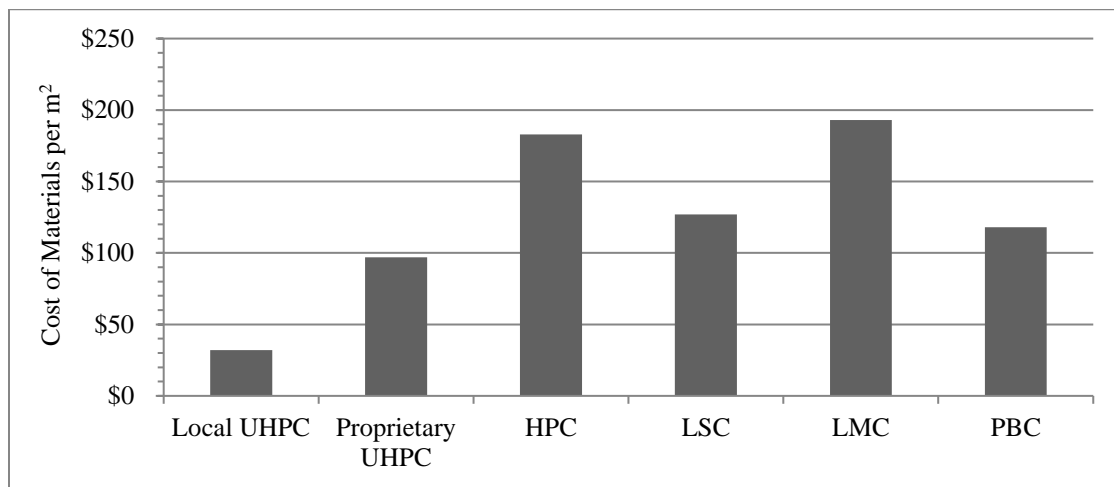


Figure 3. Material cost per m<sup>2</sup> of different overlaying material alternatives (2).

### 3.4. UHPC as an Overlay Material

Concrete bridge decks play a crucial role in protecting structural elements beneath the deck from various environmental and physical attacks while providing a comfortable riding surface. However, deterioration of bridge decks, caused by exposure to environmental and mechanical distress, often requires rehabilitation or, in extreme cases, replacement. As stated in the previous sections, UHPC has excellent mechanical and durability properties that make it a prime candidate for use as a concrete deck overlay material (28).

#### 3.4.1. Quantifying Bonding between UHPC and NSC

The effectiveness of an overlay material is governed by the strength of bond between the overlay and the substrate material. A study conducted by Aaleti and Sritharan (29) investigated the bond characteristics between UHPC and normal strength concrete (NSC) for bridge deck overlay applications. In that study, sixty slant-shear test specimens with five surface textures and three NSC strengths were conducted. Flexural testing was also conducted on 7.75 x 24 x 108 in. (197 mm x 610 mm x 2740 mm) deck specimens with 1.5 in. (38 mm) thick UHPC overlays. The results demonstrated adequate shear transfer for all surface textures with depths equal to or greater than 0.12 in. (3 mm), regardless of the strength of the substrate material.

Valikhani et al. (30) correlated the bond strength between UHPC and NSC with surface roughness for repair applications. In that study, thirty bi-surface shear tests were conducted on

UHPC-NSC composite specimens to evaluate bond strength. The results showed that greater bond strengths were achieved with specimens that had adequate surface roughness compared to specimens without any surface preparation. Valikhani et al. (30) also noted the strength of the bond between the UHPC and the NSC could be harmed by the use of bonding agents.

#### ***3.4.2. UHPC Overlay Projects***

UHPC's exceptional mechanical and durability properties make it a viable option for repair applications. Consequently, many researchers have studied UHPC as a thin-bonded overlay to rehabilitate concrete bridge decks. Ju et al. (21) investigated the use of UHPC as an overlay to rehabilitate concrete bridge decks. Ju et al. (21) also reported that as of June 2019, there were eight bridges in North America with UHPC overlays.

### **3.5. Assessment of Non-Proprietary UHPC as an Overlay Material at NMSU**

NMSU investigated the use of a locally produced UHPC as an alternative to typical overlay materials. To assess the potential of the non-proprietary UHPC, several small-scale laboratory tests were conducted that investigated bond strength, shrinkage, and coefficient of thermal expansion. Large-scale tests were conducted to investigate shrinkage and thermal effects of NSC slabs overlaid with the non-proprietary UHPC. A large-scale test was also conducted to assess a full-scale pre-stressed channel girder with a 1 in. (25 mm) UHPC overlay subjected to flexural loading. The results indicated that the non-proprietary UHPC has the potential to serve as an overlay material as long as proper measures are used to prepare the substrate surface and ensure high quality bond with the existing deck (1).

#### ***3.5.1. Bond Strength Testing***

Several bond strength tests including slant-shear and direct tension tests (Figure 4) were performed to assess the bond strength between UHPC and NSC substrate with different surface textures. Results from the slant-shear tests showed that regardless of the texture depth, shear strengths of the bonded interface were greater than the required strength. However, greater bond strengths were achieved from textures that provided greater interlocking. Results from direct tension tests showed that the type of texture greatly affected the tensile bond strength. Grooved specimens had strengths less than 150 psi (1 MPa), which is considered unacceptable according to ACI 546 (31). Rough and chipped textures had average strengths greater than 150 psi (1 MPa). This was attributed to greater surface area and exposure of aggregate and pores that allowed UHPC to develop a better bond (1).

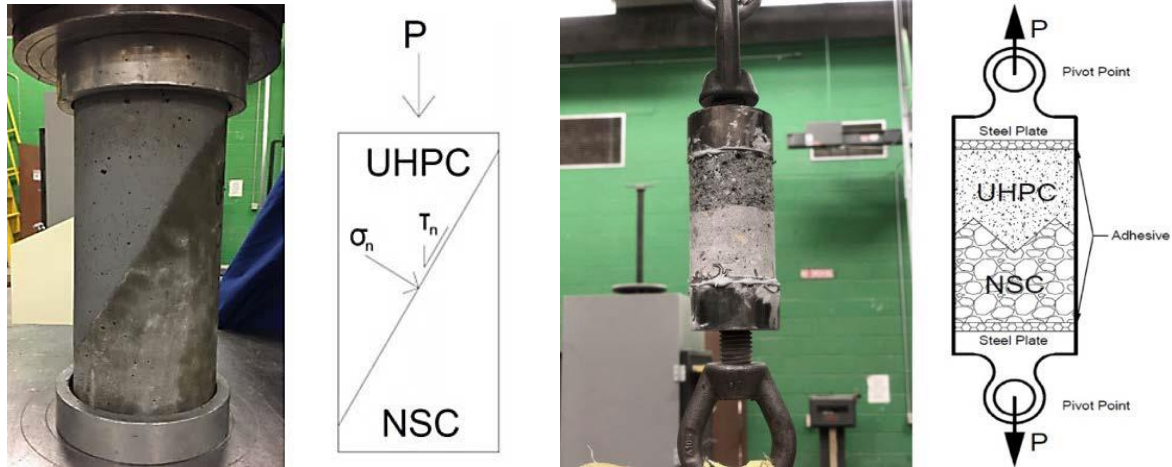


Figure 4. Slant-shear and direct tension test setups (1).

### 3.5.2. Shrinkage and Coefficient of Thermal Expansion

Tests were also conducted to assess the early-age and longer-term shrinkage behaviors and the coefficient of thermal expansion of the UHPC. The early-age shrinkage results showed that although the total UHPC shrinkage (approximately 1400  $\mu$ strain) was substantial at an early age (24 hours), 71% (approximately 1000  $\mu$ strain) of the early-age shrinkage occurred in the plastic state and may not contribute to bond stresses. Longer-term (28 days) shrinkage was 475  $\mu$ strain on average, which is well below the 600-1000  $\mu$ strain maximum values permitted by most state departments of transportation.

Coefficient of thermal expansion tests yielded a coefficient of thermal expansion of 10.8  $\mu$ /°F (19.5  $\mu$ /°C). This value is about 60% greater than what would be commonly expected for NSC concrete (typically near 5.5  $\mu$ /°F [10  $\mu$ /°C]), indicating that the thermal movements of the UHPC overlay may be significantly greater than the substrate concrete that will typically have a lower coefficient of thermal expansion and also experience smaller temperature swings (1).

### 3.5.3. Slab Testing

Combined shrinkage and thermal effects were investigated for NSC slabs overlaid with the non-proprietary UHPC by analyzing five slab-overlay specimens. Each slab-overlay specimen had a single parameter varied to isolate the effects of thickness of the NSC substrate, substrate reinforcement ratio, and exposure conditions. Increasing steel reinforcement and increasing thickness of the NSC substrate were observed to reduce UHPC overlay shrinkage (1).

### 3.5.4. Full-Scale Channel Girder Testing

The final major experiment was to overlay a full-scale channel girder to assess the response of a high-performance concrete, pre-stressed bridge girder with a 1 in. (25 mm) UHPC overlay to flexural loading as shown in Figure 5. The girder was subjected to 1000 load-unload cycles to specified service load conditions. Cyclic loading was applied both before and after application of the UHPC overlay to provide a comparison of global behavior and performance of the girder and overlay. Finally, the UHPC overlaid girder was loaded to failure to investigate post-cracking and ultimate behavior of the composite member. Little to no visible distress was

observed in the overlay until loads were applied that were substantially greater than expected under normal service conditions (1).



Figure 5. UHPC overlaid girder flexural testing setup (1).

### 3.6. UHPC Bond Performance with Delay in Cold Joint Formation

A study conducted by Lee et al. (32) conducted direct shear tests on UHPC to study monolithicity with the possibility of cold joint formation. Cold joints were formed with varying placement time delays. A reduction in bonding shear strength of approximately 8.0% was observed with a 15-minute delay. It was also noted that an extensive decrease in bonding shear performance was observed for delays greater than 15 minutes. Based on visual observations, degradation of the bonding shear performance was attributed to the formation of a surface film of  $\text{SiO}_2$  that formed approximately 15 minutes after placement and increased in thickness at approximately 60 minutes. Lee et al. (32) recommended physical or chemical treatment of the bonding surface in the occurrence of any delay.

### 3.7. Factors That Influence Bond Strength

According to Silfwerbrand and Beushausen (33), the most important factors that affect the bond between the overlay material and the substrate material include cleanliness of the prepared surface, the presence of micro-cracks, compaction of the overlay material, and curing of concrete overlays. However, many researchers and practitioners emphasize the importance of workability of the overlay material, pre-wetting of the prepared surface to promote

hydration, and both the micro-texture and the macro-texture of the substrate surface (34-36). ACI 546 recommends a minimum surface texture depth of 0.25 in. (6.35 mm) (31). Another factor that affects bond strength is age (maturity) of the overlay.

### **3.8. Surface Preparation**

Concrete overlays on bridge decks are intended to prolong the life of the deck by removing the top layer of deteriorated concrete and replacing it with a higher quality overlay material (37). To prepare the surface of the deck, all deteriorated or delaminated concrete must be removed and the deck must be properly cleaned. Removal of deteriorated concrete is accomplished by scarifying. Scarifying a deck makes abrasions in the deck and removes surface finishes such as paint and deck tining. It is important to note that removal of surface finishes is critical because if not adequately removed from the surface, finishes will break the bond between the substrate and the overlay. Four common mechanisms used to remove damaged concrete are presented in ICRI 310's guidelines for selecting and specifying concrete surface preparation (37). The four methods of scarification are impact, abrasion, pulverization, and high-pressure water erosion.

Although the scarification methods include impact and abrasion, these methods may induce micro-cracking. It is important to note that if these methods of scarification are used, inspections should be conducted to ensure sound and structurally durable concrete is maintained. Damaged concrete should be removed by sandblasting or high-pressure water erosion (37).

It is recommended that substrate surfaces be cleaned of any debris such as dirt, dust, oil, and grease to adequately anchor the overlay to the substrate. Pre-wetting the substrate surface is also recommended to prevent rapid water loss from the concrete overlay material (37).

In a study conducted by Valikhani et al. (30), the effect of substrate surface preparation on UHPC-substrate bond strength was investigated. Roughness, mechanical connection, and bonding agents were included in the study to evaluate their effects on bond strength. It was observed that there was a significant increase in bond strength of substrate surfaces that were sandblasted as opposed to substrate surfaces without any surface preparation (30).

A study conducted by Valipour and Khayat (38) also investigated bond strength between UHPC and NSC substrate. In that study, sand blasting was the method used to prepare the surface of the substrate for overlay installation. The study concluded that excellent bond can be achieved with proper surface preparation and without the use of bonding agents.

### **3.9. Bonding Agents**

When the deck is cleaned of all loose material and the aggregate is exposed, a tack coat may be applied. In some overlay alternatives, a tack coat may be used to ensure that there will be a good bond between the overlay and the substrate. The tack coat for an overlay may come in a variety of forms, such as a neat cement grout, sand-cement-water grout, or epoxy. Although common practice is to use a tack coat when applying overlay, a tack coat is not always recommended. Using a tack coat with a high water-to-cement ratio will cause the bond strength at the interface to decrease (39).

In another study evaluating bond strength between a concrete substrate and repair materials, sand-cement mortars were used as tack coats. In the study conducted by Momayez et al. (40), the percentage of silica fume in the sand-cement mortar was varied. It was concluded that the bond strength increased with the percentage of silica fume, up to an optimum 7% silica fume content (40).

Climaco and Regan (41) performed 223 slant-shear tests to assess the effects that bonding agents, surface texturing, and age of the substrate concrete had on the bond strength between the repair concrete and the substrate concrete. They concluded that using cement-based bonding agents was not required to achieve sufficient bond strengths between the substrate and the repair concrete (41).

In a study conducted by Valikhani et al. (30), UHPC-substrate bond strength with different substrate surface preparation was investigated. Roughness, mechanical connection, and bonding agents were included in the study to evaluate their effects on bond strength. It was observed that the bond strength between UHPC repair concrete and the NSC substrate was reduced by half due to the bonding agent reducing cohesion between the two materials.

### **3.10. Stresses at the Bonded Interface**

UHPC is often cast against hardened NSC when used as a repair material. Therefore, the bond interface between these two concretes needs to be assessed (42, 43). To perform adequately, the bond between the overlay and substrate must be able to withstand the deck deformations (44). Flexural deformation from loads, thermal expansion from environmental effects, and overlay shrinkage can contribute to deck deformation. Deformation of the deck can cause shear and tensile stresses at the bond interface. Slant-shear and direct tension tests are often used in the laboratory to assess the bond strength between two concrete materials. However, direct tension pull-off tests are commonly used in field projects to assess the bond strength between overlay and substrate materials.

#### ***3.10.1. Mechanical Stresses at the Bonded Interface***

The slant-shear test (ASTM C882 / C882M) (45) is widely used to assess the bond shear strength between substrate and overlay materials (41). The slant-shear test induces a combination of compressive and shear stresses (46).

The direct tension pull-off test, performed by partially coring an overlaid specimen and applying a tensile force until failure, is often used to measure bond tensile strength (46).

#### ***3.10.2. Thermal Compatibility***

Bond stresses can also be caused by differences in material properties, such as the coefficient of thermal expansion. It is desirable to have similar coefficients of thermal expansion between the overlay and substrate materials (thermal compatibility). Areas subjected to large temperature changes are the areas in which the coefficient of thermal expansion is most important (31). The coefficient of thermal expansion values for the two concrete materials can be used to analyze the differences in the thermal movements of the two materials. A common coefficient of thermal expansion test used in the south-central states is TxDOT Tex-428-A (47).

### ***3.10.3. Shrinkage Compatibility***

Shrinkage is another concern when considering a potential concrete repair material. ACI 546 recommends using an overlay material that can shrink without breaking the bond with the substrate since shrinkage of the overlay can cause shear and tensile stresses at the bond interface that can lead to cracking and delamination (31).

Shrinkage of repair concrete is particularly important when using a material with a high cementitious materials content, such as UHPC. Because UHPC has a high percentage of cementitious material, it is prone to excessive shrinkage (48). In a study conducted by Chilwesa et al. (48), curling, de-bonding, and cracking in slab elements with different overlay materials was investigated. The study found that overlay de-bonding or cracking depends on the rate and magnitude of shrinkage, especially at early ages. Shrinkage reducing admixtures (SRAs) were also assessed for their ability to mitigate shrinkage of the overlay material. It was observed that SRAs prevented de-bonding, curling, and cracking by reducing the rate and magnitude of overlay shrinkage.

A study conducted by Hong (49) investigated edge curling effects on interface delamination of concrete overlays for bridge decks. It was observed that saturated substrate surfaces exhibited less relative displacement at the interface than dry substrate surfaces. Therefore, dry substrate surfaces should be avoided.

## 4. METHODOLOGY

The following sections present details regarding the bridge description and location, condition of the bridge, the design of the overlaid bridge deck, mixture proportion adjustments, UHPC overlay mock-up placements, and preliminary testing.

### 4.1. Bridge Description and Location

Bridge 7032 off Exit 150 in Socorro, New Mexico is the bridge that was overlaid with a non-proprietary UHPC (Figure 6). The bridge is a two-lane bridge with a center median and is approximately 300 ft. (91.4 m) in length and 54 ft. (16.5 m) in width. This bridge is a four-span, multi-cell box girder bridge with three intermediate supports provided by column bents (integral caps) containing six cylindrical columns as shown in Figure 6. A site visit allowed the researchers to assess what instrumentation would be feasible for this bridge. Because of the box girder superstructure (shown in Figure 6), the underside of the deck could only be accessed by entering the box girders. The bridge is a two-lane bridge with the traffic lanes separated by a small concrete median as shown in Figure 7. The concrete deck has a tined finish to provide skid resistance.

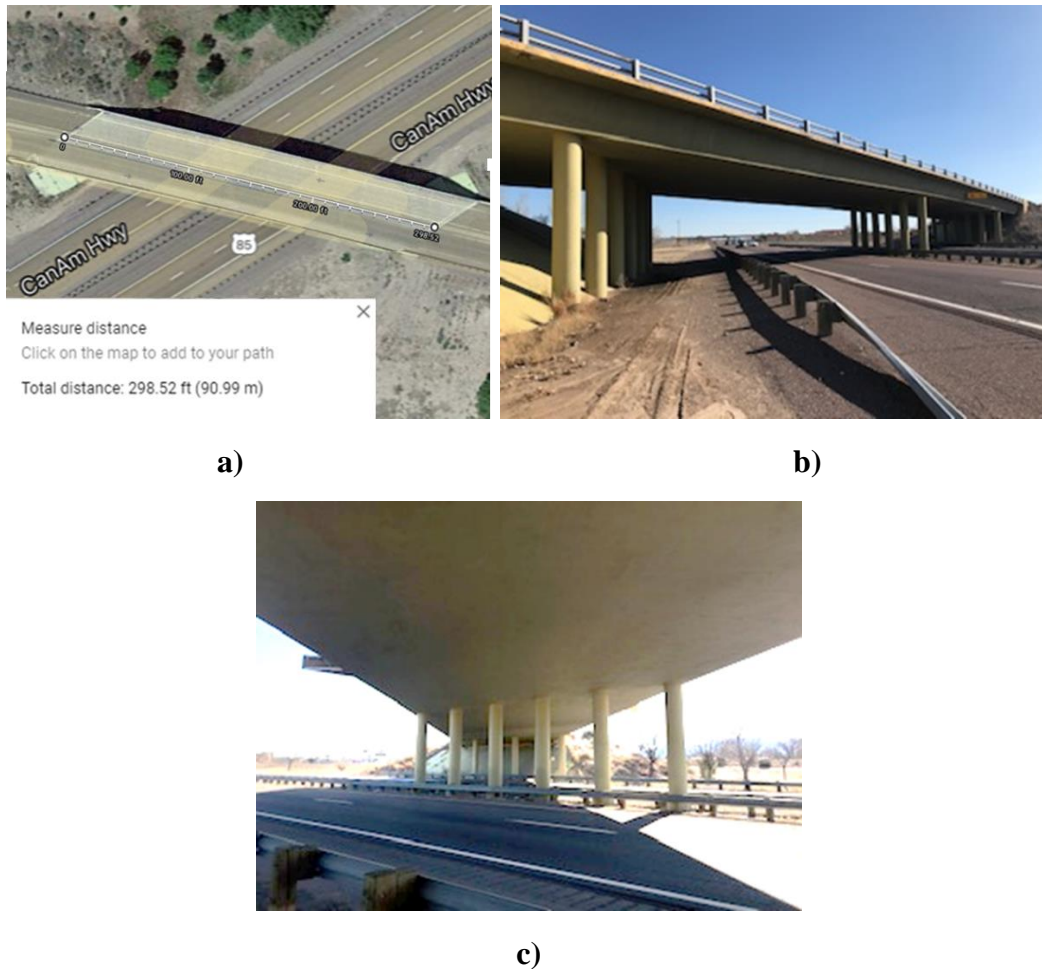


Figure 6. a) Top view of bridge 7032, b) plan view of bridge 7032, and c) bottom of multicell box girder superstructure.



Figure 7. Bridge 7032 concrete deck with two lanes separated by a median.

## 4.2. Condition Assessment of Existing Deck

At several locations along the bridge deck there were transverse cracks approximately 1/16 in. (1.59 mm) in width as shown in Figure 8. The transverse cracks were primarily located at the negative moment regions over column bents and potentially full depth. During assessment it was noted that there was no evidence of delamination on the bridge deck.



Figure 8. Transverse cracks observed on the concrete bridge deck.

## 4.3. Design

The scope of the bridge rehabilitation project included removal of deteriorated concrete from the existing deck, installation of a high-performance deck (HPD) layer to replace removed concrete, and installation of a 1 in. (25 mm) thick UHPC overlay.

### 4.3.1. Removal of Deteriorated Concrete

The removal of deteriorated concrete included removing existing metal railing and the deck overhang as shown in Figure 9. Along with the removal of deteriorated concrete, the expansion joint seals were also removed and replaced as shown in Figure 10.



Figure 9. Condition of deck on southbound lane after removal of deteriorated concrete.



Figure 10. Replacement of the expansion joint seal.

#### ***4.3.2. Design of Bridge Rehabilitation***

The design for the rehabilitation of the bridge included a 33-inch (838-mm) concrete barrier railing as shown in Figure 11. The raised median was also to be replaced after construction of the 1 inch (25.4 mm) thick UHPC overlay as shown in the illustration presented in Figure 12.

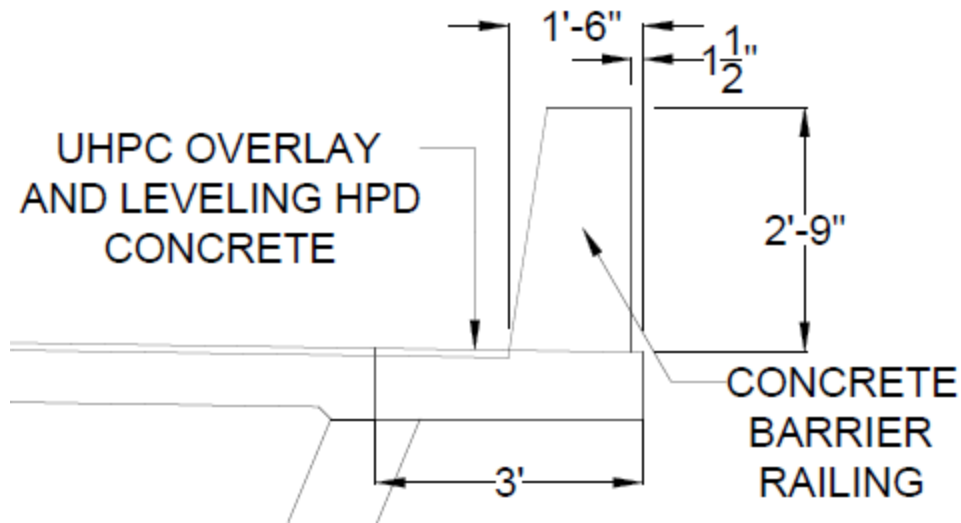


Figure 11. Concrete barrier railing.

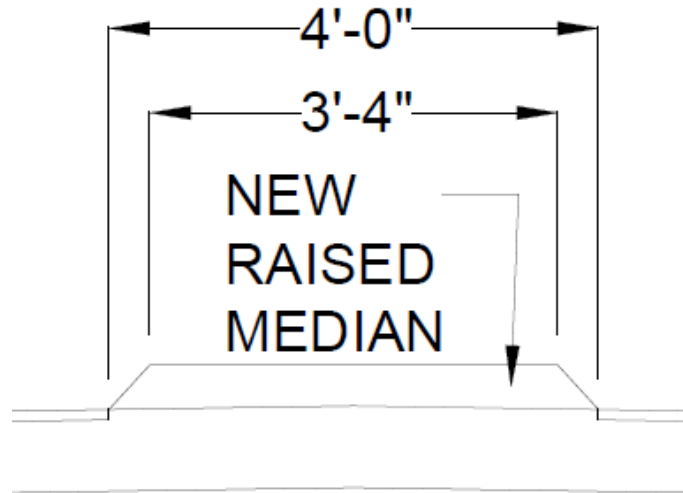


Figure 12. Raised median after placement of UHPC overlay.

#### 4.4. Mixture Proportions

This project was conducted as the implementation of a sequence of research projects that were conducted in collaboration with the NMDOT and Tran-SET. The mixture proportions proposed for use on this project were selected based on results from those prior research projects.

##### 4.4.1. Proposed UHPC Mixture Proportions

A 2017-2018 research project at NMSU (funded by Tran-SET) demonstrated that UHPC produced with local materials was able to achieve adequate bond strength with substrate concrete when used as an overlay material in the laboratory (1). Based on these observations, NMDOT decided to implement the locally produced UHPC overlay on a concrete bridge deck in Socorro, NM. The mixture proportions developed in the 2017-2018 Tran-SET project, presented earlier in Table 1, were proposed for the NMDOT field implementation project.

#### 4.4.2. Buy America (49 U.S. Code § 5323 [jj]) Enforcement

NMDOT enforced the Buy America (49 U.S. Code § 5323[jj]) requirement that steel (fibers) purchased for the bridge rehabilitation project be produced in the United States. The fibers recommended in the UHPC mixture proportions used by NMSU were produced in China, and production of those fibers had ceased in the United States. Fibers produced by Concrete Fiber Solutions (CFS) that were the same length as the original fibers, 0.5 in. (13 mm) with a length/diameter aspect ratio of 22 and a tensile strength that meets the requirements of ASTM A820 (50) were identified as the most suitable replacement.

#### 4.4.3. Selection of the New Steel Fibers

The CFS fibers were selected based on previous research conducted at NMSU. Visage (51) investigated the flexural behavior of UHPC beams using local materials at NMSU. In the study conducted by Visage (51), compressive strength tests were conducted on UHPC using the mixture proportions shown in Table 2 and the CFS steel fibers. This UHPC mixture had an average 28-day compressive strength of 19.5 ksi (134 MPa) as shown in Figure 13, which provided the basis for using the CFS fibers to accommodate NMDOT’s requirement.

Table 2. UHPC Mixture proportions for 1.5% by volume fibers.

Constituents	Unit	Unit/yd <sup>3</sup> [m <sup>3</sup> ]
Cement	lb. [kg]	1242 [737]
Silica Fume	lb. [kg]	194 [115]
Fly Ash	lb. [kg]	116 [68.8]
Sand	lb. [kg]	1900 [1127]
Fibers <sup>1</sup>	lb. [kg]	198 [117]
HRWRA	gal. [L]	8.57 [42.4]
Water	lb. [kg]	233 [138]

<sup>1</sup> - 1.5% steel fibers by volume.

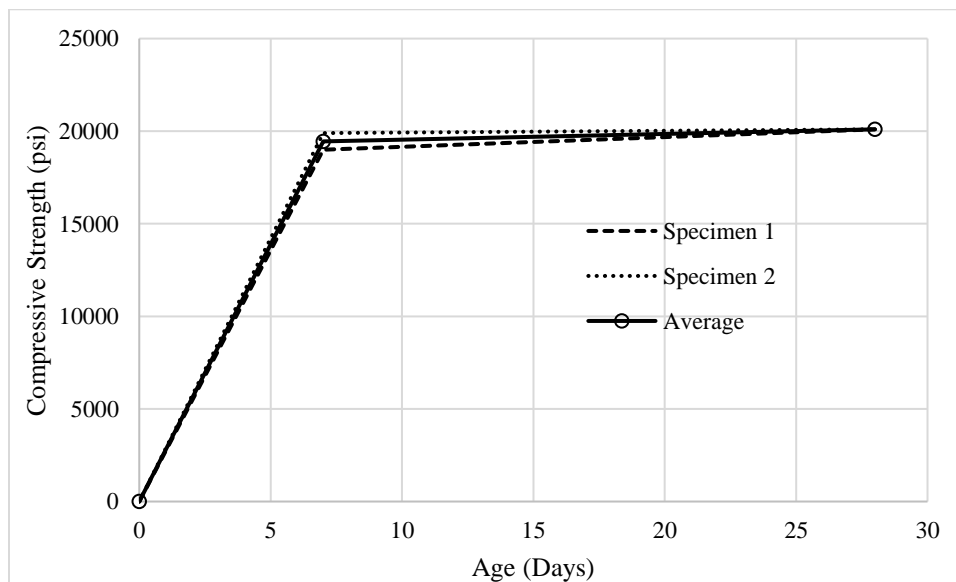


Figure 13. Compressive strength curve of UHPC.

It should be noted that the UHPC mixture was a prescribed specification for the NMDOT construction project. Based on experiences gained during this project, it is recommended that agencies should endeavor to transform the process into performance-based specifications for UHPC mixtures.

#### **4.5. UHPC Overlay Mock-Up Placements**

NMSU researchers worked closely with NMDOT to ensure adequate transfer of the UHPC overlay technology. To prepare for construction, mock-up placements were conducted that allowed NMSU to instruct NMDOT personnel and contractors on the batching, mixing, placing, and finishing of the UHPC overlay material. The mock-up placements were conducted at A1 Quality Ready Mix located in Socorro, NM.

##### ***4.5.1. Mock-Up Placement 1 (May 29, 2020)***

The first mock-up placement was conducted on May 29, 2020 at a temperature of 85°F (29.4°C). The contractor made little effort to batch or mix UHPC prior to the mock-up placement. Consequently, the objective of this mock-up placement became to educate the contractor on UHPC batching and mixing procedures to transfer the UHPC technology. During mock-up placement 1, the contractor attempted to batch larger volumes that the pan mixers could handle, requiring adjustments to batch volumes for later mock-up placements. It was also observed that the UHPC mixture produced was too fluid because the contractor did not account for the moisture in the sand. Since the contractor was unable to demonstrate batching, mixing, and placing the UHPC, a second mock-up placement was scheduled.

##### ***4.5.2. Mock-Up Placement 2 (June 24, 2020)***

The second mock-up placement was conducted on June 24, 2020 at a temperature of 92°F (33.3°C). During the second mock-up placement, the contractor was able to correctly adjust the batch quantities to properly account for the moisture in the sand. However, the contractor continued to attempt to mix large volumes of UHPC that overloaded the mixers. This resulted in the contractor using mock-up placement 2 to determine the maximum volume of UHPC that could be mixed in the pan mixers, which was determined to be 0.2 yd<sup>3</sup> (0.153 m<sup>3</sup>). Although the contractor was able to demonstrate batching and mixing proficiency, placement and curing of an UHPC overlay was not demonstrated. Therefore, a third mock-up placement was scheduled.

##### ***4.5.3. Mock-Up Placement 3 (July 7, 2020)***

The third mock-up placement was conducted the night of July 7, 2020 at a temperature of 83°F (28.3°C). The mock-up placement slab (substrate) was constructed using an approved Class HPD concrete, produced by A1 Quality Ready Mix. The substrate concrete surface was finished with a tine rake that provided a minimum average texture height of 0.25 in (6.35 mm). The 20 ft. by 20 ft. (6.1 m by 6.1 m) HPD slab was unreinforced and field-cured for eight days. After the curing time, the HPD slab was thoroughly pressure-washed to remove any debris or surface contaminants. Then, the surface was maintained in a saturated condition until placement of the UHPC overlay was initiated. However, the surface was allowed to dry after the first batch of UHPC was placed and appeared dry prior to placement of subsequent batches of UHPC.

After curing the UHPC overlay, direct tension pull-off tests were conducted on the overlaid slab to investigate the bond performance between the UHPC overlay and the HPD substrate. Reasonable strengths were achieved in areas where the first batches of UHPC produced were placed on visibly moist surfaces, while zero strengths were observed in areas where the substrate appeared dry during placement of the UHPC overlay. Although some zero strength pull-off tests were observed, the reason was known for the loss of bond. Therefore, this mock-up placement was considered to be successful because the contractor demonstrated the ability to batch, mix, and place the overlay material.

#### ***4.5.4. Mock-up Placement 4 (April 5, 2021)***

The construction season in 2020 ended prior to construction of the UHPC overlay. Consequently, the contractor scheduled a fourth mock-up placement in April 2021 to refresh the construction crew's knowledge of UHPC practices. For this mock-up placement, new high-energy, horizontal shaft mixers (Figure 14) with a 1.0 yd<sup>3</sup> (0.76 m<sup>3</sup>) capacity were introduced to accelerate UHPC placement on bridge 7032. The new mixers were 40 hp (30kW) mixers (one electric and one hydraulic).

The mock-up placement was conducted at A1 Quality Ready Mix located in Socorro, NM on Monday, April 5, 2021. Again, a 20 ft by 20 ft (6.1 m by 6.1 m) HPD slab was placed and was cured for 7 days prior to placing the UHPC overlay. The substrate surface had a tined texture with an average texture depth of 0.25 in. (6.35 mm). After curing, the concrete surface was sandblasted to remove surface paste in an effort to facilitate bond between the UHPC overlay and the substrate concrete. The HPD was maintained between wet and visibly moist conditions prior to overlay placement.



**Figure 14. Horizontal shaft mixers.**

A 0.77 yd<sup>3</sup> (0.59 m<sup>3</sup>) batch volume was selected as the batch size for production placements on bridge 7032. Figure 15 shows the UHPC placement on the HPD slab. During placement, Confilm<sup>®</sup>, an evaporation retardant from BASF was used to reduce surface moisture evaporation against the rapid drying conditions. Figure 16 shows the placement and UHPC finish during mock-up placement 4. The white film on the UHPC overlay, after finishing, is a curing compound applied to the top surface of the overlay.



a)

b)

**Figure 15. Mock-up placement 4 – a) UHPC placement and b) UHPC screeding.**



**Figure 16. Mock-up placement 4 – UHPC finish.**

Following the mock-up placement, cracking was observed because the UHPC overlay was not covered with plastic sheeting immediately after screeding and finishing were completed. As a result, cracks were visible within 10 minutes, as shown in Figure 17. Subsequently, the UHPC overlay was covered with a plastic tarp and maintained wet for the following seven days. To assess the integrity of the bond, direct tension pull-off testing was conducted on the overlaid mock-up placement slab. Inadequate pull-off strengths (less than 150 psi [1.0 MPa]) were observed. This can be attributed to improper substrate surface preparation, specifically, the slab was only maintained saturated for one hour prior to overlay placement, and within that hour the surface was lightly sandblasted which caused localized evaporation. However, this mock-up placement was considered successful since the cause of inadequate strengths were known the contractor was allowed to continue with the overlay construction.



Figure 17. Mock-up placement 4 – UHPC overlay cracking.

## 4.6. Test Methods

Workability of each UHPC overlay batch was assessed using slump and spread tests. Compressive strength tests were performed at two, four, seven, 14, 28, and 56 days and flexural strength tests were performed at seven and 56 days. Additionally, direct tension pull-off tests were conducted on the overlaid bridge.

### 4.6.1. Slump Flow Test

To analyze workability of the UHPC, slump and spread tests were performed on each batch in accordance with ASTM C143 (52) and ASTM C1611 (53), respectively. For these tests, a standard slump cone with dimensions of 12 in. (305 mm) in height, a base diameter of 8 in. (203 mm), and a top diameter of 4 in. (102 mm) was used. To conduct slump tests, the slump cone was placed upright over a stainless-steel base plate. The cone was filled with UHPC in increments of 1/3 the cone volume and rodded 25 times after each increment. When the cone was filled completely, the top surface was screeded flush with the rim of the slump cone. Then, slowly and in a straight single motion, the cone was pulled directly up allowing the UHPC to slump and spread. Measurements were taken using a tape measure as shown in Figure 18.

For slump measurements, the cone was inverted, and a steel rod was placed flush with the top of the slump cone. The slump measurement was taken from the center of the top of the UHPC mixture to the bottom of the rod as shown in Figure 18a. The spread was determined by taking average of three measurements across the width of the slumped UHPC as shown in Figure 18b. The target slump and spread measurements were between 8 and 10.5 in. (205 and 265 mm) for slump and between 12 and 19.5 in. (305 and 495 mm) for spread.



Figure 18. a) Slump and b) spread measurements.

#### 4.6.2. Compressive Strength Test

Compressive strength of UHPC was tested in accordance with the British Standard (BS) 1881 (54) at two, four, seven, 14, 28, and 56 days. A minimum of four cube samples were cast for each test day, resulting in a total of 24 samples. Cube specimens used for two, four, and seven-day compressive strengths were cured at ambient conditions (68 °F [20 °C] and 30% relative humidity). Samples for the 14, 28, and 56-day strengths were cured in a moist room (73°F [23°C] and 98% relative humidity). Cube specimens (3.94-in. [100-mm] cubes) from each batch of UHPC were tested at seven and 28 days, for compressive strength. Specimens were loaded to failure, as shown in Figure 19, at a rate of 9000 psi/min (62 MPa/min) following recommendations to accelerate the test (8). The target compressive strengths for the UHPC were 14,000 psi (96.5 MPa) at seven days and 17,000 psi (117.2 MPa) at 28 days. Target strengths were selected by the NMDOT, at seven days, and to meet the minimum strength requirement from ASTM 1856 (14) at 28 days.



Figure 19. UHPC cube sample at failure under compression test.

### ***4.6.3. Flexural Strength Test***

To assess the flexural strength (modulus of rupture [MOR]), testing was conducted according to ASTM C1609 (55) at 7 and 56 days. A minimum of two prismatic samples (3x4x16 in. [76x102x406 mm]) were cast for each test day. Samples used for seven-day flexural strength testing were cured at ambient conditions (68 °F [20 °C] and 30% relative humidity). Samples for 56-day strengths were cured in a moist room (73°F [23°C] and 98% relative humidity). The flexural tests were performed by placing a UHPC prism over a bearing point near each end of the prism, then applying a split load symmetrically about the mid-span location of the specimen. As shown in Figure 20, the four-point flexural tests used linear-variable displacement transducers (LVDTs), load cells, and string potentiometers to monitor the behavior of the specimens. The data obtained from the LVDTs facilitated identification of the first crack load and moment. Then, the first crack load was used to calculate the flexural strength of each prismatic specimen in terms of MOR. The prisms were loaded to failure at a rate of 1500 lbs per minute (6.7 kN per minute).



**Figure 20. UHPC prismatic sample at failure during flexural test.**

### ***4.6.4. Direct Tension Pull-off Tests***

Direct tension pull-off tests were conducted on overlaid slabs produced for mock-up placements 3 and 4.

#### ***4.6.4.1. Direct Tension Pull-off Tests for Mock-up Placement 3***

The first step of these tests was to saw 1.875 in. (47.6 mm) diameter cores through the overlay material and approximately 0.5 in. (12.7 mm) into the substrate material as shown in Figure 21a. After completing the coring process the area was dried and debris was removed from the top surface before steel load platens were epoxied to the tops of the cores. The epoxy used to adhere the load platens to the cores (ChemCo Systems Bonder Paste LWL) required 24 hours to cure. After the epoxy had cured for 24 hours, the direct tension tests were conducted using the testing setup shown in Figure 21b.



**Figure 21. a) Core drilling and b) pull-off test setup.**

Figure 22 is an illustration that shows the general locations of the direct tension pull-off tests. The UHPC was mixed in batches and was placed on the slab in sections beginning at the west end of the slab, which is the top of the slab illustration in Figure 22. Subsequent batches were placed where the previous overlaid section stopped, and the placements continued eastward (downward in Figure 22). The lower portion of the figure identifies where the overlaid section stopped by labeling the location that was not overlaid as “No UHPC Overlay”. The locations of the direct tension pull-off tests are identified by the circles shown in Figure 22. On September 7, 2020, NMSU attempted to conduct pull-off tests in the areas depicted as “Zero Strength Locations”. These locations were denoted as “Zero Strength Locations” because the UHPC overlay broke from the substrate during core drilling and pull-off tests could not be conducted. However, locations 1 through 6, were located in the portion of the overlay that was placed first. This portion of the slab was overlaid while the substrate surface was still wet. These core locations were successfully cored and pull-off tests were conducted on September 20, 2020.

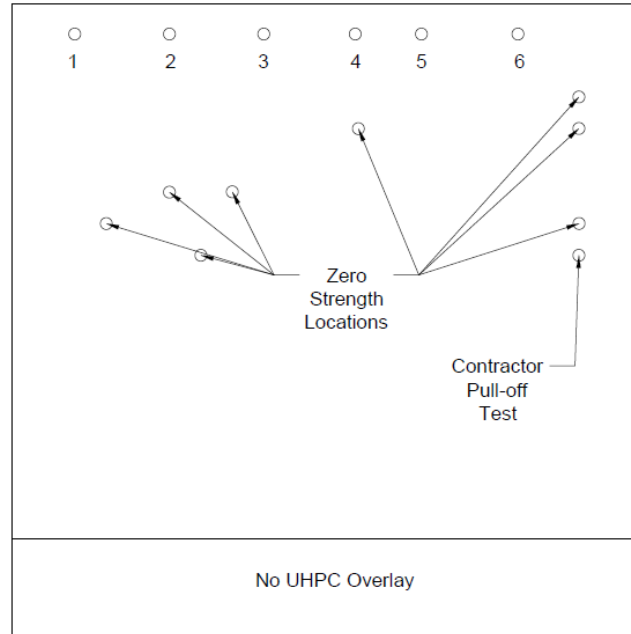


**Figure 22. Direct tension pull-off locations on the mock-up placement 3 slab.**

#### *4.6.4.2. Direct Tension Pull-off Test for Mock-up Placement 4*

Additional pull-off tests were conducted on the 20 ft by 20 ft (6.1 m by 6.1 m) mock slab constructed for the fourth mock-up placement. Core drilling, pull-off test setup, and pull-off testing were performed as described in Section 4.6.4. A total of five core drillings were attempted, with one zero-strength location.

Figure 23 illustrates the locations of the core drillings and the pull-off tests performed on the mock slab. The UHPC was placed on the HPD from northeast to southwest (from top to bottom as shown in Figure 23). UHPC was placed up to the “No UHPC Overlay” mark. A total of five pull-off tests were conducted, as numbered from 1 to 5 in Figure 23. Core sample no. 2 debonded while setting up the pull-off test equipment, so it was considered a zero-strength location. The 4 successful pull-off tests (1, 3, 4, and 5) were located on the northeast side of the slab as shown in Figure 23. Locations where pull-off tests were successfully conducted are identified by circles and their order number, and the zero-strength location is identified by a circle with a cross mark.

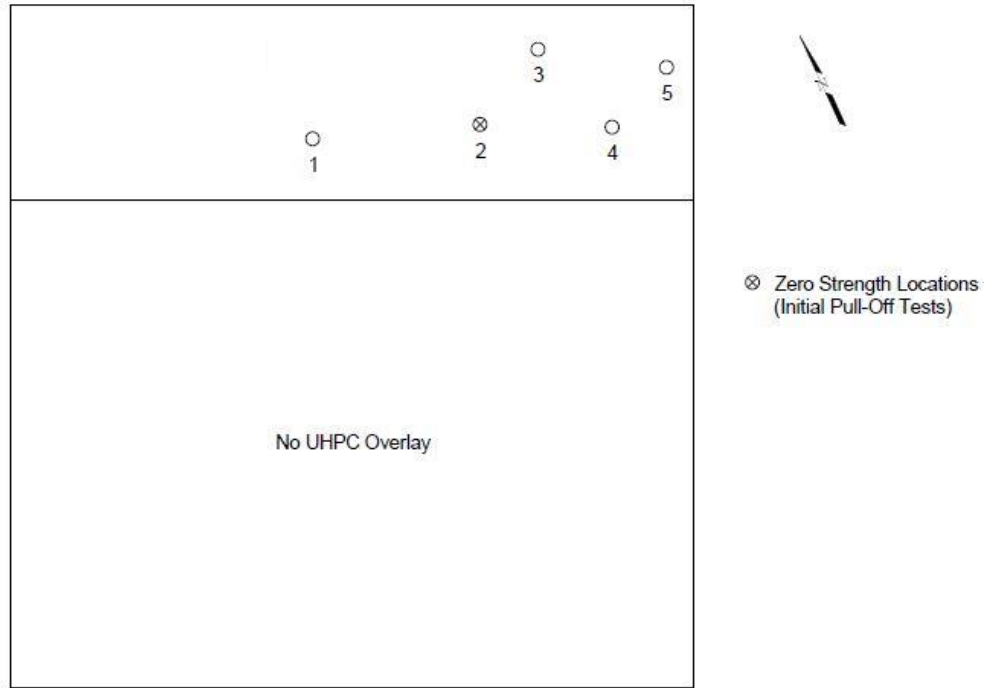


Figure 23. Direct tension pull-off test locations on mock-up placement 4 slab.

#### 4.7. HPD Installation

As described in Section 4.3.1, deteriorated concrete was removed to expose the reinforcing steel. The removed deteriorated concrete was replaced volumetrically by placing a HPD leveling layer. The HPD concrete placement started November 5, 2020 at the northeast corner of the bridge.

The construction sequence of the HPD placement began by removing the deteriorated concrete in the weeks prior to placement of the HPD. The construction sequence consisted of preparing for HPD placement, initiation of field measurements (slump, unit weight, air content, concrete temperature, air temperature, wind speed, and relative humidity), placing the HPD concrete, and finishing and surface texturing of the HPD.

The exposed deck was cleaned of debris and contaminants and the concrete surface appeared dry. During the cleaning of the deck, the construction workers made final adjustments to the reinforcing steel. The HPD was placed using a concrete pump, consolidated, and screeded. The screeded concrete surface was then misted with water and floated. The floated surface of the HPD was textured using the tine rake as shown in Figure 24.

The tined surface appeared to have a texture depth that was at least 0.25 in. (6.35 mm), which is the minimum recommended texture depth for applying repair concrete according to ACI 546 (46).



Figure 24. Tine rake used to texture the HPD surface.

## **4.8. UHPC Production Placement**

Prior to overlay installation the substrate surface was ceramic bead blasted and maintained saturated up to placement. A total of 105 batches were placed on bridge 7032 (53 batches on the eastbound lane and 52 batches on the westbound lane). Additionally, workability tests were conducted on the UHPC batches to ensure that acceptable slump and spread were obtained. Spread measurements between 12 and 19.5 in. (305 and 495 mm) and slump measurements between 8 in. and 10.5 in. (205 mm and 265 mm) were considered acceptable since mixtures with lower slumps were challenging to handle, place, and finish. Samples were also taken for compressive and flexural strength testing as required by NMDOT.

### ***4.8.1. Substrate Surface Preparation***

Before placement of the UHPC overlay, the substrate surface was prepared by providing a surface texture and saturated surface conditions. Surface texturing was achieved using the ceramic bead blaster shown in Figure 25.



**Figure 25. Ceramic bead blaster.**

#### ***4.8.2. Material Preparation and UHPC Mixing***

The material preparation consisted of using pre-loaded bags containing sand, cement, and fly ash. Bags contained the quantities (masses) required for a 0.77 yd<sup>3</sup> (0.59 m<sup>3</sup>) total batch volume. Mixing was performed using the two 1.0 yd<sup>3</sup> (0.76 m<sup>3</sup>) high-energy horizontal shaft mixers described in Section 4.5.5.

#### ***4.8.3. UHPC Placement***

A total of 105 batches were placed on bridge 7032 (53 batches on the eastbound lane and 52 batches on the westbound lane). Production Placements 1 and 2 (eastbound lane) started from the west end of the bridge, and Production Placements 3 and 4 (westbound lane) started from the east end of the bridge. The first placement experienced visible cracking (Figure 26) because the UHPC overlay was not covered under plastic sheets and burlap as soon as surface finishing was completed. Therefore, curing procedures were modified for Production Placements 2 through 4. The revised curing procedures required application of curing compound immediately after screeding and finishing were completed, and then coverage with plastic sheets as soon as possible after the curing compound is applied. The revised curing practices resulted in no significant cracking being observed for the remaining production placements.



Figure 26. Production placement 1 – UHPC overlay cracking.

#### ***4.8.4. Data Collection during Construction of UHPC Overlay***

Data were collected during construction of the UHPC overlay that included weather conditions, construction sequence, substrate surface condition, and UHPC quality assurance testing. These data are of interest because they are expected to influence quality of the completed overlay construction project.

##### *4.8.4.1. Weather Conditions*

Weather condition data included temperature, wind speed, and relative humidity during construction of the UHPC overlay. These data are of interest because they can influence evaporation from the UHPC overlay material. Temperature during installation of the overlay was documented because temperature can influence rate of hydration and water evaporation as well as reduce workability (accelerate slump loss) of the overlay material.

##### *4.8.4.2. Construction Sequence*

Construction sequence data that were collected include production times for each batch, timing and location of any cold joints observed during construction, and methods for vibrating the overlay material.

##### *4.8.4.3. Substrate Surface Conditions*

Substrate surface conditions included characterization of the surface texture (texture depth and exposure of aggregate particles), cleanliness of the substrate surface, pre-wetting of the substrate surface prior to overlay installation, and the moisture condition at the time of placement.

##### *4.8.4.4. UHPC Quality Assurance Testing*

Testing of the UHPC began by measuring the temperature and workability of freshly mixed batches. The target slump and spread measurements were between 8.5 and 10.5 in. (215 and 265 mm) for slump and between 12 and 19.5 in. (305 and 495 mm) for spread. After fresh properties of the UHPC were assessed, samples were cast for compressive and flexural strength testing. Compressive strength testing was conducted at ages of two, four, seven, 14, 28, and 56 days. A minimum of four 3.94-in. (100-mm) cube samples were cast for each testing age. Target compressive strengths identified by NMDOT were 10,000 psi (68.9 MPa) at seven days

and 17,000 psi (117.2 MPa) at 56 days. Flexural strength tests were performed at seven and 56 days. A minimum of two 3x4x16 in. (76x102x406 mm) prismatic samples were cast for each testing age.

#### 4.9. Instrumentation on Bridge 7032

Preceding the placement of the HPD on bridge 7032, internal and embedded sensors were installed to monitor the structural performance of the bridge superstructure and, eventually, the UHPC overlay. Figure 27 shows bridge 7032 before and after initial deck removal. External sensors were attached to the ceiling inside the cells of the multi-cell box girder superstructure, while embedded sensors were installed inside the HPD. Figure 28 illustrates the external sensors used inside the box girders cells (strain gauges only) and Figure 29 shows the embedded sensors in the deck prior to placement of the concrete (strain gauges and thermocouple). During UHPC placement, embedded sensors were installed inside the UHPC to monitor the overlay behavior. Figure 30 shows the embedded sensors attached to steel bolts resting on the HPD. Sensors were placed inside the overlay material as it was being placed (strain gauges only).



Figure 27. Bridge 7032 before and after first deck section removal.



Figure 28. External sensor installation inside box girder cells.



**Figure 29. Embedded sensor installation in HPD.**



**Figure 30. Embedded sensor installation in UHPC overlay.**

All sensor wires extended below the deck through drilled openings, to the inside of the box girder cells, and were connected to multiplexors inside protective boxes that were placed near midspan of the first two (western most) bridge spans. Each multiplexor was connected to a datalogger that collects data continuously. A solar panel was installed near the bridge to power the 12V battery of the datalogger. Figure 31 presents the datalogger box set up (datalogger, 12V battery, and charge controller).

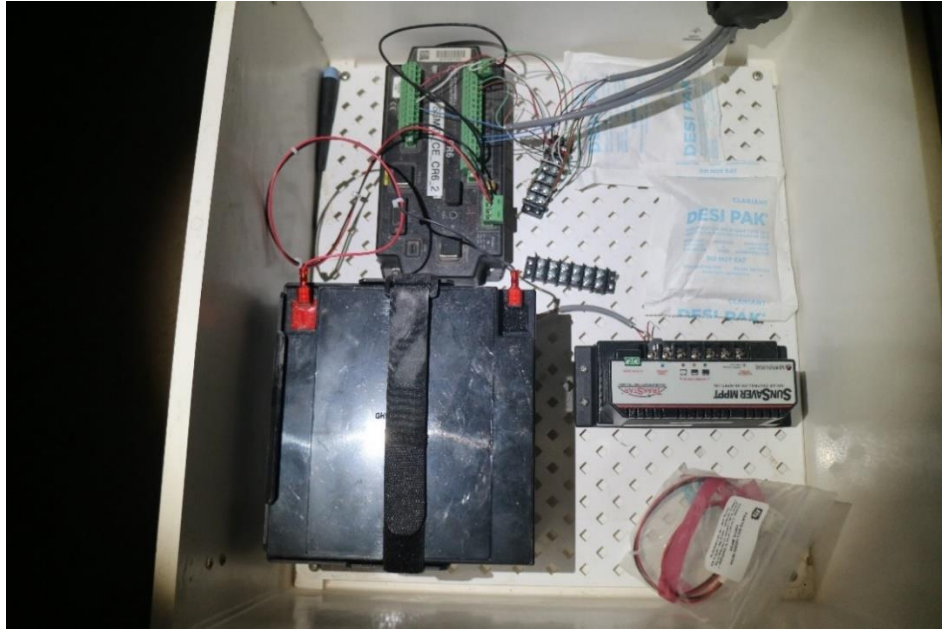


**Figure 31. Data-logger box setup.**

A total of 156 strain gauges and 26 thermocouples were installed in the eastbound lane of bridge 7032. Strain gauges were used to measure compressive and tensile strains in the bridge, and thermocouples were used to measure the temperature at different bridge locations. Figure 32 shows the sensors used on bridge 7032 (strain gauge for steel embedded in concrete, external strain gauge for concrete, and thermocouple). Strain gauges for steel were 0.08-in. (2-mm) long with a resistance of  $120 \pm 5$  ohms ( $\Omega$ ) and strain gauges for concrete were 3.5-in. (90-mm) long with a resistance of  $120 \pm 5$  ohms ( $\Omega$ ).

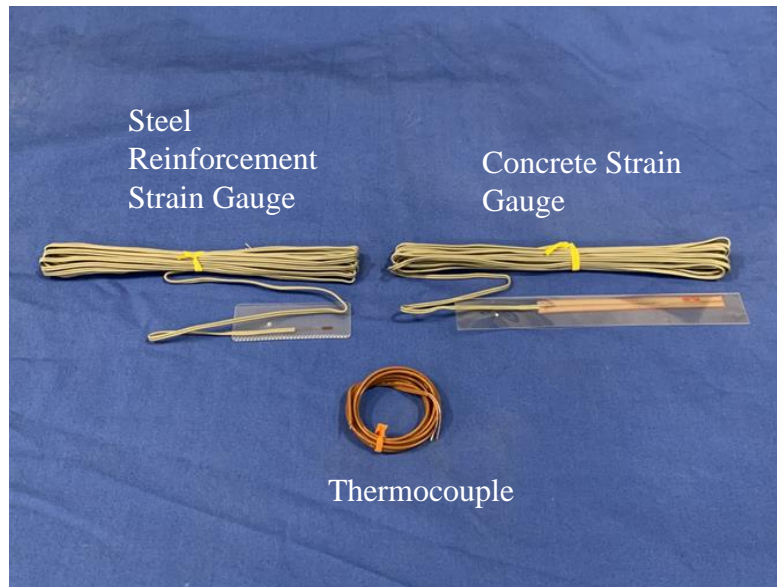
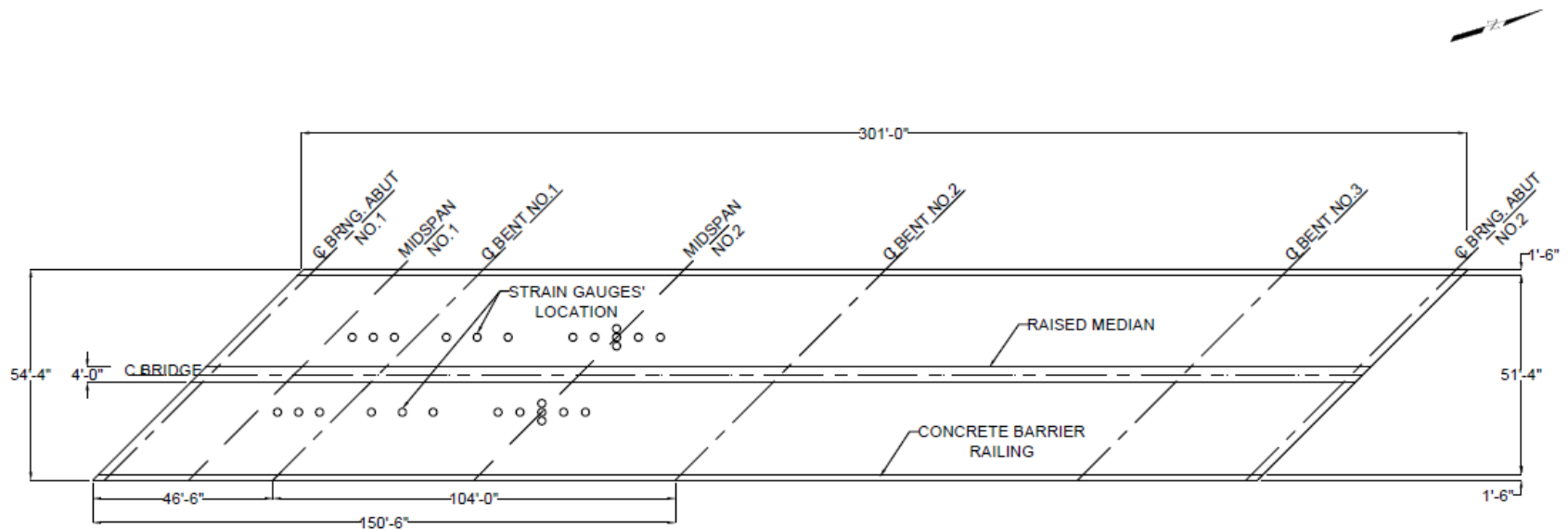


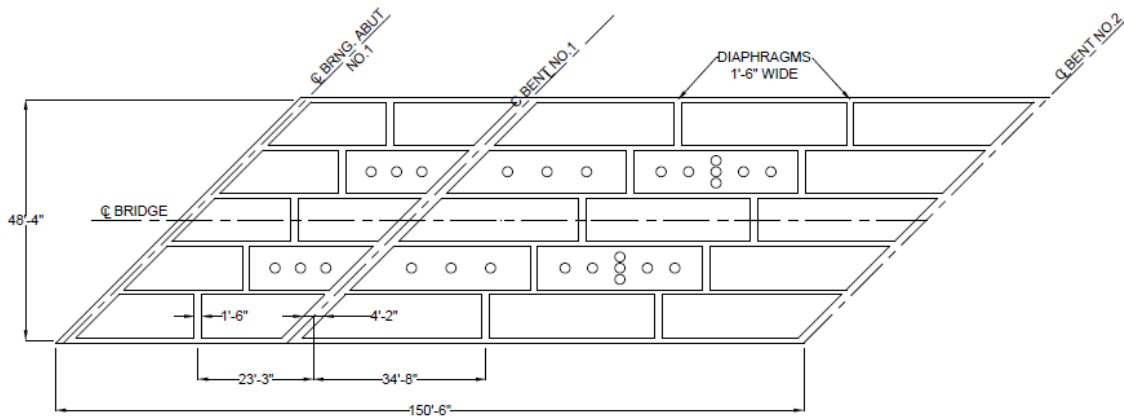
**Figure 32. Sensors used on bridge 7032.**

To place steel strain gauges, a Dremel rotary tool was used to create a flat and smooth surface on the steel where the gauge was installed (e.g. steel reinforcement). After cleaning the surface, strain gauges were attached by applying a certified two-part adhesive kit for strain gauge use (M-Bond 200 Adhesive Kit). After ensuring a good bond between the steel surface and the strain gauge, a sealant was used to protect the exposed side of the strain gauge. To place external concrete strain gauges and thermocouples, sandpaper was used to remove any roughness on the concrete surface. After cleaning the concrete surface, concrete strain gauges were attached by applying a two-part adhesive compound, Loctite 410 adhesive and Loctite SF 7452 activator.

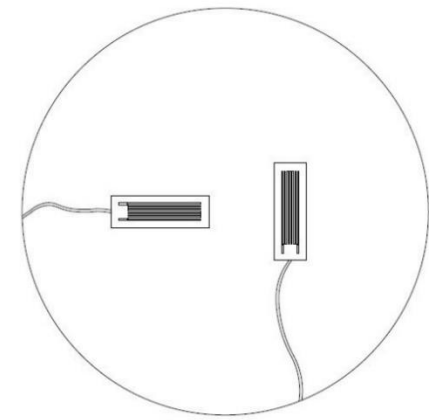
Half of the total sensors (78 strain gauges and 13 thermocouples) were installed on the westbound side of the bridge, and the remaining half on the eastbound side. Figure 33a illustrates the plan view of the strain gauge location layout. Sensors were spaced equidistant from west to east in three different sections (referred to as bays) between diaphragms inside the multi-cell box girders. As shown in Figure 33b, the bridge had straight diaphragms at mid-span and end-span locations as well as skewed diaphragms at the abutments. Therefore, sensors were installed in bay 1 (between the diaphragm at midspan no. 1 and the diaphragm at bent no. 1), in bay 2 (between the diaphragm at bent no. 1 and the first intermediate diaphragm in span no. 2), and in bay 3 (mid-span no. 2, between the two intermediate diaphragms). All sensors were placed above the second or fourth cells (counting from the south side of the bridge) of the multi-cell box girder. The sensors in bay 1 and bay 2 contained strain gauges longitudinally separated at quarter points from diaphragm to diaphragm. The sensors in bay 3 had strain gauges longitudinally separated at sixth points from diaphragm to diaphragm. Additionally, the bay 3 sensors had strain gauges transversely separated at quarter points from cell wall to cell wall of the multi-cell box girder at the center location of the longitudinally spaced gauges. Figure 33c shows the direction of the strain gauges attached to the bridge. At every strain gauge location, two strain gauges were installed, a gauge in the longitudinal direction and a second gauge in the transverse direction.



a)



b)



c)

Figure 33. a) Plan view, b) west end plan view, and c) strain gauge direction layout.

Figure 34a and 34b illustrate the strain gauge layout on the cross-section of the superstructure. As illustrated in Figure 34b, every strain gauge location consists of a three-level strain gauge profile. The external strain gauges were placed at the bottom of the existing deck (inside the box girder cells). Then, embedded strain gauges were installed on the top reinforcement embedded in the HPD. A final set of strain gauges were installed in the UHPC overlay.

In summary, each of the first two bays (Figure 33b) had 18 strain gauges and three thermocouples. Specifically, there are six strain gauges and one thermocouple at each cross-section elevation (box girder cell ceiling, HPD leveling course, and UHPC overlay). The bay 3 sensors included 42 strain gauges and seven thermocouples. Specifically, there are 14 strain gauges and one thermocouple for the box girder and 14 strain gauges and three thermocouples each for the HPD and UHPC layers.



## **4.10. Initial, Early-age, and Longer-term Monitoring Programs**

The monitoring program for the constructed UHPC overlay included initial, early-age, and longer-term monitoring. Initial monitoring included strain and temperature monitoring before UHPC overlay placement during installation of the HPD concrete. Early-age monitoring included assessing overlay bond using non-destructive testing (NDT) methods to identify delaminated locations and using direct tension pull-off tests to measure bond strengths. Strain and temperature monitoring during the first 28 days after placement of the UHPC were also included in the early-age monitoring program. Longer-term monitoring included strain and temperature monitoring after an overlay age of 28 days. Detailed descriptions of the initial, early-age, and longer-term monitoring programs are provided in the following sub-sections.

### ***4.10.1. Initial Monitoring Program***

After the initial deck removal, external sensors inside the multi-cell box girder and embedded sensors in the HPD were installed prior to placing HPD concrete. Using the instrumentation described in Section 4.9, initial strain and temperature data were monitored prior to placement of the UHPC overlay.

### ***4.10.2. Early-age Monitoring Program***

Early-age monitoring included overlay bond assessment, as well as strain and temperature monitoring for the first 28 days after overlay placement. After construction of the UHPC overlay, the overlay-substrate bond was assessed using hammer soundings and chain drags to identify areas that might be delaminated. Additionally, NDT methods were used to perform tests at locations that were identified as possibly being delaminated by hammer soundings and chain drags. Strength of the overlay-substrate bond was then measured using direct tension pull-off tests in both suspect and intact areas of the overlay.

#### ***4.10.2.1. Overlay-Substrate Bond Assessment***

Bond assessment between the substrate concrete and UHPC was conducted after the overlay was cured and grooved. Physical tests, such as hammer sounding and chain drag, were performed to identify potential delamination of the overlaid UHPC. NDT technologies were primarily intended to evaluate the condition between the overlay and concrete bridge deck without causing any damage. Strength of the overlay bond and verification of delaminated areas were evaluated directly by coring and conducting pull-off tests on bridge 7032.

##### ***4.10.2.1.1. Hammer Sounding and Chain Drag***

Physical testing was performed over the entire UHPC overlaid bridge deck to identify potential locations of delamination by conducting hammer soundings and chain drags. The chain drag method involves dragging several chains attached to a handle across a bridge deck. These methods rely on interpretation of the inspector for the tone of the sound caused by metal impacting the concrete surface. Higher pitched tones indicate sound bond between the substrate and the overlay and lower pitched tones indicate potential delamination between the overlay and the substrate.

#### 4.10.2.1.2. Ground Penetrating Radar

The GPR equipment used in this work consisted of a pushcart, SIR 3000 control system, and a 1.5 GHz Model 5100 Antenna (Figure 35) from Geophysical Survey Systems, Inc. (56). This NDT method utilizes a transmitter and receiving antenna. The transmitter sends short electromagnetic pulses (EMP) through concrete bridge decks. EMPs are then reflected at interfaces of materials with different electric properties, such as steel reinforcement and concrete within a bridge deck. GPR imaging devices also detect variation in the composition of the ground material. If the EMPs hit an object, the density of the object reflects and scatters the signal.

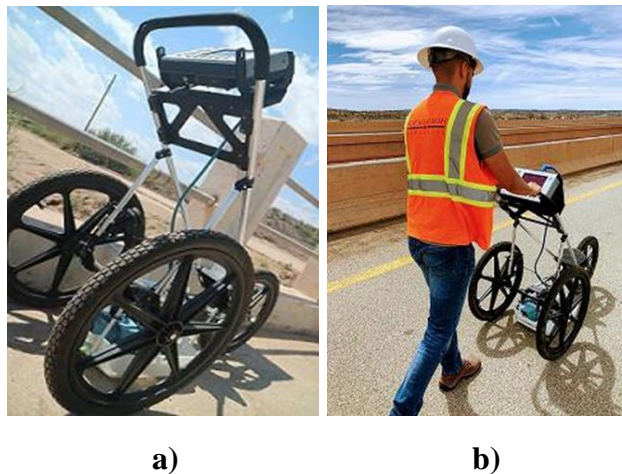


Figure 35. a) GPR system and b) GPR system in use (56).

#### 4.10.2.1.3. Infrared Thermal Imaging

Infrared thermal imaging uses electromagnetic surface radiation to identify internal anomalies. Special infrared cameras are used to produce images of the surface temperature. For instance, the presence of an internal anomaly in a bridge deck (e.g., delamination) will create a disturbance of heat transfer that will affect the surface temperature recorded in the image produced by the infrared camera. This technique becomes less sensitive with increasing anomaly depth. It should be noted that an anomaly can be present near the surface of a concrete deck, but the actual depth of the anomaly would be unknown.

#### 4.10.2.1.4. Direct Tension Pull-Off Testing

After completing physical testing and NDT to detect locations of potential delamination, direct tension pull-off tests were conducted on bridge 7032. Core drilling, pull-off test setup, and pull-off testing were performed as described in Section 4.6.4 with the only difference being the use of a different epoxy. ASF-GEL from E-Chem, a two-component, fast-cure, epoxy acrylate adhesive gel was used to accelerate curing. Table 3 shows the minimum cure times, based on the temperature of the substrate, used when epoxying the steel platens on the core samples. Direct tension pull-off tests were performed after 20-30 minutes of ambient curing as recommended by the technical data sheet. Figure 36 presents the pull-off testing procedure on

the bridge which was to first core saw (Figure 36a), epoxy steel platens to tops of cores (Figure 36b), then perform test as shown in Figure 36c.

**Table 3. ASF-GEL Minimum Cure Time Based on Substrate Temperature.**

Substrate Temperature °F [°C]	Working Time (Minutes)	Cure Time Dry Concrete	Cure Time Damp Concrete
95 [35]	3	20 min	40 min
77 [25]	5	30 min	60 min
59 [15]	9	60 min	2 hr
41 [5]	20	90 min	3 hr
23 [-5]	40	3 hr	6 hr
15 [-9]	50	4 hr	8 hr



**a)**

**b)**



**c)**

**Figure 36. Direct tension pull-off test on bridge 7032 - a) core sawing, b) epoxying of steel platens, and c) test set up.**

#### 4.10.2.2. Strain and Temperature Monitoring

For the first 28 days after construction of the overlay, the instrumentation described in Section 4.9 was used for early-age strain monitoring of the non-proprietary UHPC overlay.

Specifically, embedded strain gauge sensors were used to monitor strain. Other early-age monitoring included internal temperature monitoring of the UHPC overlay with embedded thermocouples.

#### ***4.10.3. Longer-term Monitoring Program***

Longer-term monitoring of the overlay included strain and temperature monitoring from an overlay age of 28 days to December 15, 2021. The longer-term monitoring of the overlay utilized the instrumentation described in Section 4.9 to monitor structural behavior of the overlaid deck. Specifically, the external and embedded strain gauge sensors and thermistors were used to measure the combined thermal and shrinkage movements of the UHPC overlay and the substrate. Coefficient of thermal expansion data collected during the 2017-2018 Tran-SET project is used in the analysis of the thermal movements. Long-term monitoring of the overlaid bridge will continue for two more years as part of a NMDOT research contract.

## 5. FINDINGS

This chapter covers the findings from the implementation of a non-proprietary UHPC overlay on an existing concrete bridge deck. The findings include discussion on mock-up placement direct tension test results, as well as data collection during overlay construction. Initial, early-age, and longer-term monitoring results are also presented in this chapter.

### 5.1. Mock-up Placement Direct Tension Test Results

The mock-up placements were conducted at A1 Quality Ready Mix located in Socorro, NM. These mock-up placements were used to prepare for the UHPC overlay construction on bridge 7032. During these mock-up placements, HPD slabs were overlaid with UHPC for mock-up placement 3 and 4. The integrity of the bond was assessed using direct tension pull-off tests and the results of those tests are presented in the following sub-sections.

#### 5.1.1. Direct Tension Pull-off Test Results for Mock-up Placement 3

Table 4 presents the strengths obtained from the direct tension tests conducted on September 20, 2020 on the mock-up placement 3 slab. As stated previously, a majority of the pull-off strengths were zero because failure occurred during core sawing. The lack of bond is attributed to improper surface preparation of the substrate concrete. The inadequate surface preparation in this region included drying of the substrate surface prior to overlay application and a surface texture that did not remove surface paste to expose the aggregate, which is essential for bonding the UHPC to the substrate concrete.

Table 4. Direct tension pull-off test results for mock-up placement 3.

Specimen	Strength, psi [MPa]	Failure
1	100 [0.7]	Bond
2	462 [3.2]	Bond
3	199 [1.4]	Bond
4	263 [1.8]	Bond
5	254 [1.8]	Bond
6	100 [0.7]	Bond

Although a majority of the strengths were zero, six spots located along the edge of the slab that was overlaid first produced cores that appeared to be reasonably well bonded. As stated in the previous chapter, the HPD slab used in the third mock-up placement was saturated overnight and maintained at a saturated surface condition until application of the UHPC overlay. However, the substrate surface was allowed to dry after the first batch of UHPC overlay material was applied. Direct tension pull-off test results from the six intact core locations are presented in Table 4. The bond strengths presented in Table 4 indicate that there was some bonding between the UHPC and HPD concrete. However, the average bond strengths are not acceptable (less than 250 psi [1.7 MPa]). This can be attributed to the surface texture of the slab not having any aggregate particles exposed.

### 5.1.2. Direct Tension Pull-off Test Results for Mock-up Placement 4

Table 5 presents the direct tension pull-off strengths of five locations on the overlaid slab produced during the fourth mock-up placement. Two core samples had inadequate bond strengths (less than 150 psi [1.0 MPa]) with tensile strengths of 54.3 psi (0.374 MPa) and 72.4 psi (0.499 MPa). Specimens at locations 4 and 5 had adequate direct tensile strengths of 154 psi (1.06 MPa) and 226 psi (1.56 MPa), respectively. However, the average bond strength was 127 psi (0.873 MPa) indicating inadequate bond strength (less than 150 psi [1.0 MPa]) as stated by ACI 546 (2014). These results were considerably lower than the cores tested for the third mock-up placement (230 psi [1.58 MPa] average strength). This can be attributed to improper surface preparation, specifically, the substrate was only maintained saturated for one hour prior to overlay placement. Furthermore, the slab was then lightly sandblasted which introduced localized evaporation of the substrate surface.

Table 5. Direct tension pull-off test results from fourth mock-up placement.

Specimen	Strength, psi [MPa]	Failure
1	54.3 [0.374]	Bond
2 <sup>1</sup>	- <sup>1</sup>	- <sup>1</sup>
3	72.4 [0.499]	Bond
4	154 [1.06]	Bond
5	226 [1.56]	Bond
Avg.	127 [0.873]	Bond

<sup>1</sup> – Core sample was accidentally detached while setting up pull-off tester.

## 5.2. Data Collection During Construction of UHPC Overlay

Data was collected during construction of the UHPC overlay that included weather conditions, substrate surface conditions, construction sequence, and UHPC quality assurance testing.

### 5.2.1. Weather Conditions

The UHPC overlay construction was divided into four production placements (two placements per lane). The first production placement began on April 10, 2021 from the west end of the eastbound lane at around 10:00 pm (60°F [15.6°C] and wind speed of approximately 5 mph [2.24 m/s]) and was stopped the next day at around 12:00 pm (64°F [17.8°C] and wind speed of 0 mph). Production Placement 2 began on April 13, 2021 at around 12:00 am (52°F [11.1°C] and windspeed of 6 mph [2.68 m/s]) and was completed by 5:00 am (42°F [5.6°C] and windspeed of 3 mph [1.34 m/s]).

UHPC placement on the westbound lane began on the east end and was divided into two production placements as well. The third production placement was placed on April 24, 2021 starting from the east end of the bridge at around 2:00 am (52°F [11.1°C] and windspeed of 0 mph) and was paused the same day at around 7:00 am (43°F [6.1°C] and windspeed of 7 mph [3.13 m/s]). The fourth production placement began April 27, 2021 at 9:00 pm (64°F [17.8°C]

and windspeed of 5 mph [2.24 m/s]) and was completed the next morning by 5:00 am (44°F [6.7°C] and windspeed of 0 mph).

### **5.2.2. Substrate Surface Conditions**

The substrate (HPD leveling course) surface had been finished to provide a tined texture. Prior to overlay placement, it was ceramic bead blasted to remove surface paste. This texturing method was able to partially expose fine aggregate as shown in Figure 37a. After the surface was textured, the deck was thoroughly cleaned of any debris and the deck was maintained saturated for 24 hours prior to UHPC overlay placement. The deck appeared moist at installation of the UHPC overlay, as shown in Figure 37b.

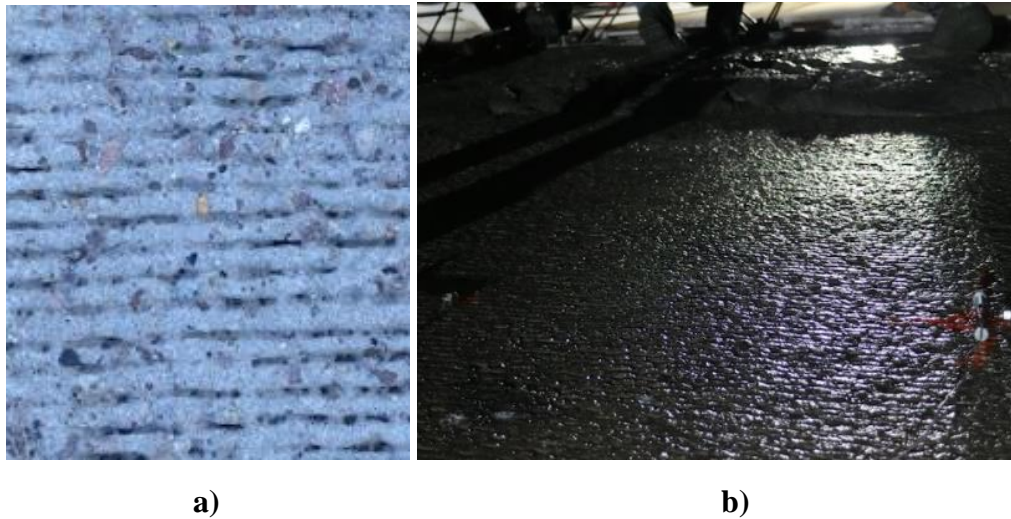


**Figure 37. a) Substrate surface texture and b) substrate surface moisture condition during placement.**

### **5.2.3. Construction Sequence**

This section presents observations related to construction of the UHPC overlay. Specifically, the placement, screeding, and curing practices as well as construction joint practices that were used on this project are described.

#### **5.2.3.1. Placement**

Concrete buggies, shown in Figure 38, with a 16 ft<sup>3</sup> (0.45 m<sup>3</sup>) capacity were used to transport the UHPC from the mixers to the location of placement. Then, construction workers used shovels to spread the UHPC, as shown in Figure 39, in front of a vibrating screed.



**Figure 38. Concrete buggy delivering UHPC.**



**Figure 39. Construction workers spreading UHPC with shovels prior to screeding.**

#### *5.2.3.2. Vibrating and screeding the overlay material.*

The overlay material was consolidated using a combination of concrete vibrating tools. After initial placement, a handheld concrete vibrator was used as shown in Figure 40a. Then, the vibrating screed shown in Figure 40b was used to finish the UHPC overlay and control thickness.



a)



b)

**Figure 40. a) Handheld concrete vibrator and b) vibrating screed.**

#### *5.2.3.3. Curing*

After screeding, curing compound was applied as soon as possible to the finished overlay surface as shown in Figure 41. Then, within only a few minutes after application of the curing compound, the UHPC overlay was covered with plastic sheeting as shown in Figure 42.



**Figure 41. Application of curing compound after screeding.**



**Figure 42. UHPC overlay covered with plastic sheeting.**

#### *5.2.3.4. Construction joints*

When overlay construction was halted, construction joints were installed as shown in Figure 43. These joints were formed in positive moment regions and were formed using blocking (shown in Figure 43) that provided a 90-degree cold joint. The first construction joint was formed on the eastbound lane, 68.42 ft (20.9 m) from the east end of the bridge, and the second was on the westbound lane, 122.17 ft (37.2 m) from the east end of the bridge.



Figure 43. Images of construction joint blocking.

#### 5.2.4. UHPC Temperature and Workability Data

Evaluation of the UHPC produced on site began by measuring the temperature and workability of each UHPC batch. Table 6 presents the temperatures, slump, and spread values from all production placement batches. Temperatures from the production placements are comparable to each other since all four overlay placements were performed at night. As mentioned in Section 4.8.4.4, the acceptable slump range was between 8.5 and 10 in. (215 and 255 mm) and the acceptable spread range was 12 and 19.5 in. (305 and 495 mm). The average slump and spread values for the 105 accepted batches were 9.25 in. (235 mm) and 15.75 in. (405 mm), respectively.

Table 6. Temperature and workability measurements from all batches.

Batch No.	Start Time	Temperature, °F (°C)	Slump, in. (mm)	Spread, in. (mm)	ACCEPT/REJECT
1	11:22 PM	69.6 (20.9)	10.5 (270)	22 (560)	ACCEPT
2	11:45 PM	REJECT	REJECT	REJECT	REJECT
3	12:06 AM	71.9 (22.2)	10 (250)	19.25 (490)	ACCEPT
4	1:01 AM	68.3 (20.2)	9.25 (235)	17.5 (445)	ACCEPT
5	1:22 AM	71.7 (22.1)	9 (230)	15.5 (390)	ACCEPT
6	1:42 AM	72.8 (22.7)	8.5 (220)	15.25 (385)	ACCEPT
7	1:50 AM	67.1 (19.5)	8 (205)	14 (355)	ACCEPT
8	2:07 AM	75.1 (23.9)	8.75 (220)	14.75 (380)	ACCEPT
9	2:16 AM	75.9 (24.4)	8.75 (220)	15 (385)	ACCEPT
10	3:00 AM	76.4 (24.7)	9 (230)	15.5 (395)	ACCEPT
11	3:11 AM	73.4 (23.0)	8.75 (220)	15.25 (385)	ACCEPT
12	3:30 AM	69 (20.6)	9.25 (235)	16.5 (420)	ACCEPT
13	3:46 AM	72.4 (22.4)	9.25 (235)	16.5 (415)	ACCEPT
14	4:00 AM	66.7 (19.3)	9.5 (240)	18 (455)	ACCEPT
15	4:17 AM	64.7 (18.2)	9.25 (235)	16.25 (410)	ACCEPT

16	4:39 AM	65.4 (18.6)	9.5 (240)	17.5 (445)	ACCEPT
17	4:52 AM	71.2 (21.8)	8.5 (215)	13.25 (340)	ACCEPT
18	5:10 AM	69 (20.6)	9.75 (250)	19.25 (490)	ACCEPT
19	5:23 AM	70.8 (21.6)	9.75 (250)	18.75 (475)	ACCEPT
20	5:30 AM	70 (21.1)	9.5 (240)	15 (380)	ACCEPT
21	6:00 AM	71 (21.7)	9 (230)	14.5 (370)	ACCEPT
22	6:26 AM	69 (20.6)	8 (205)	14 (355)	ACCEPT
23	6:40 AM	70.5 (21.4)	9 (230)	15 (380)	ACCEPT
24	6:50 AM	72 (22.2)	10 (255)	15.25 (385)	ACCEPT
25	7:22 AM	71.6 (22.0)	9.5 (240)	17 (430)	ACCEPT
26	7:30 AM	72 (22.2)	10 (255)	15 (380)	ACCEPT
27	7:48 AM	74.9 (23.8)	9.5 (240)	16 (410)	ACCEPT
28	7:55 AM	73.9 (23.3)	9.75 (250)	17.25 (435)	ACCEPT
29	8:16 AM	74.1 (23.4)	9.25 (235)	16.25 (415)	ACCEPT
30	8:36 AM	67.6 (19.8)	10 (255)	17.25 (440)	ACCEPT
31	8:52 AM	REJECT	REJECT	REJECT	REJECT
32	8:20 AM	69 (20.6)	10.25 (260)	17.25 (435)	ACCEPT
33	9:31 AM	70.2 (21.2)	10.5 (270)	17.5 (440)	ACCEPT
34	9:50 AM	72.1 (22.3)	9.25 (235)	16.25 (415)	ACCEPT
35	10:00 AM	75.9 (24.4)	9.5 (240)	15.25 (385)	ACCEPT
36	10:20 AM	76.8 (24.9)	9 (230)	14 (360)	ACCEPT
37	10:30 AM	77.7 (25.4)	8.5 (215)	13.25 (340)	ACCEPT
38	11:00 AM	76 (24.4)	10 (255)	15 (380)	ACCEPT
39	12:00 AM	75.2 (24.0)	9.25 (235)	16.5 (420)	ACCEPT
40	12:14 AM	75.5 (24.2)	9.5 (240)	16.25 (415)	ACCEPT
41	12:25 AM	76.4 (24.7)	9.75 (250)	18 (460)	ACCEPT
42	12:35 AM	77.7 (25.4)	9.5 (240)	17.25 (440)	ACCEPT
43	12:52 AM	77.9 (25.5)	9.5 (240)	16.5 (420)	ACCEPT
44	1:06 AM	77.1 (25.1)	9.75 (250)	17.75 (450)	ACCEPT
45	1:19 AM	80.6 (27.0)	8.5 (215)	14 (360)	ACCEPT
46	1:34 AM	REJECT	REJECT	REJECT	REJECT
47	1:52 AM	73.2 (22.9)	9.5 (240)	17.25 (440)	ACCEPT
48	2:03 AM	76.2 (24.6)	9.5 (240)	17.25 (435)	ACCEPT
49	2:14 AM	74.8 (23.8)	9.5 (240)	15.75 (400)	ACCEPT
50	2:30 AM	75 (23.9)	9.5 (240)	17.25 (435)	ACCEPT
51	2:46 AM	68.4 (20.2)	7.5 (190)	11.75 (295)	ACCEPT
52	2:55 AM	REJECT	REJECT	REJECT	REJECT
53	3:10 AM	75.5 (24.2)	9.25 (235)	15 (380)	ACCEPT
54	3:25 AM	79.7 (26.5)	9.75 (250)	15.75 (400)	ACCEPT

55	3:38 AM	74.1 (23.4)	9.5 (240)	14.75 (380)	ACCEPT
56	3:49 AM	71.4 (21.9)	10.25 (260)	16.75 (430)	ACCEPT
57	4:05 AM	69.9 (21.1)	9.75 (250)	15.75 (400)	ACCEPT
58	2:06 AM	66.2 (19.0)	9.75 (250)	17 (430)	ACCEPT
59	2:18 AM	61.7 (16.5)	9 (230)	15.25 (385)	ACCEPT
60	2:40 AM	66.9 (19.4)	9.5 (240)	17.25 (435)	ACCEPT
61	2:47 AM	64 (17.8)	9.5 (240)	16.25 (410)	ACCEPT
62	3:05 AM	69 (20.6)	9.25 (235)	16.5 (415)	ACCEPT
63	3:15 AM	71.6 (22.0)	8.5 (215)	14.25 (365)	ACCEPT
64	3:27 AM	69 (20.6)	8.5 (215)	13.5 (340)	ACCEPT
65	3:37 AM	69.4 (20.8)	9 (205)	13 (335)	ACCEPT
66	3:51 AM	69.6 (20.9)	8.5 (215)	14.25 (360)	ACCEPT
67	3:58 AM	68.7 (20.4)	9.25 (235)	15 (380)	ACCEPT
68	4:11 AM	67.2 (19.6)	9.5 (240)	16 (405)	ACCEPT
69	4:19 AM	Not Tested	Not Tested	Not Tested	ACCEPT
70	4:29 AM	68.7 (20.4)	9.5 (240)	17 (430)	ACCEPT
71	4:45 AM	65.3 (18.5)	9.5 (240)	16.75 (430)	ACCEPT
72	5:02 AM	67.6 (19.8)	9.5 (240)	15.25 (390)	ACCEPT
73	5:10 AM	64.7 (18.2)	9.5 (240)	16.25 (410)	ACCEPT
74	5:15 AM	66.4 (19.1)	9.5 (240)	16.25 (415)	ACCEPT
75	5:22 AM	65.7 (18.7)	9.75 (250)	16.75 (430)	ACCEPT
76	5:30 AM	Not Tested	Not Tested	Not Tested	ACCEPT
77	8:12 PM	79.5 (26.4)	9.25 (235)	14.5 (370)	ACCEPT
78	8:16 PM	74.8 (23.8)	9.5 (240)	15.75 (400)	ACCEPT
79	8:26 PM	74.1 (23.4)	9 (230)	14.75 (375)	ACCEPT
80	8:42 PM	76.1 (24.5)	9.5 (240)	16.5 (420)	ACCEPT
81	8:50 PM	77.7 (25.4)	9.25 (235)	15 (380)	ACCEPT
82	8:59 PM	77.7 (25.4)	9 (230)	15.25 (385)	ACCEPT
83	9:10 PM	77.7 (25.4)	9.5 (240)	16.25 (410)	ACCEPT
84	9:17 PM	75.7 (24.3)	9.25 (235)	15 (380)	ACCEPT
85	9:30 PM	77.9 (25.5)	9 (230)	14.75 (375)	ACCEPT
86	12:56 AM	69.2 (20.7)	9.25 (235)	15.5 (395)	ACCEPT
87	1:08 AM	69.9 (21.1)	9 (230)	14.25 (360)	ACCEPT
88	1:14 AM	71 (21.7)	9.5 (240)	15 (380)	ACCEPT
89	1:22 AM	70.1 (21.2)	9.5 (240)	16.5 (420)	ACCEPT
90	1:31 AM	72.6 (22.6)	9 (230)	14.75 (375)	ACCEPT
91	1:40 AM	75.5 (24.2)	9 (230)	14.75 (380)	ACCEPT
92	1:49 AM	Not Tested	Not Tested	Not Tested	ACCEPT
93	1:58 AM	71.9 (22.2)	9.5 (240)	16.75 (430)	ACCEPT

94	2:08 AM	Not Tested	Not Tested	Not Tested	ACCEPT
95	2:20 AM	Not Tested	Not Tested	Not Tested	ACCEPT
96	2:32 AM	71.7 (22.1)	9 (230)	14.75 (375)	ACCEPT
97	2:40 AM	Not Tested	Not Tested	Not Tested	ACCEPT
98	2:51 AM	Not Tested	Not Tested	Not Tested	ACCEPT
99	2:58 AM	71.5 (21.9)	9.5 (240)	17 (430)	ACCEPT
100	3:08 AM	75.2 (24.0)	9.75 (250)	17.5 (440)	ACCEPT
101	3:10 AM	Not Tested	Not Tested	Not Tested	ACCEPT
102	3:26 AM	75.2 (24.0)	9 (230)	15 (380)	ACCEPT
103	3:37 AM	69.4 (20.8)	9.25 (235)	17 (435)	ACCEPT
104	3:46 AM	Not Tested	Not Tested	Not Tested	ACCEPT
105	3:55 AM	Not Tested	Not Tested	Not Tested	ACCEPT
106	4:04 AM	69.6 (20.9)	9.25 (235)	15 (385)	ACCEPT
107	4:15 AM	72.6 (22.6)	8.25 (210)	13.5 (340)	ACCEPT
108	4:27 AM	Not Tested	Not Tested	Not Tested	ACCEPT
109	4:40 AM	Not Tested	Not Tested	Not Tested	ACCEPT
110	4:58 AM	Not Placed	Not Placed	Not Placed	Not Placed

### 5.2.5. UHPC Strength Data

Average compressive and flexural strength results from the production placements are presented in Table 7. Cube and prism specimens were cast after workability testing was performed and were placed in a shaded area (under ambient field conditions) and covered with plastic until the production placement concluded. After completing a production placement, the specimens were kept covered with plastic sheeting and cured under ambient field conditions for a minimum of 24 hours. Approximately 24 hours after casting, the specimens were transported two hours to the testing laboratory where they were de-molded and laboratory curing was initiated. Cube specimens tested at two, four, and seven days were cured under ambient laboratory conditions (20 °C [68 °F] and 30% relative humidity), and the remaining samples tested at 14, 28, and 56 days were cured inside a moist room (73°F [23°C] and 98% relative humidity). Prismatic specimens for flexural strength testing were cured in a moist room (73°F [23°C] and 98% relative humidity) for seven days, and then cured at ambient laboratory conditions (20 °C [68 °F] and 30% relative humidity) until they were tested.

**Table 7. Production Placement – compressive and flexural strength results.**

Curing Regimen	Avg. 3.94-in (100-mm) Compressive Strength, psi [MPa]			Curing Regimen	Avg. MOR, psi [MPa]
	2-Day	4-Day	7-Day		
Ambient	8470	10,351 [71.4] ± 540 [± 3.7]	11,380 [78.5] ± 604 [± 4.2]	Wet Room Cured for 7 Days, Then Ambient Until Testing Age	1408
	[58.4]				[9.70]
	± 566 [± 3.9]				± 68 [± 0.47]
Wet Room	11,960	12590 [86.8] ± 919.5 [± 6.3]	13,630 [94.0] ± 929 [± 6.4]		1039
	[82.5]				[7.17]
	± 716 [± 5.7]				± 118.7 [± 0.82]

All production placements had average compressive strengths that exceeded the target compressive strength of 10,000 psi (68.9 MPa) at seven days. However, the target compressive strength of 17,000 psi (117.2 MPa) at 56 days was not met. The average 56-day compressive strength obtained for the production placements was 13,630 psi (94.0 MPa). The low strengths observed for the field samples are attributed to a lack of precise control on the water content of the field batches and lack of tight control on the initial curing temperature of the compression test samples. Specifically, field batches were produced by controlling workability within an acceptable range of slump and spread. Exact water contents of the final batches were not known since the sand was pre-bagged with a moisture content that was not precise for the time at which the bags were filled. Also, field curing was performed at ambient temperature in plastic covered steel molds for the first 24 hours. During this time, the plastic was not always in tight contact with the concrete surface and some evaporation from the samples is believed to have occurred. After the initial 24 hours of curing, field samples were transported to the testing laboratory on the second day.

Flexural strengths were measured at ages of seven and 56 days. The average MOR was 1408 psi (9.7 MPa) at seven days and decreased significantly to 1039 psi (119 MPa) at 56 days. The decrease in MOR between seven and 56 days is attributed to the lack of precise control of the curing environment described previously for the compression test samples and the dry curing that occurred after an age of seven days that might have caused shrinkage at the surface of flexural strength samples (extreme fiber location in flexure) that led to stresses near individual fibers that restrained shrinkage.

### 5.3. Initial Monitoring

Initial monitoring data collection began during placement of the HPD (prior to UHPC placement). Sensors were installed in three layers (on the ceiling of the cells of the multi-cell

box girder, in the HPD leveling course, and in the UHPC overlay that was not installed until after initial monitoring was completed). After the initial deck removal, external sensors in the box girder and embedded sensors in the HPD were installed prior to placing HPD concrete on the westbound lane. Similarly, during the eastbound lane deck removal, external sensors in the box girder and embedded sensors in the HPD were installed before placing HPD concrete on the eastbound lane. After completion of the HPD placement and curing, embedded sensors were placed in the UHPC overlay. Throughout placement of the HPD substrate and UHPC overlay, strain and thermal data were recorded to monitor the behavior of the bridge during construction.

### ***5.3.1. Westbound HPD Placement***

HPD placement started at the east end of the westbound lane on November 30, 2020. Placement began at 9:00 am and was completed at approximately 6:00 pm. Strain (Figure 44 through Figure 54) and thermal data (Figure 55 through Figure 57) were collected during placement. The naming convention for each strain gauge consists of the location of the gauge (C – cell ceiling of box girder, H – HPD, or U - UHPC), lane the gauge was placed in (W - westbound or E - eastbound), bay number (1 to 3 defined in Section 4.9), position within the bay (1 to 5 defined in Section 4.9), and strain gauge orientation (transverse or longitudinal). For instance, CW11T is a concrete strain gauge installed on the cell ceiling of the multi-cell box girder on the westbound lane located in bay 1 at position 1, and oriented transversely. For bay 3 at location 3 there were additional sensors placed north and south of central sensor location. Therefore, the naming convention for sensors in bay 3 at location 3 have an additional letter (N – north or S – south) indicating location of sensor relative to central location in the transverse direction of the bridge. For instance, CW33TN is a concrete strain gauge installed on the cell ceiling of the multi-cell box girder on the westbound lane, located in bay 3, at position 3, oriented transversely, and located north of the central location. The naming convention of each thermocouple consists of the lane (W - westbound or E - eastbound), sensor type (T - thermocouple), bay number (1 to 3), and place of installation (C – cell ceiling of box girder, H – HPD, or U - UHPC). For instance, WT1C is a thermocouple located on the westbound of the first bay, installed on the ceiling of the cell in the box girder.

During initial HPD placement on the westbound lane, five of 26 strain gauges (HW33TN, HW33LN, HW33TS, HW34T, and HW35L) from bay 3 were damaged. As seen in the figures, sensors were monitored for a seven-day period. For the westbound lane, the monitoring period was November 30, 2020 (HPD placement) through December 7, 2020. During this period, temperature and shrinkage effects are perceptible in the strain data. The daily temperature cycle is easily observed in the strain results, and relative strain changes for sensors in the HPD and box girder cells provide the combined effects of HPD shrinkage and thermal effects in both the HPD and original superstructure concrete. Thermocouple measurements (Figure 55 through Figure 57) show that in all three bays, the temperatures inside the HPD fluctuate noticeably during the first six hours since the thermocouples captured the change in temperature from the concrete being placed. Additionally, temperatures in the box girders varied less than the temperature in the HPD since the inside of the girders is not as exposed to

the outside ambient weather. These measurements are being used in a detailed analysis on the bridge behavior as part of an on-going NMDOT research project that continues for another two years.

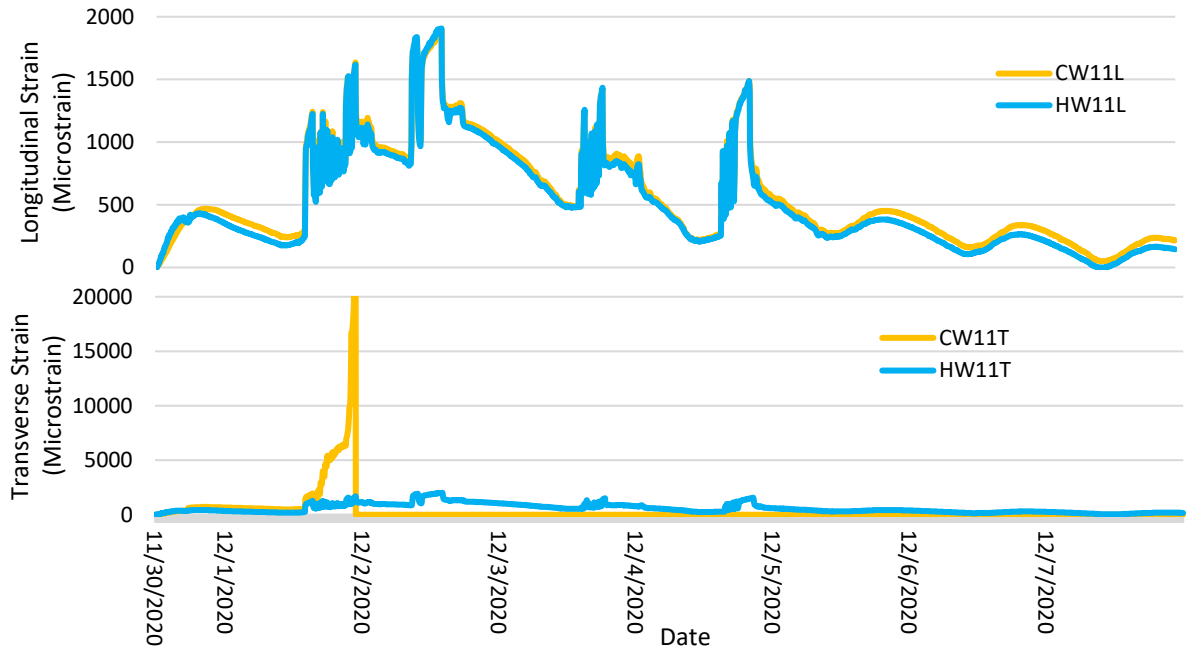


Figure 44. Longitudinal and transverse strain during HPD placement 1 (westbound lane) – bay 1 – position 1.

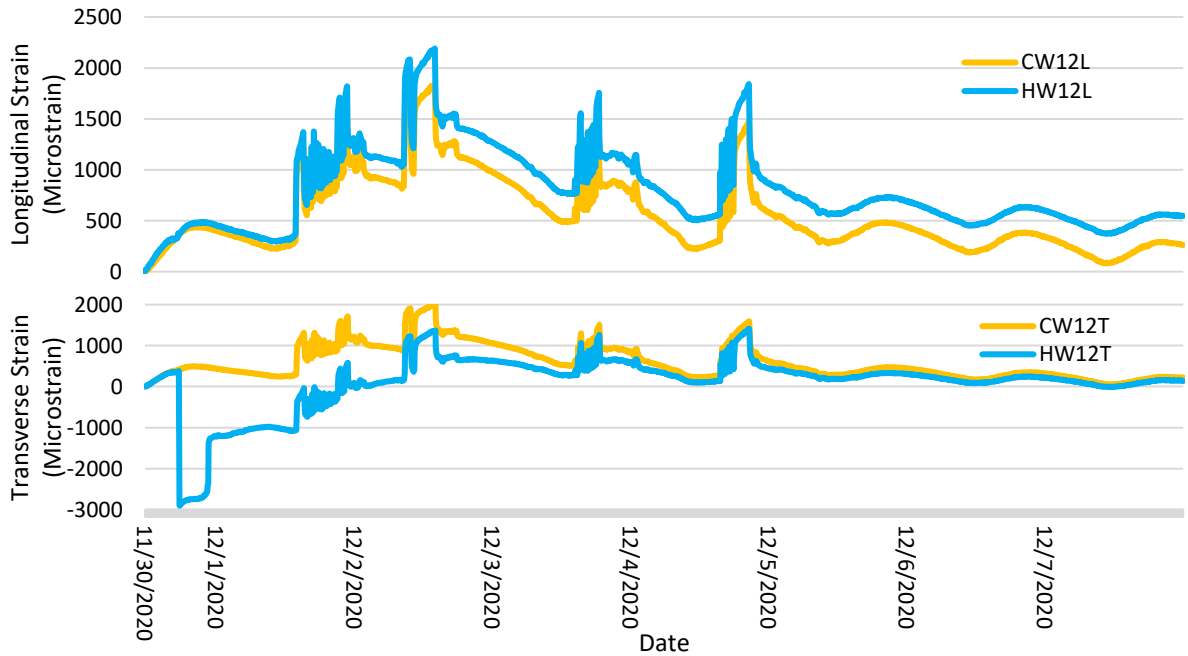


Figure 45. Longitudinal and transverse strain during HPD placement 1 (westbound lane) – bay 1 – position 2.

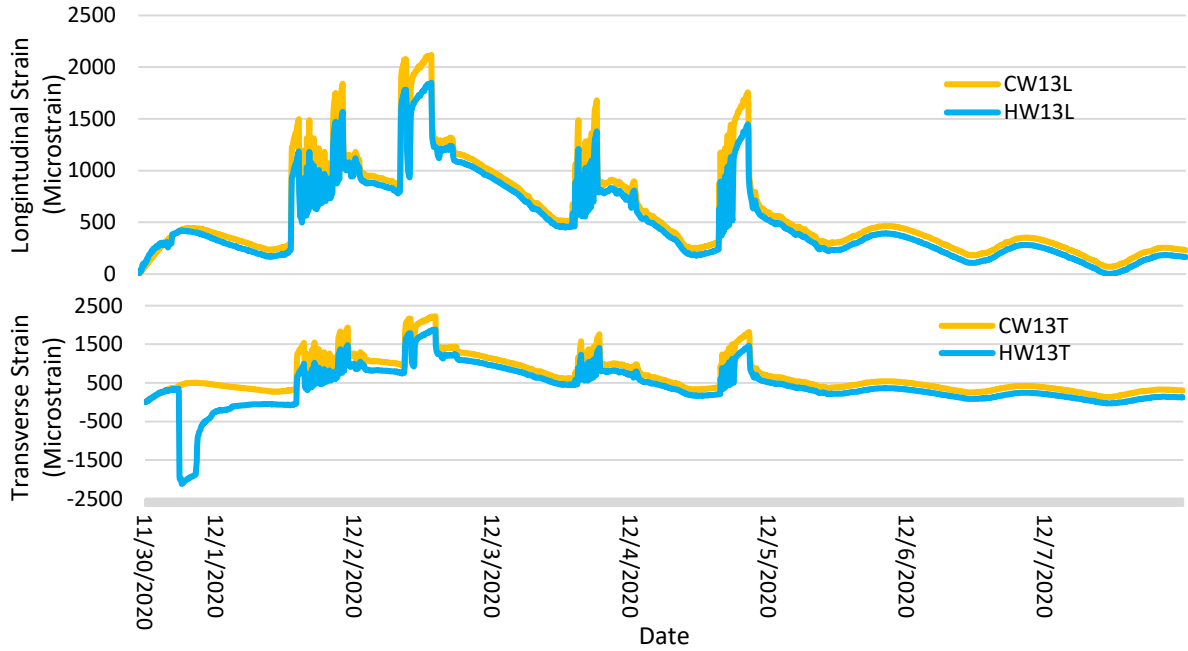


Figure 46. Longitudinal and transverse strain during HPD placement 1 (westbound lane) – bay 1 – position 3.

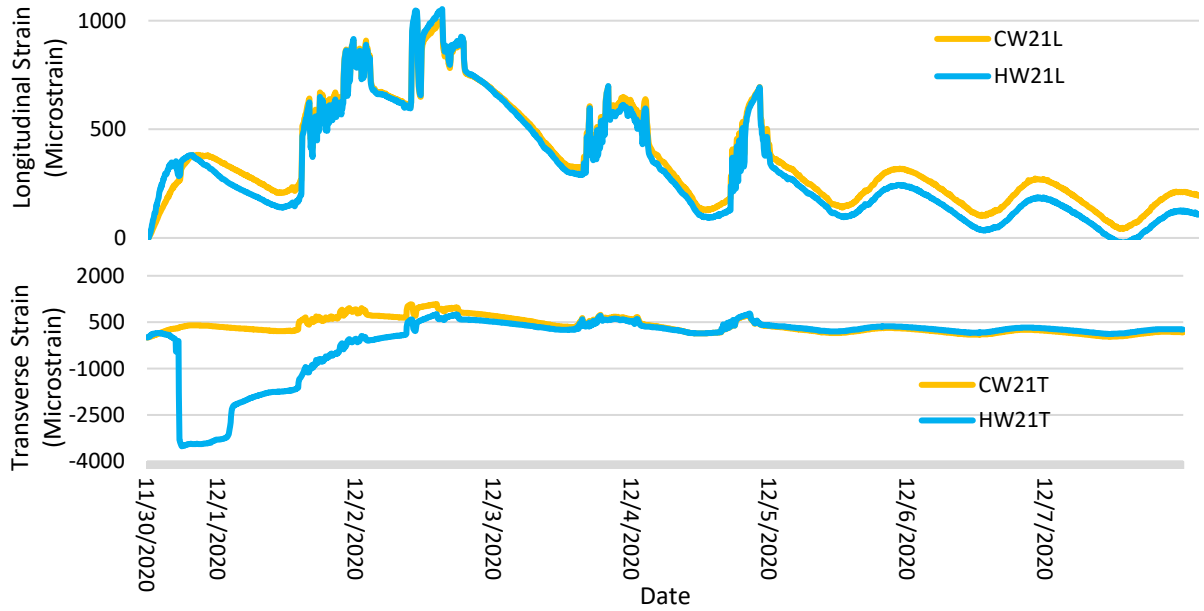


Figure 47. Longitudinal and transverse strain during HPD placement 1 (westbound lane) – bay 2 – position 1.

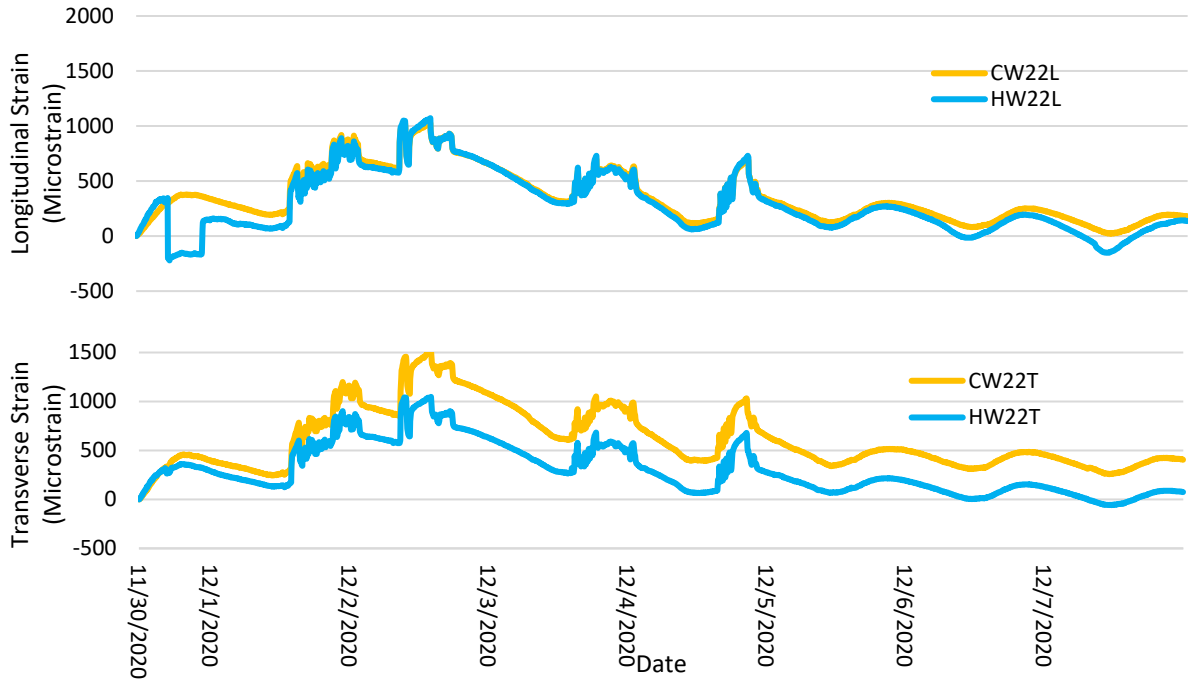


Figure 48. Longitudinal and transverse strain during HPD placement 1 (westbound lane) – bay 2 – position 2.

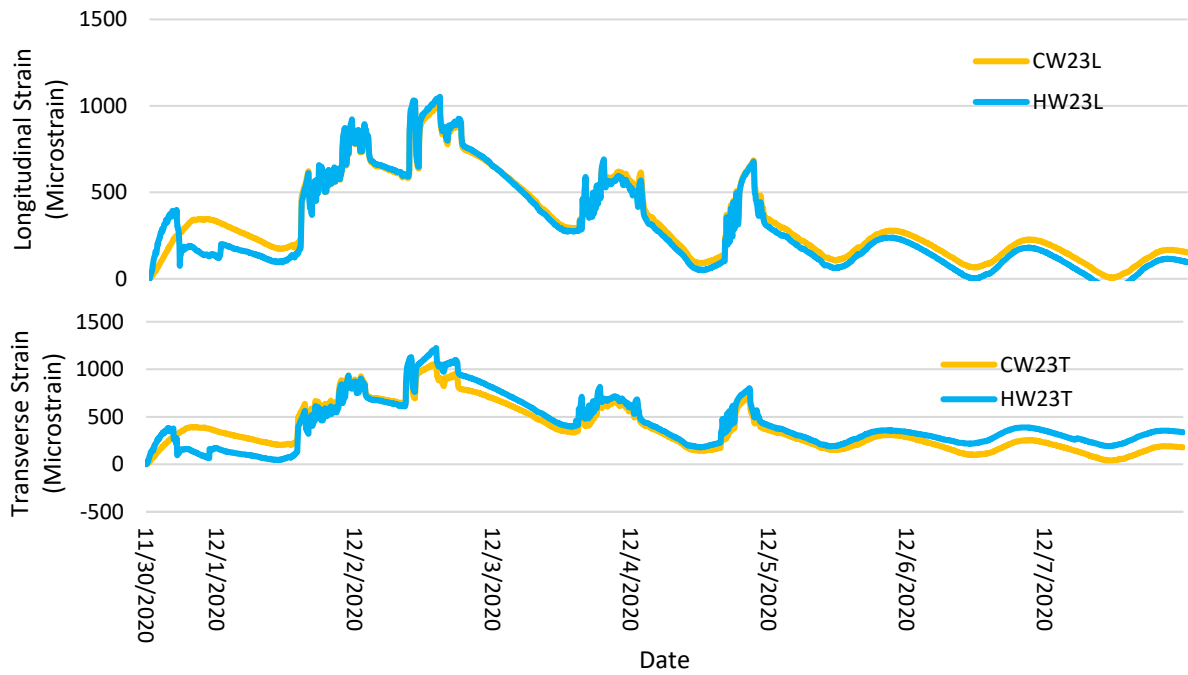


Figure 49. Longitudinal and transverse strain during HPD placement 1 (westbound lane) – bay 2 – position 3.

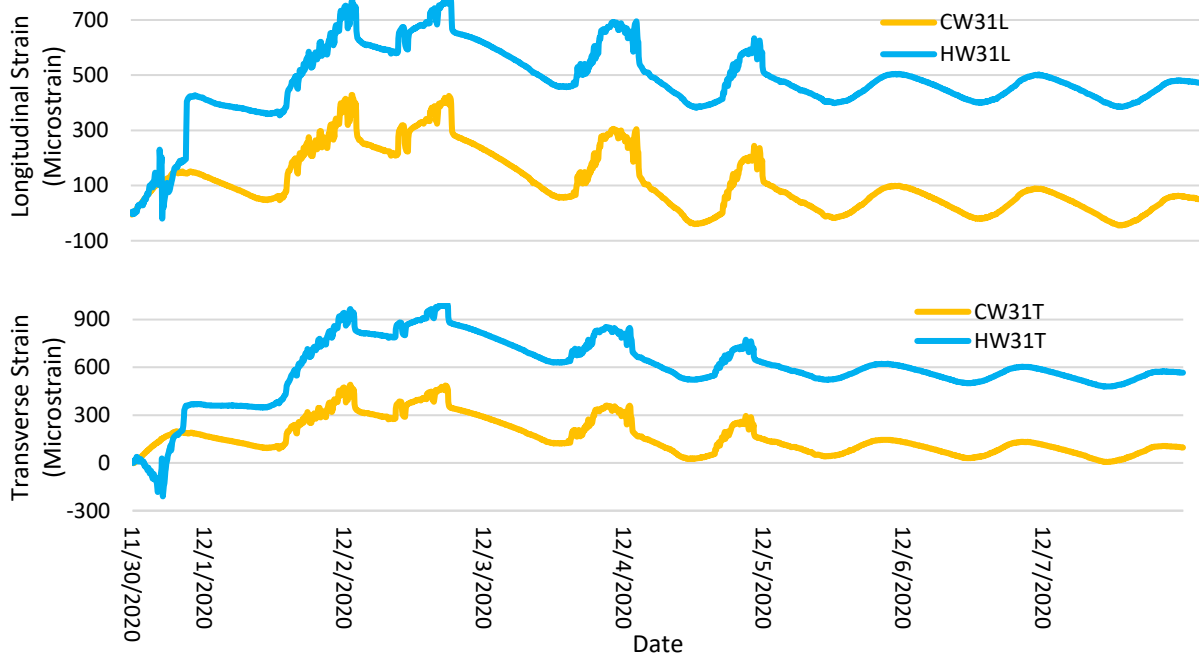


Figure 50. Longitudinal and transverse strain during HPD placement 1 (westbound lane) – bay 3 – position 1.

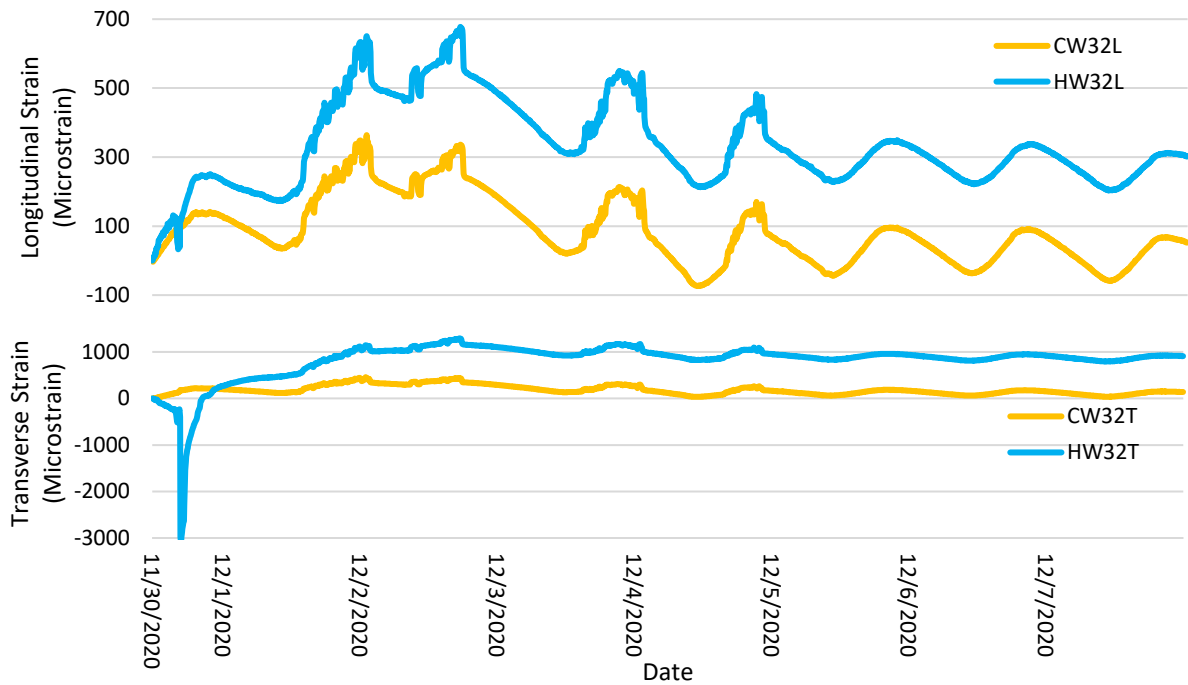


Figure 51. Longitudinal and transverse strain during HPD placement 1 (westbound lane) – bay 3 – position 2.

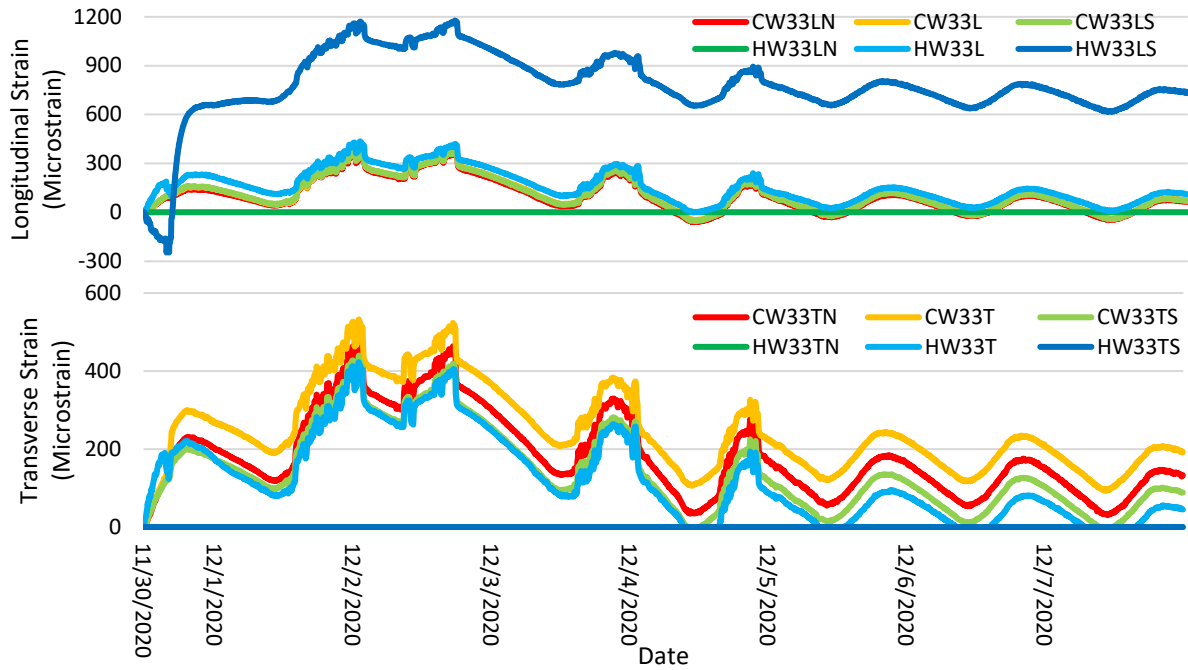


Figure 52. Longitudinal and transverse strain during HPD placement 1 (westbound lane) – bay 3 – position 3.

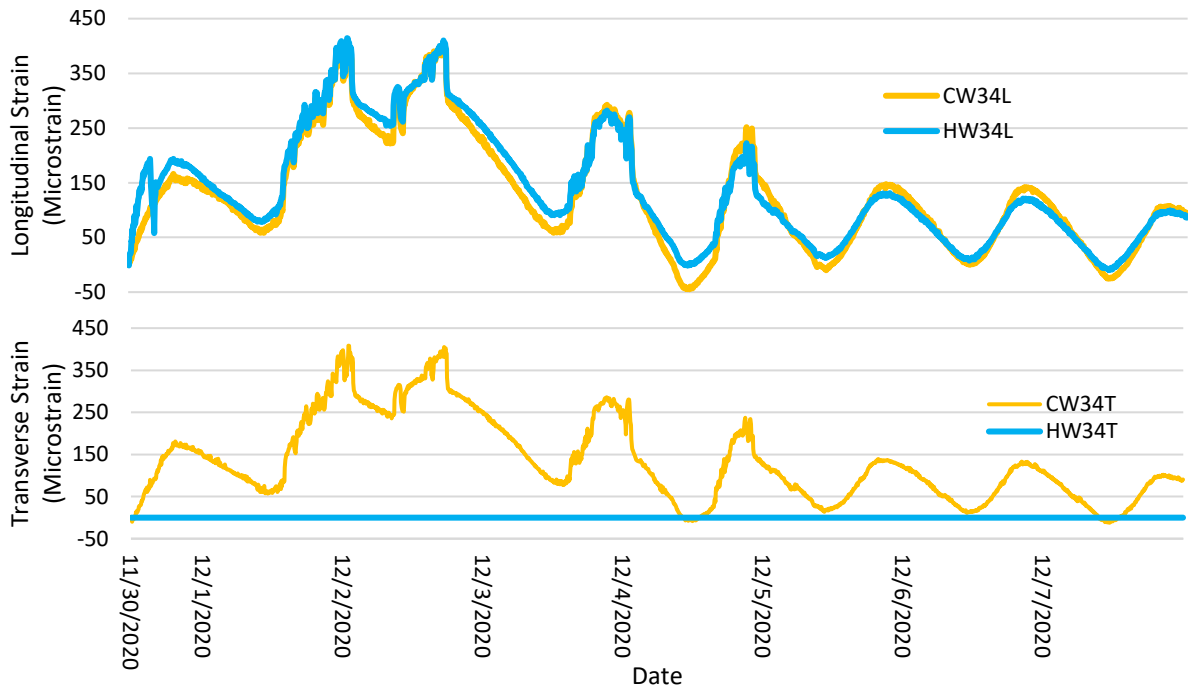


Figure 53. Longitudinal and transverse strain during HPD placement 1 (westbound lane) – bay 3 – position 4.

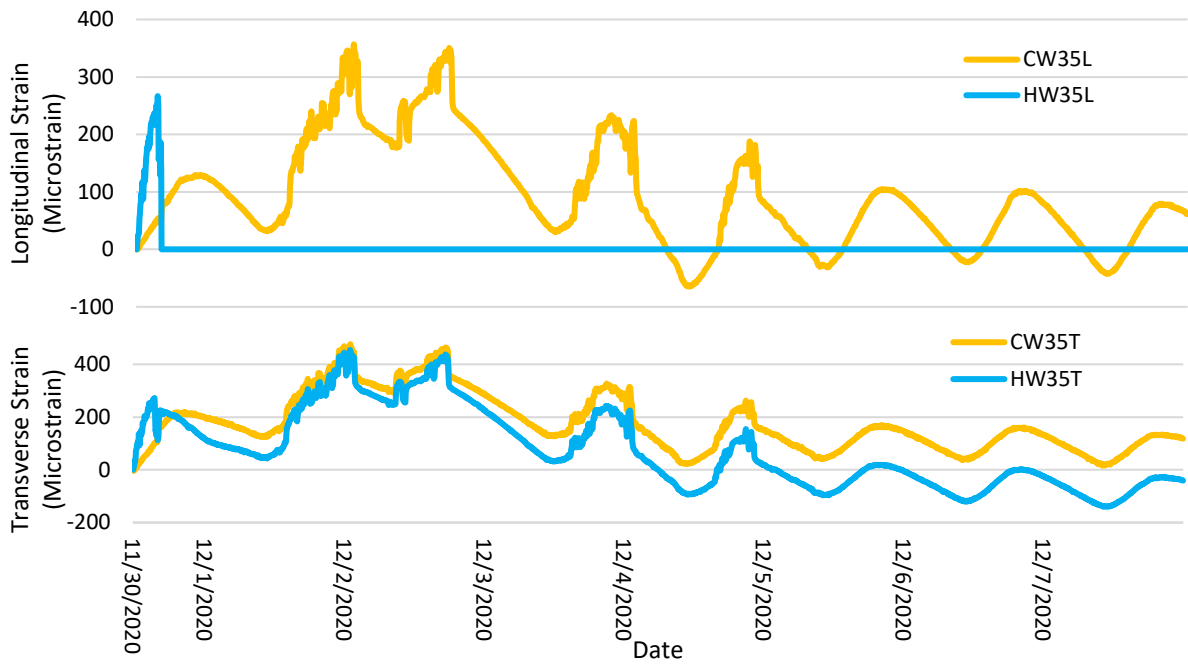


Figure 54. Longitudinal and transverse strain during HPD placement 1 (westbound lane) – bay 3 – position 5.

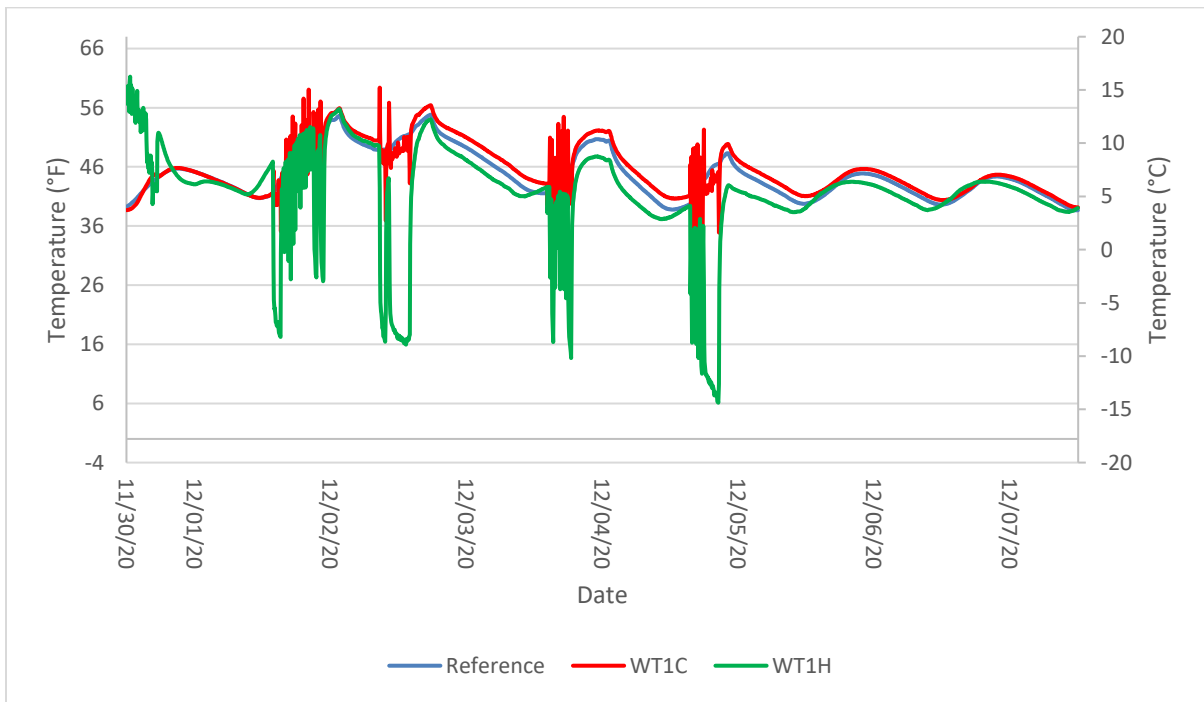


Figure 55. Temperature during HPD placement 1 (westbound lane) – bay 1.

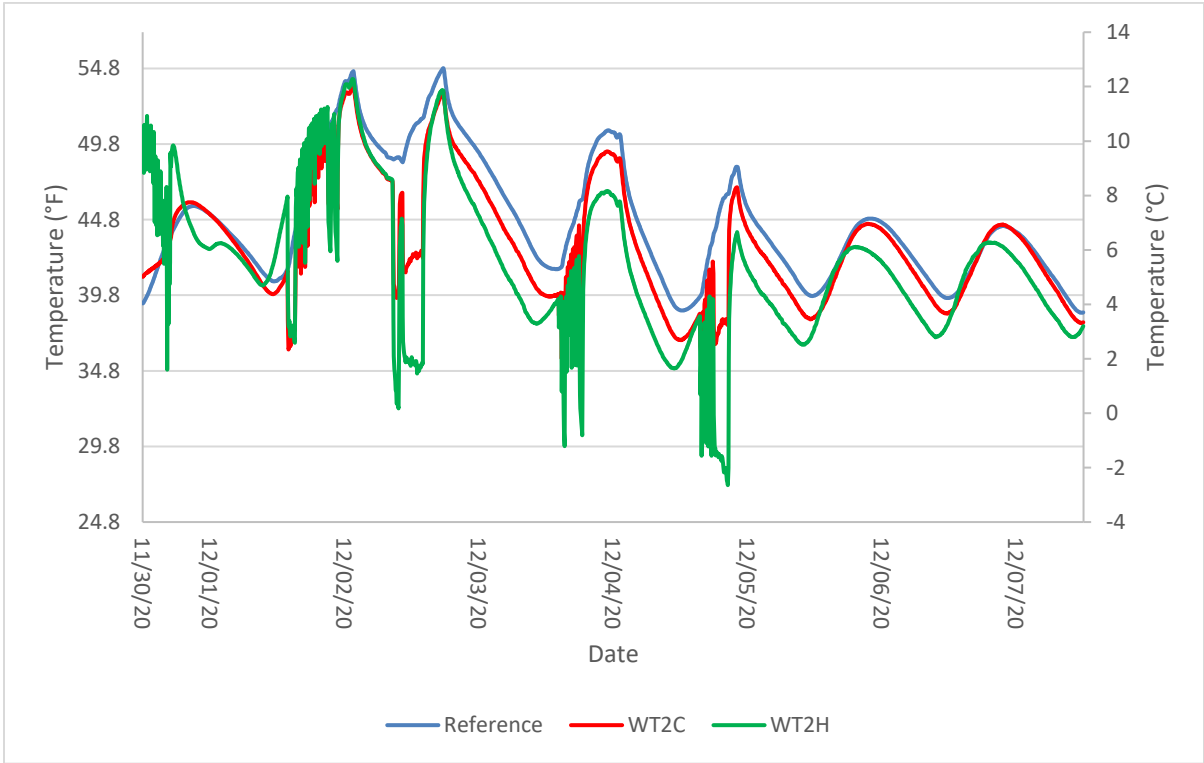


Figure 56. Temperature during HPD placement 1 (westbound lane) – bay 2.

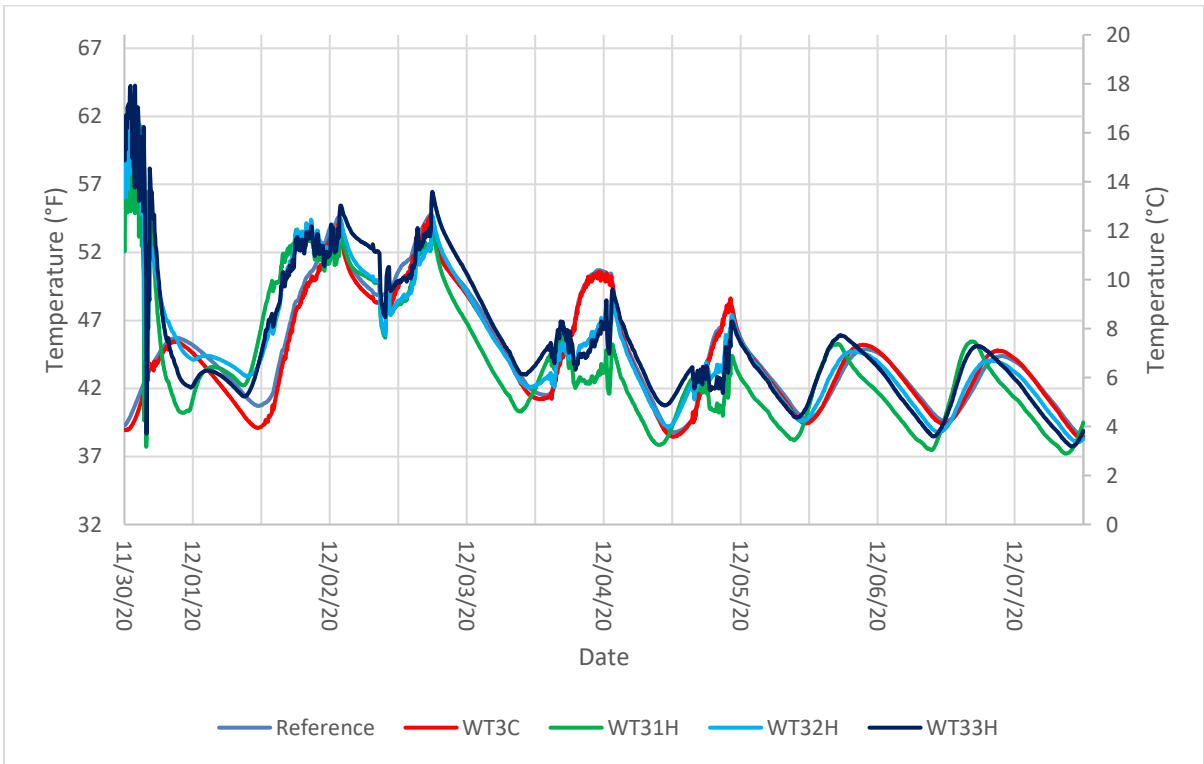
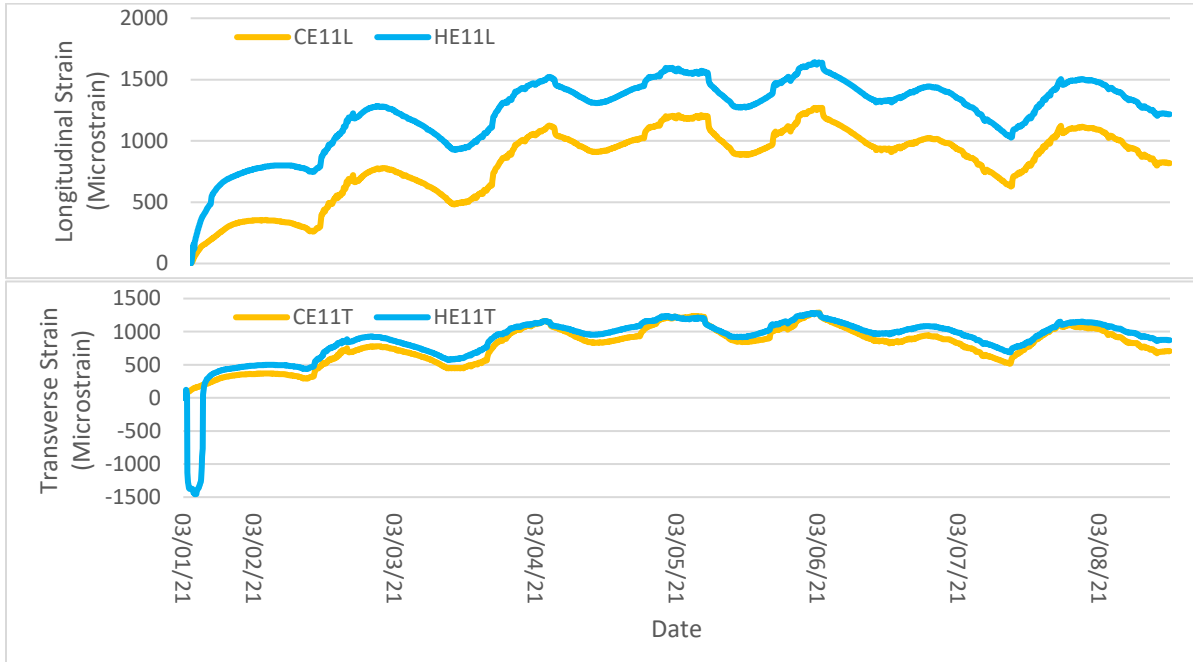


Figure 57. Temperature during HPD placement 1 (westbound lane) – bay 3.

### 5.3.2. Eastbound HPD Placement

HPD placement for the eastbound lane occurred on March 1, 2021. This time, placement started from the west end of the bridge at around 11:00 am and was completed by the evening at around 5:00 pm. Strain (Figure 58 through Figure 68) and thermal data (Figure 69 through Figure 71) were collected during placement.



**Figure 58. Longitudinal and transverse strain during HPD placement 1 (eastbound lane) – bay 1 – position 1.**

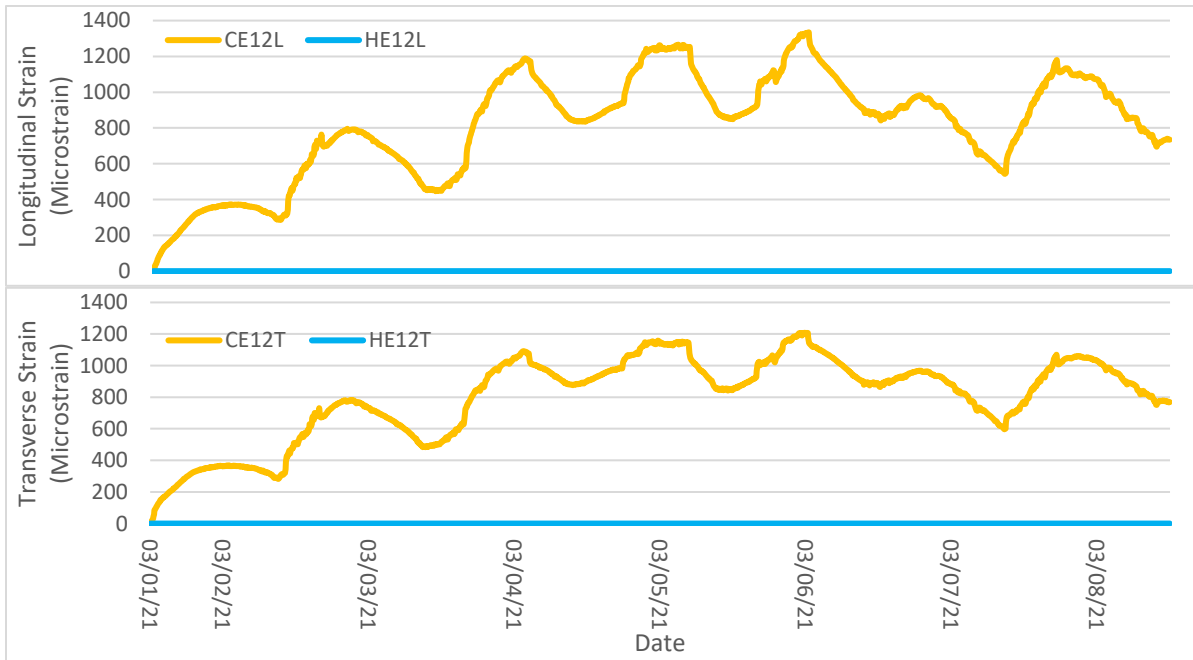


**Figure 59. Longitudinal and transverse strain during HPD placement 1 (eastbound lane) – bay 1 – position 2.**

During HPD placement on the eastbound lane, three of 12 strain gauges (HE12L, HE12T, and HE13T) failed in bay 1. For bay 2, two of 12 strain gauges (HE21T and HE21L) did not record any data as can be seen in Figure 61. Additionally, strain gauges HE23T and HE33LS experienced irregular behavior right after initiation of data collection. Lastly, bay 3 had eight of 28 strain gauges fail (HE31L, HE31T, HE32L, HE32T, HE33TN, HE33LS, HE33TS, and HE35T). As can be seen in Figure 69 through Figure 71, no thermocouples were damaged during HPD placement. The seven-day monitoring period for the initial data collection during HPD placement on the eastbound lane was from March 1, 2021 (HPD placement) through March 8, 2021.

In all three bays, sensors located in the HPD show changes in strain and temperature caused by the eastbound HPD placement. The overall temperatures from eastbound HPD placement were greater than westbound HPD placement because the first placement occurred during a colder weather in December. As with the westbound HPD placement, the daily temperature cycle is easily observed in the strain results, and relative strain changes for sensors in the HPD and box girder cells provide the combined effects of HPD shrinkage and thermal effects in both the HPD and original superstructure concrete. These results are also being used in a detailed analysis on the bridge behavior as part of the NMDOT research project that continues for another two years.

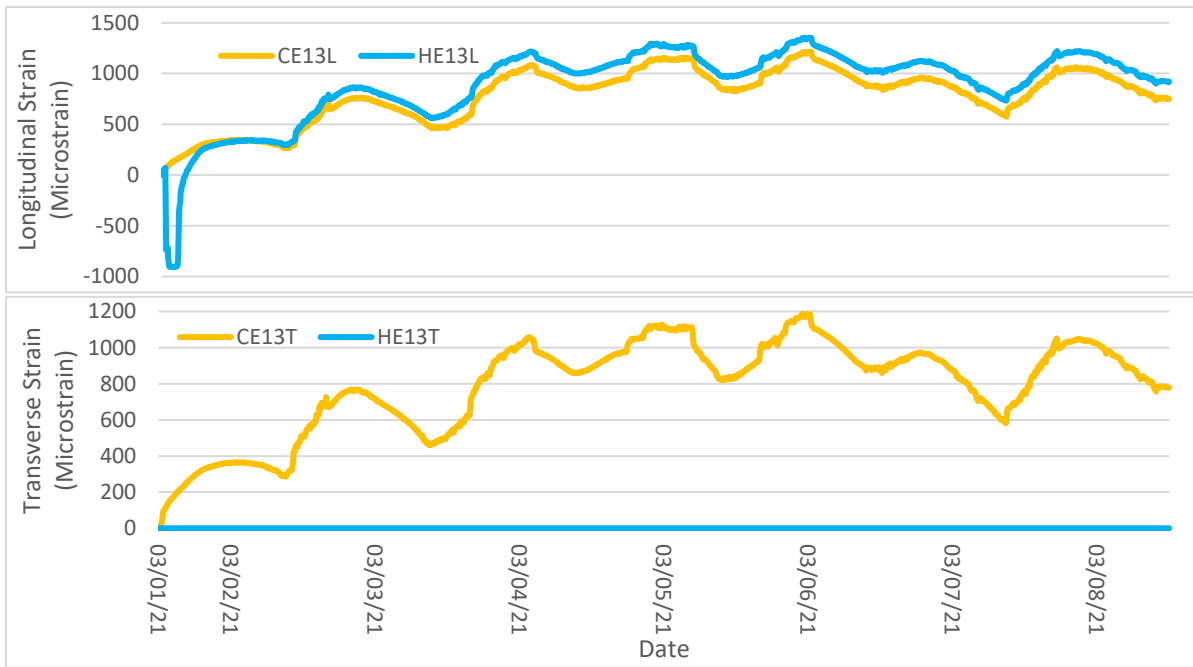


**Figure 60. Longitudinal and transverse strain during HPD placement 1 (eastbound lane) – bay 1 – position 3.**

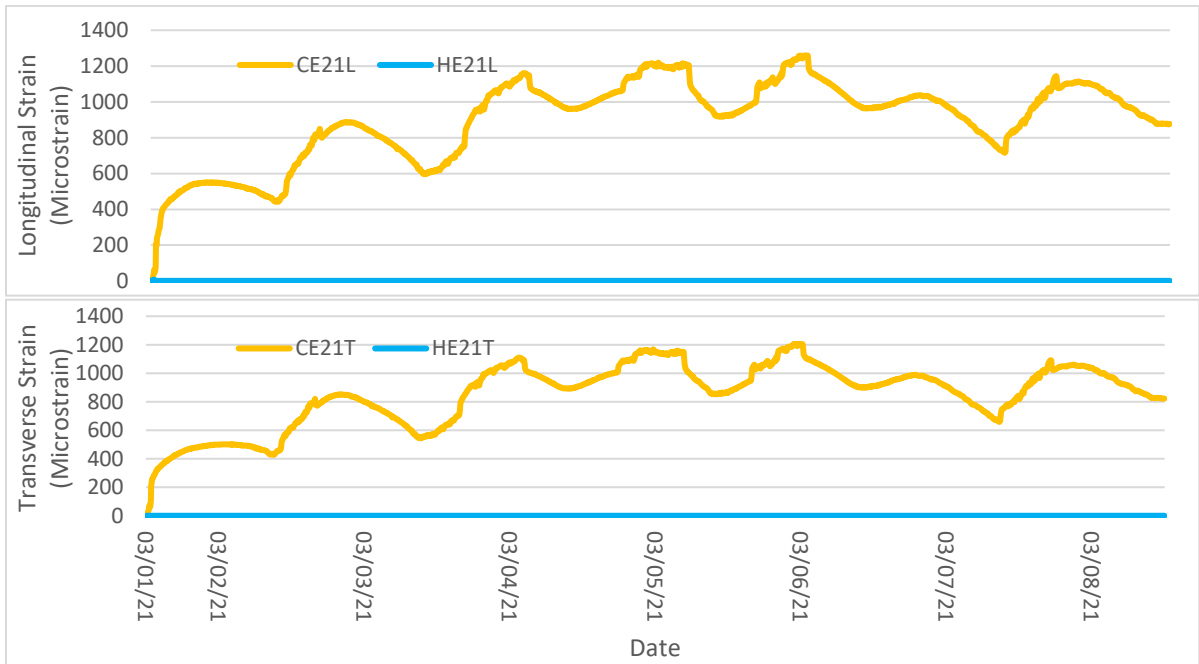


**Figure 61. Longitudinal and transverse strain during HPD placement 1 (eastbound lane) – bay 2 – position 1.**

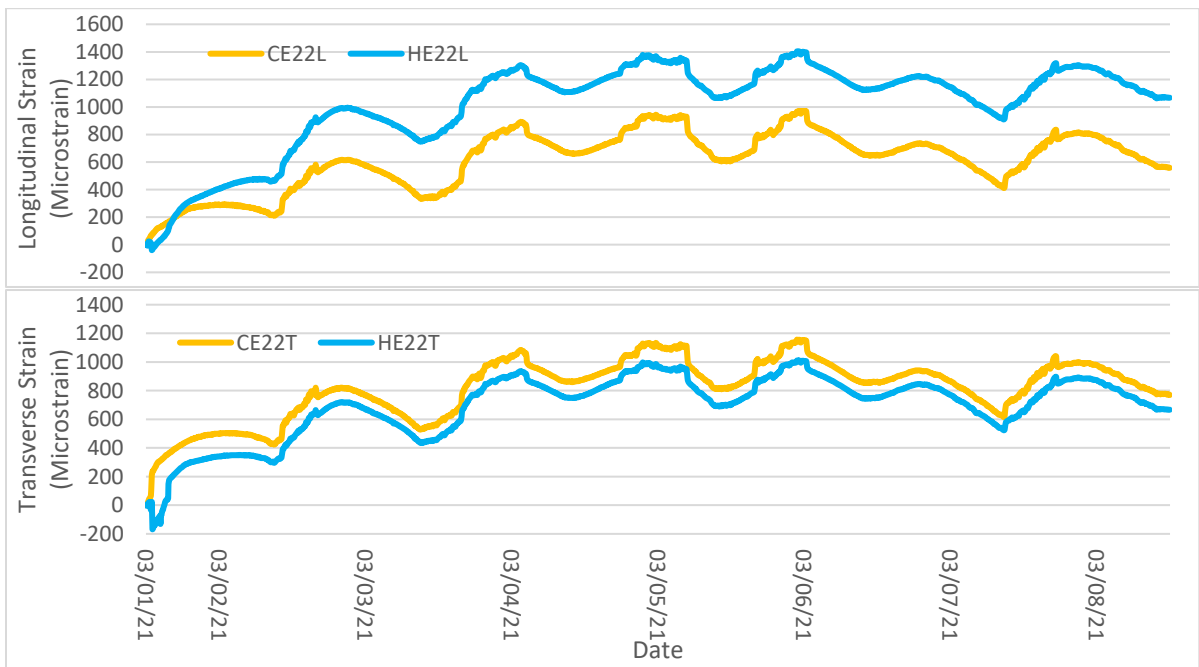


**Figure 62. Longitudinal and transverse strain during HPD placement 1 (eastbound lane) – bay 2 – position 2.**

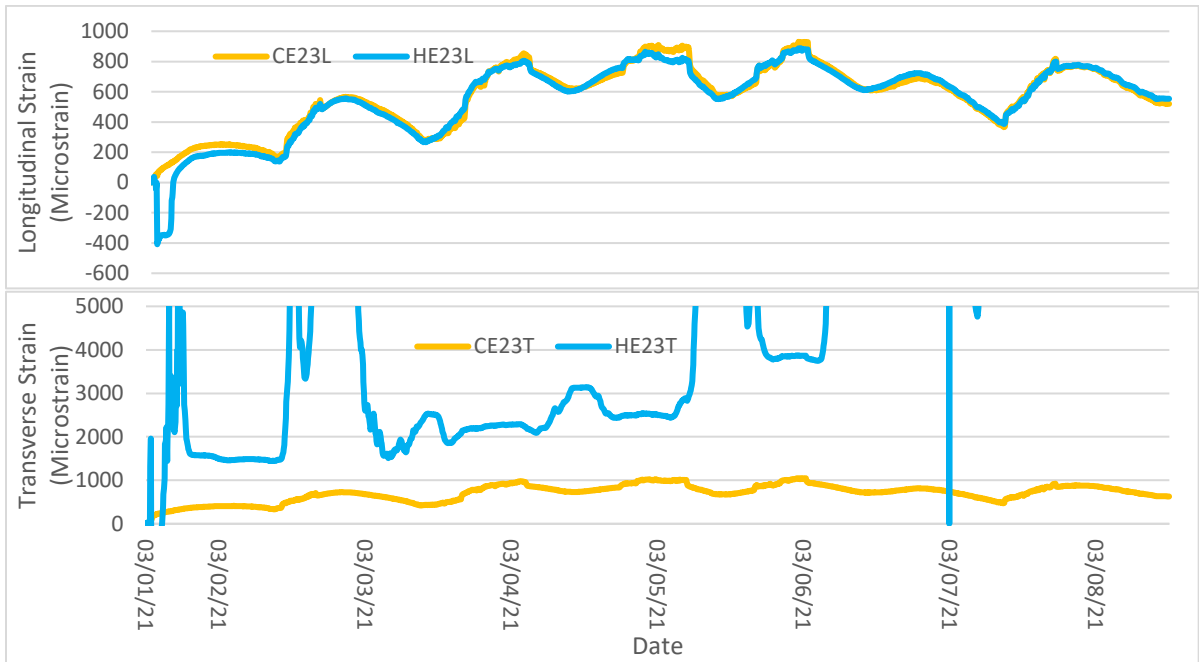


**Figure 63. Longitudinal and transverse strain during HPD placement 1 (eastbound lane) – bay 2 – position 3.**

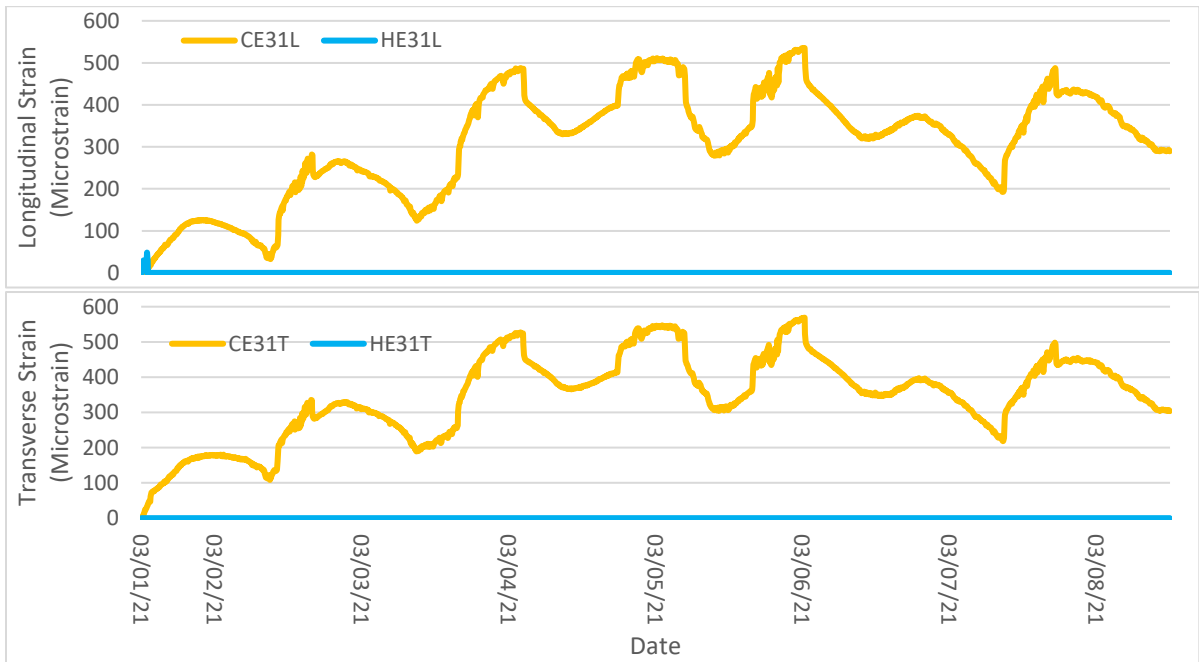


**Figure 64. Longitudinal and transverse strain during HPD placement 1 (eastbound lane) – bay 3 – position 1.**

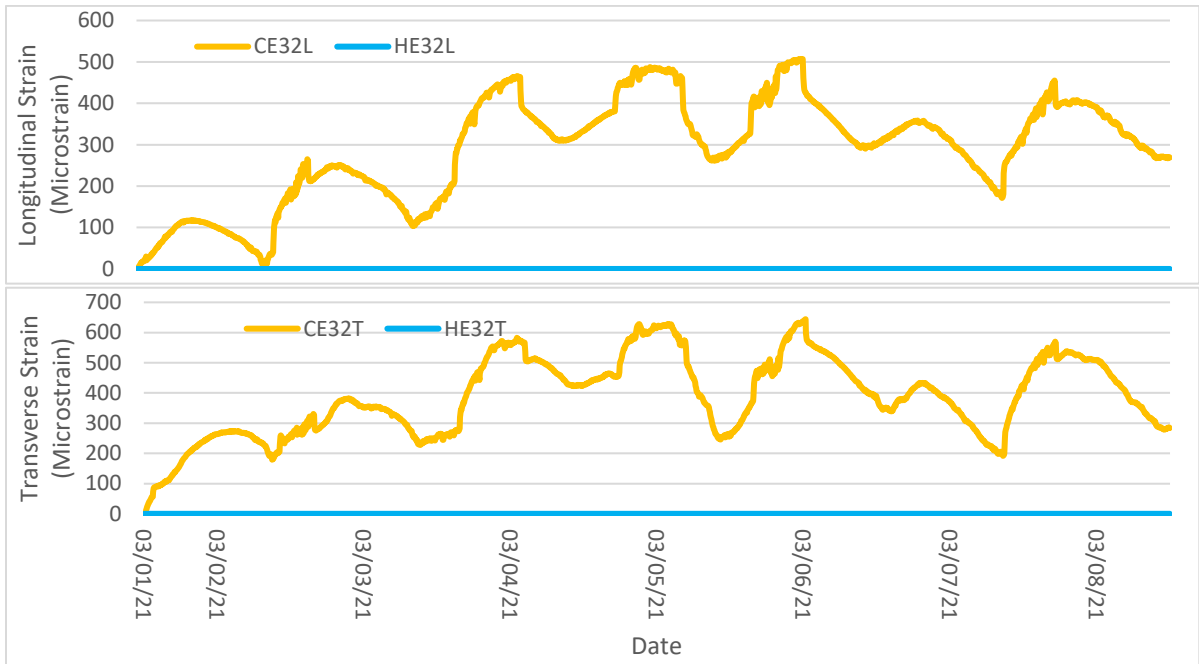


**Figure 65. Longitudinal and transverse strain during HPD placement 1 (eastbound lane) – bay 3 – position 2.**

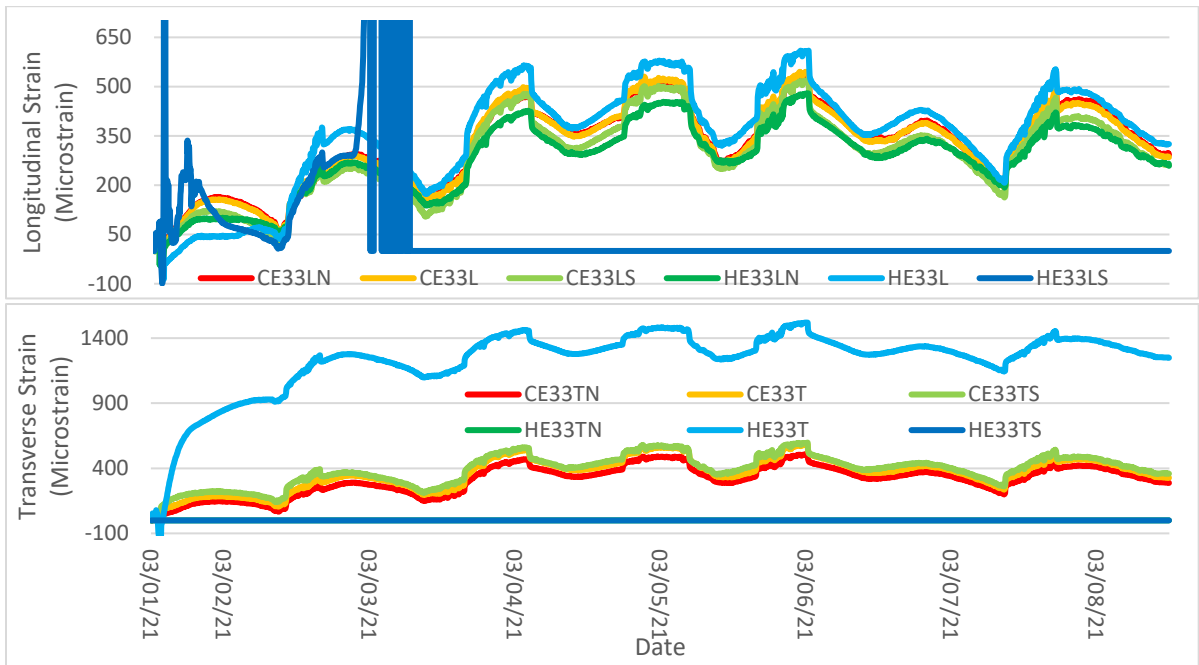


**Figure 66. Longitudinal and transverse strain during HPD placement 1 (eastbound lane) – bay 3 – position 3.**

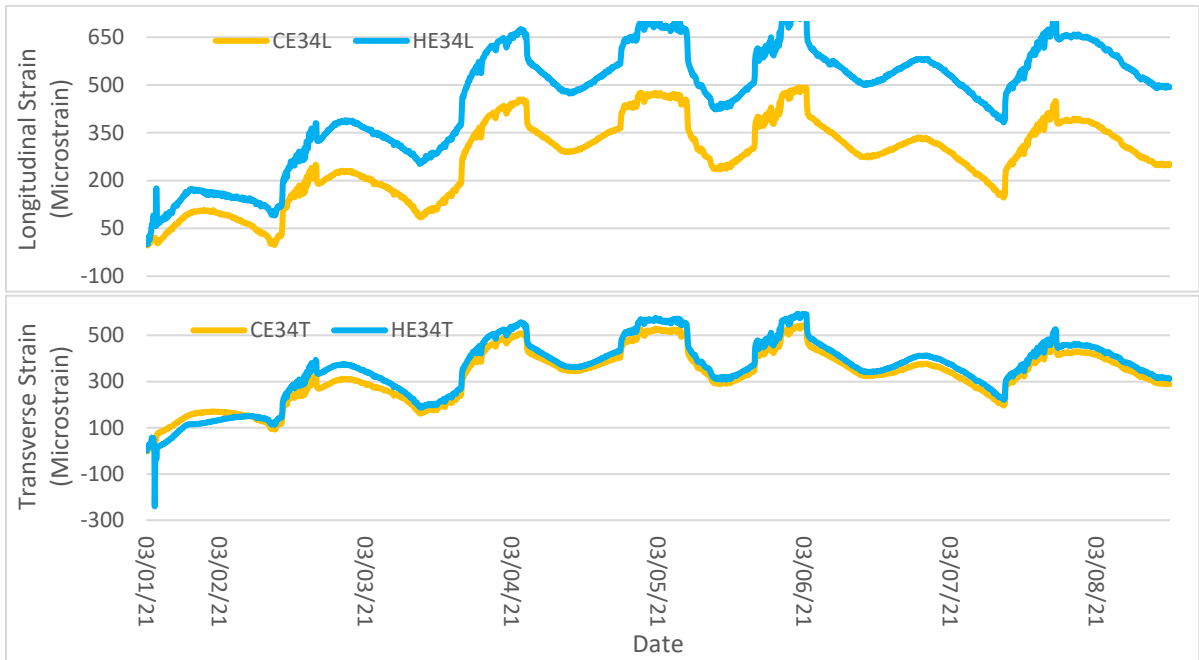


**Figure 67. Longitudinal and transverse strain during HPD placement 1 (eastbound lane) – bay 3 – position 3.**

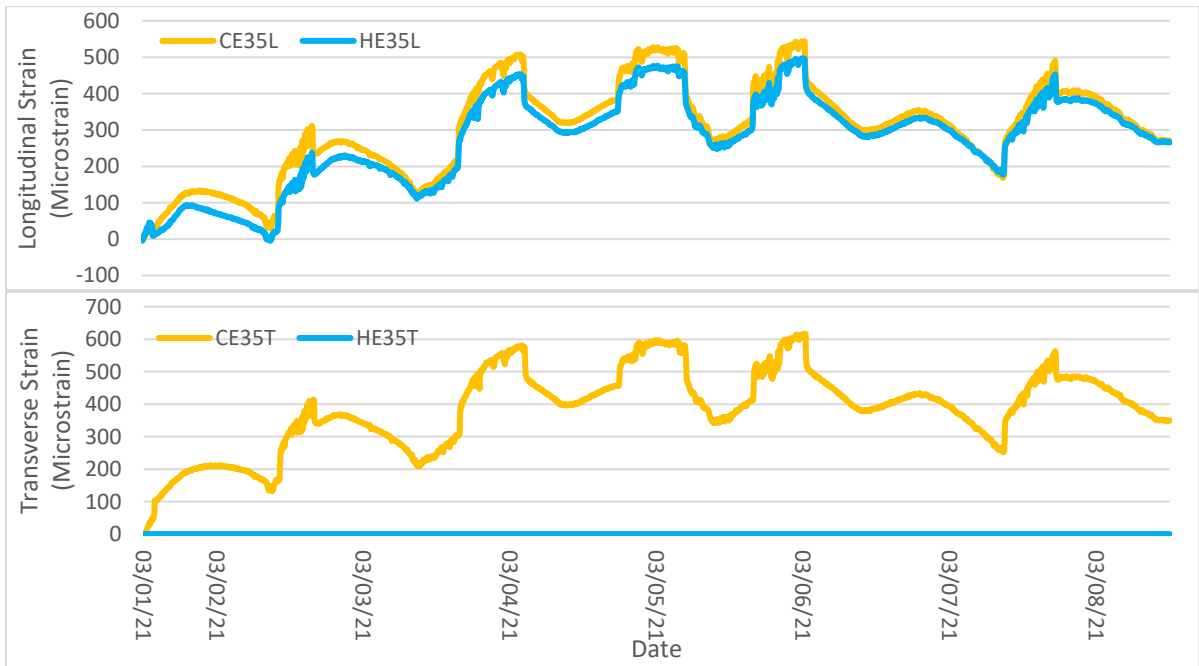


**Figure 68. Longitudinal and transverse strain during HPD placement 1 (eastbound lane) – bay 3 – position 5.**

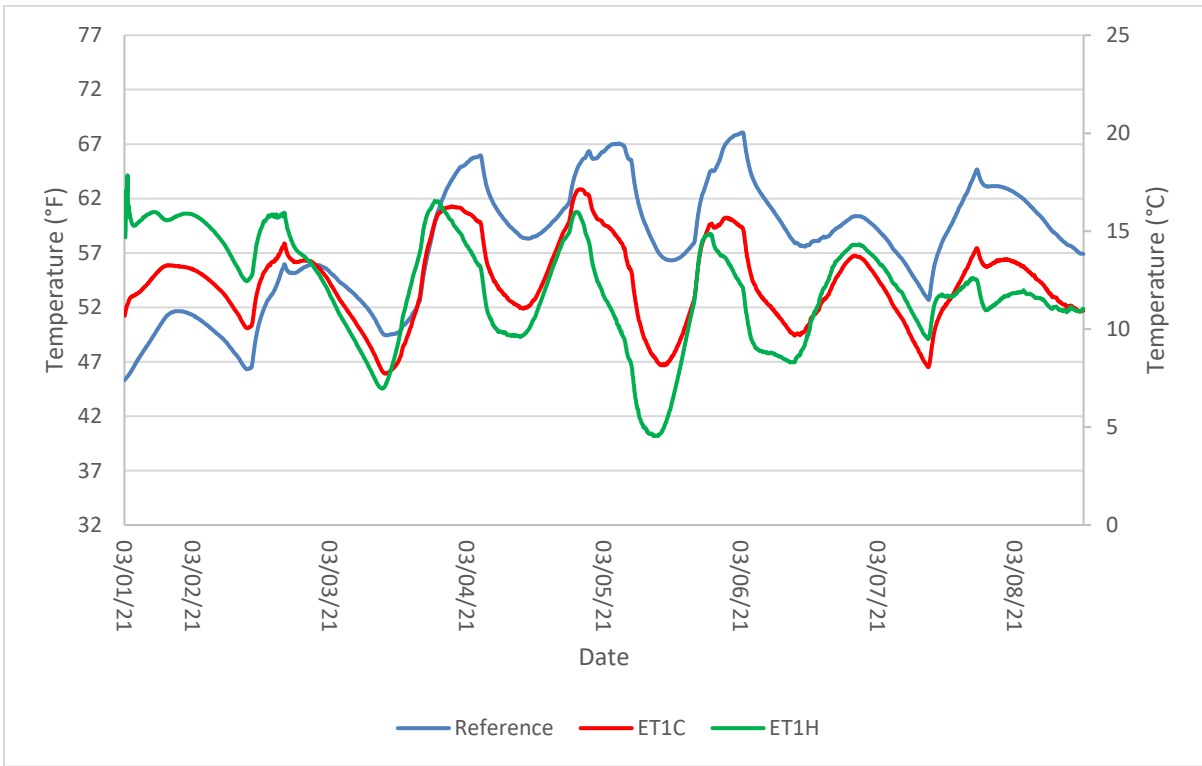


**Figure 69. Temperature during HPD placement 2 (eastbound lane) – Bay 1.**

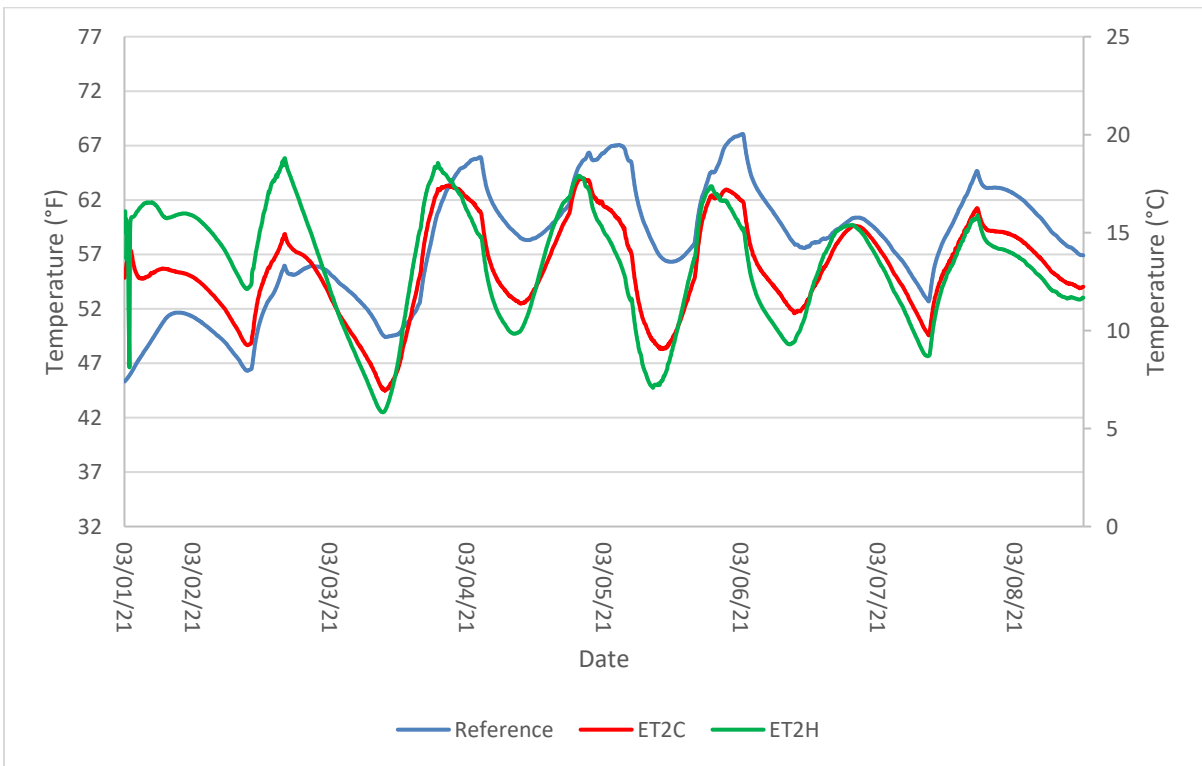


**Figure 70. Temperature during HPD placement 2 (eastbound lane) – bay 2.**

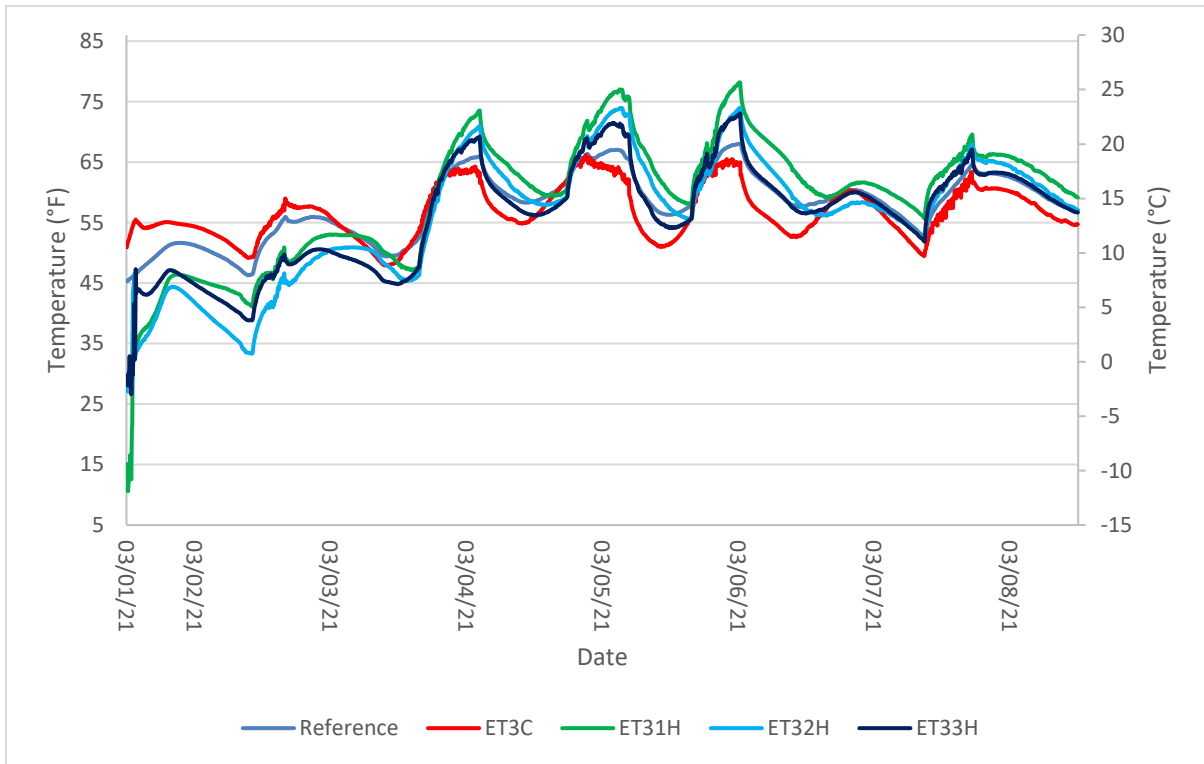


Figure 71. Temperature during HPD placement 2 (eastbound lane) – bay 3.

## 5.4. Early-age Monitoring

Early-age monitoring included overlay bond assessment, strain monitoring, and temperature monitoring. Overlay bond assessment was also considered to be early-age monitoring and included identification of possible delamination areas using hammer sounding and chain drag testing. Areas suspected of being delaminated were investigated using NDT methods (GPR and infrared thermal imaging). Direct tension pull-off tests were also conducted to obtain bond strengths between the UHPC overlay and the substrate concrete. Early-age monitoring also included strain and temperature monitoring from placement of the UHPC overlay to an overlay age of 28 days. The data collected for the early-age monitoring is presented in the following sub-sections.

### 5.4.1. Overlay-substrate Bond Assessment

After construction of the UHPC overlay, the overlay-substrate bond was assessed using hammer soundings and chain drags to identify any potentially delaminated areas. Then, GPR scans and infrared thermal imaging were performed to assess any suspected delamination. Strength of the overlay-substrate bond, as well as verification of bond or delamination, was measured using direct tension pull-off tests in both suspect and intact areas of the overlay.

#### 5.4.1.1. Hammer Sounding and Chain Drag

Figure 72 presents a diagram of the bridge with possible delaminated areas. The assessment started on the westbound lane, with no delamination found. For the eastbound lane, four potentially delaminated areas were identified. The first potential delamination was

approximately 3.5 ft. by 1 ft. (1.1 m. by 0.3 m.) located 85.25 ft. (25.98 m.) from the east end of the bridge, in the area overlaid during Production Placement 1. Two delaminated areas were identified (both approximately 2 ft. by 1 ft. [0.6 m. by 0.3 m.]) at the joint where Production Placement 1 concluded and Production Placement 2 began. The last potential delamination was approximately 2 ft. by 1 ft. (0.6 m. by 0.3 m.) found 82.08 ft. (25.02 m.) from the west end of the bridge, in the area overlaid during Production Placement 2. Pull-off testing was conducted on the potentially delaminated areas as well as at intact locations.

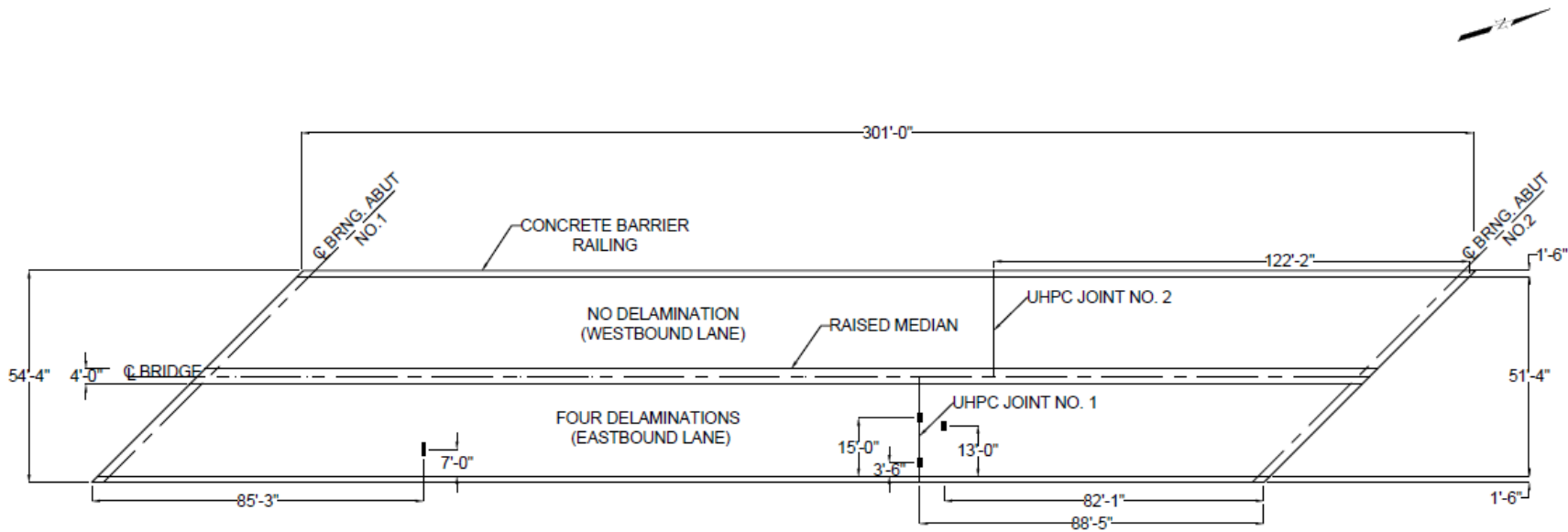


Figure 72. Delaminated areas on bridge after UHPC placement.

#### 5.4.1.2. GPR

Another NDT assessment that was performed to investigate the integrity of the overlay was GPR. The GPR equipment includes a transmitter and a receiving antenna. The transmitter sends short EMP that are reflected at interfaces of materials with different electric properties. Because of the UHPC overlay contains numerous steel fibers, too many reflections were generated for the testing to be able to provide useful results. Consequently, no useful results were obtained from the GPR testing.

#### 5.4.1.3. Infrared Thermal Imaging

To assess potential delamination, a FLIR ONE Pro thermal imaging camera was used to capture images of potentially delaminated areas identified by chain drag and hammer sounding. Figure 73 presents a photograph and color-coded thermal image for the first potential delamination, located 85.25 ft. (25.98 m.) from the west end of the bridge. Lighter color in the thermal image (amber) indicates higher temperature, while darker color (purple) indicates lower temperature. Three spots along the potentially delaminated area were selected as reference points to analyze the temperature change of the delamination and nearby cracking. As seen in the images, cracks near the suspected delamination do not show much temperature change, ranging from 107 °F (41.7 °C) to 109 °F (42.6 °C).

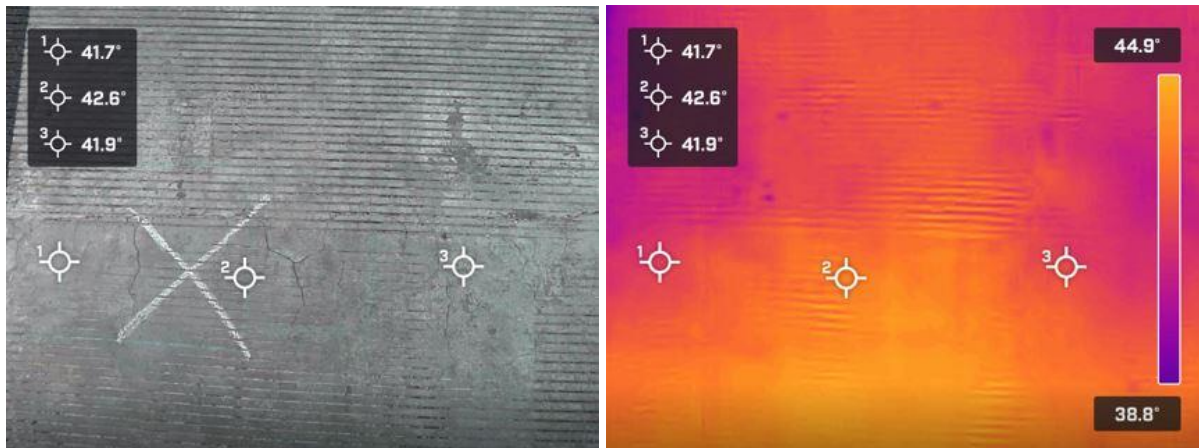


**Figure 73. Photograph and color-coded infrared thermal image at the first potential delamination.**

Figure 74 presents a photograph and a color-coded thermal image for the fourth potentially delaminated area, 82.08 ft. (25.02 m.) away from the east end of the bridge. Again, the high and low temperature points were included to analyze the temperature differential within the suspected delamination. Unlike the first delamination (Figure 73), the fourth potential delamination had a greater temperature range, 103 °F (39.7 °C) to 111 °F (44.1 °C). This large temperature differential provides an indication that the area has a greater probability of being delaminated.

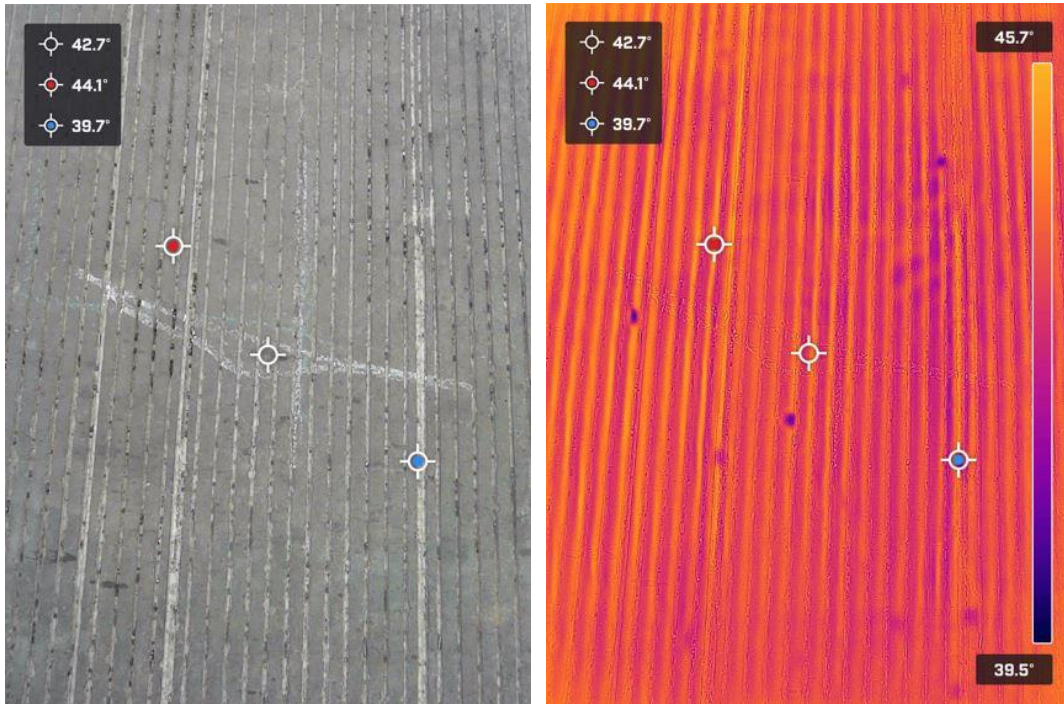


**Figure 74. Infrared thermal imaging on fourth potential delamination.**

#### *5.4.1.4. Direct Tension Pull-off Test Results for UHPC Overlaid Bridge*

Table 8 presents pull-off tensile strengths obtained from 10 locations described in Figure 75. The only zero-strength location was at the fourth suspected delamination. The average bond strength of the nine intact core samples was 239 psi (1.65 MPa), which is slightly less than the recommended tensile bond strength of 250 psi (1.72 MPa) as stated by ACI 546 (2014). However, it should be recognized that four of the tests had failures that occurred at the epoxy, which provides a conservative measurement of the overlay bond strength. Additionally, a low bond strength was obtained for core sample no. 6 that occurred at a location where the concrete substrate surface was not rough, as shown in Figure 76. Figure 77 shows the UHPC/Epoxy type of failure for core samples no. 3, 7, 9, and 10, respectively.

Table 8. Direct tension pull-off test results from bridge 7032.

Core Sample	Delamination	Load, lbs. [kN]	Tensile Strength, psi [MPa]	Failure
Eastbound Lane				
1	On Delam 1	325 [1.45]	118 [0.814]	Bond
2	-	650 [2.89]	235 [1.62]	UHPC/Bond
3	-	550 [2.45]	199 [1.37]	UHPC/Epoxy
4 <sup>1</sup>	On Delam 4 <sup>1</sup>	- <sup>1</sup>	- <sup>1</sup>	- <sup>1</sup>
5	-	400 [1.78]	145 [1.00]	Bond
Westbound Lane				
6	-	200 [0.890]	72.4 [0.499]	Bond
7	-	850 [3.78]	308 [2.12]	UHPC/Epoxy
8	-	875 [3.89]	317 [2.19]	Bond
9	-	1130 [5.03]	407 [2.81]	UHPC/Epoxy
10	-	975 [4.34]	353 [2.43]	UHPC/Epoxy
Avg.		662 [2.94]	239 [1.65]	UHPC

<sup>1</sup> – Core debonded from concrete substrate while drilling (zero-strength location).

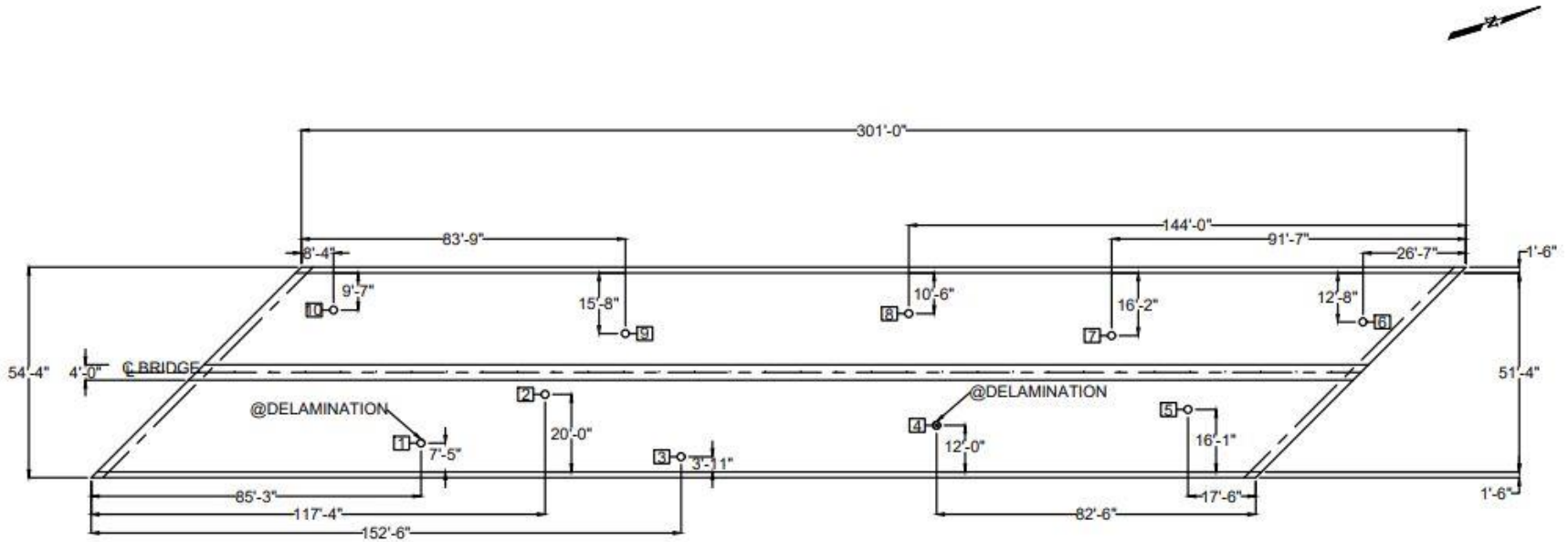


Figure 75. Direct tension pull-off test locations on bridge 7032.



Figure 76. Core sample with substrate that lacks roughness.



Figure 77. UHPC/epoxy failure.

#### ***5.4.2. Eastbound Early-age Monitoring***

The UHPC overlay was divided into four production placements (two placements per lane). Early-age monitoring of the eastbound side includes strain and temperature monitoring data for the first 28 days after placement of the UHPC overlay. The first production placement began on April 10, 2021 from the west end of the eastbound lane at around 10:00 pm and was stopped the next day at around 12:00 pm. The second production placement began on April 13, 2021 at around 12:00 am and was completed by 5:00 am. Strain (Figure 78 through Figure 88) and thermal data (Figure 89 through Figure 91) were collected from UHPC placement to an overlay age of 28 days.

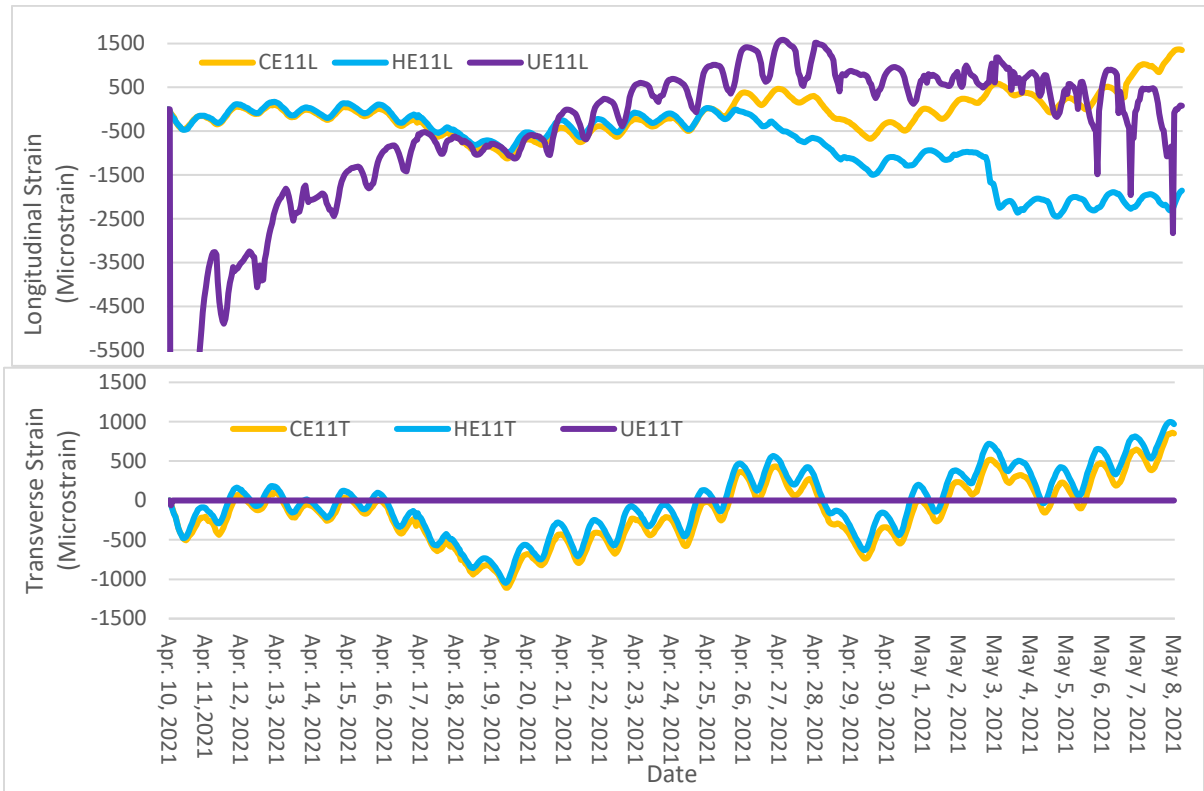


Figure 78. Early-age longitudinal and transverse strain in eastbound lane - bay 1 – position 1.

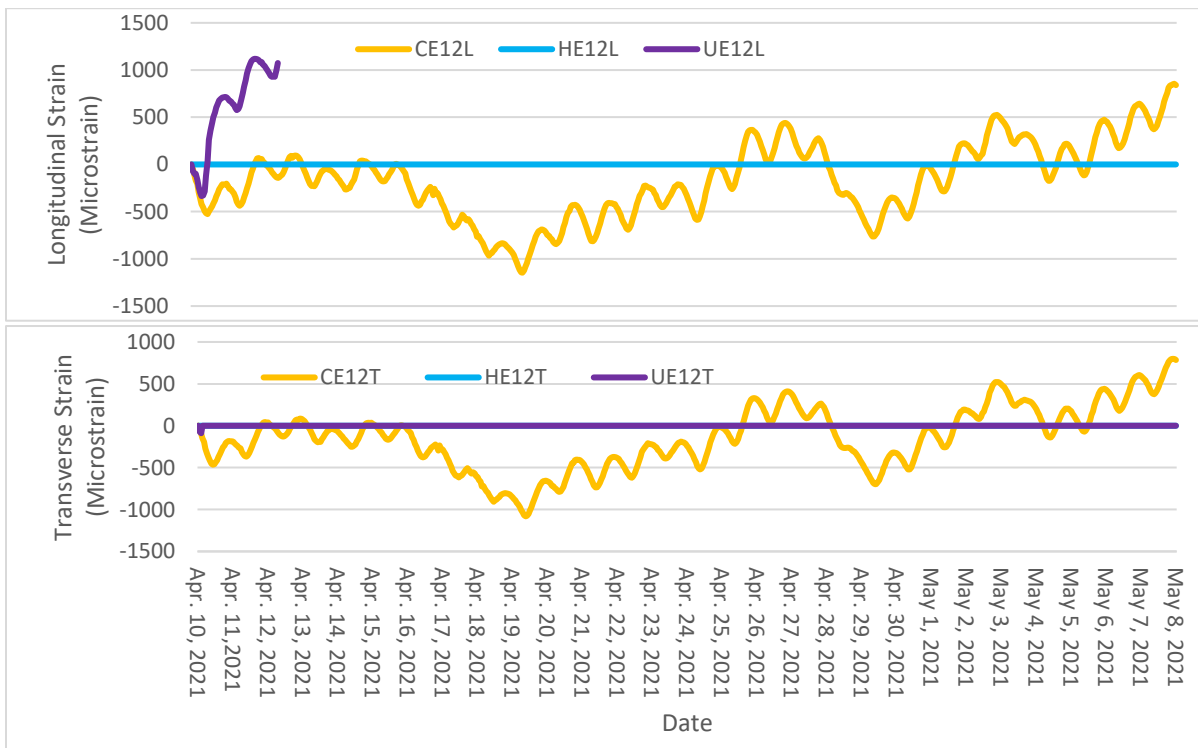
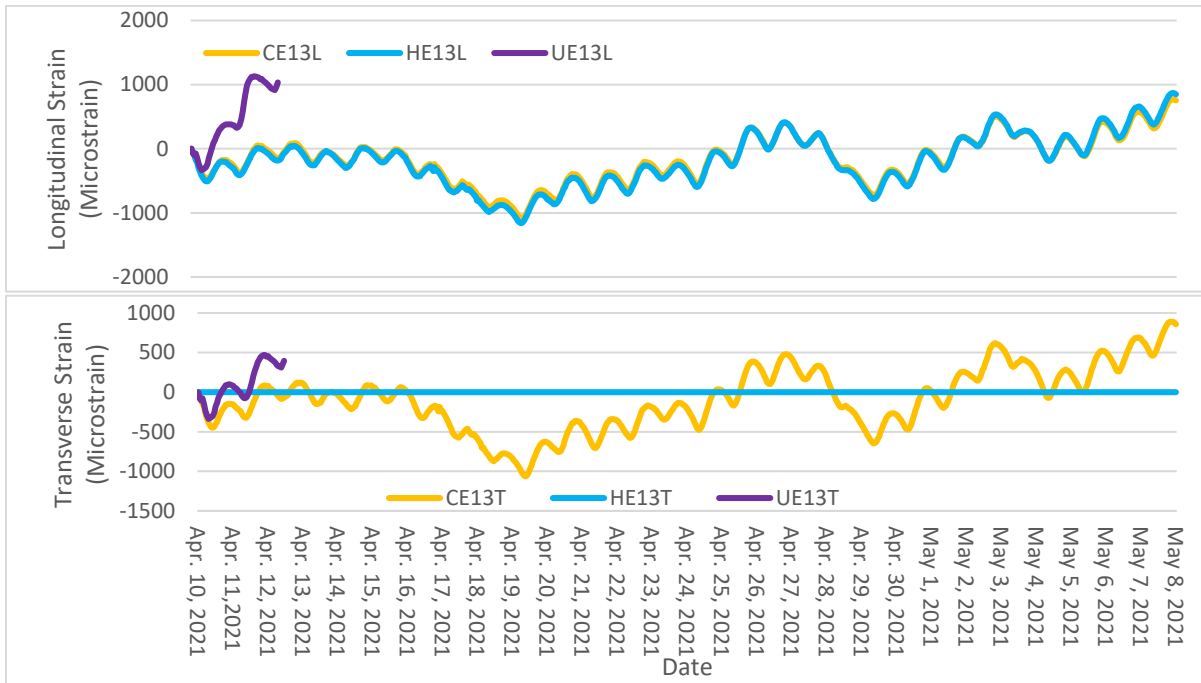
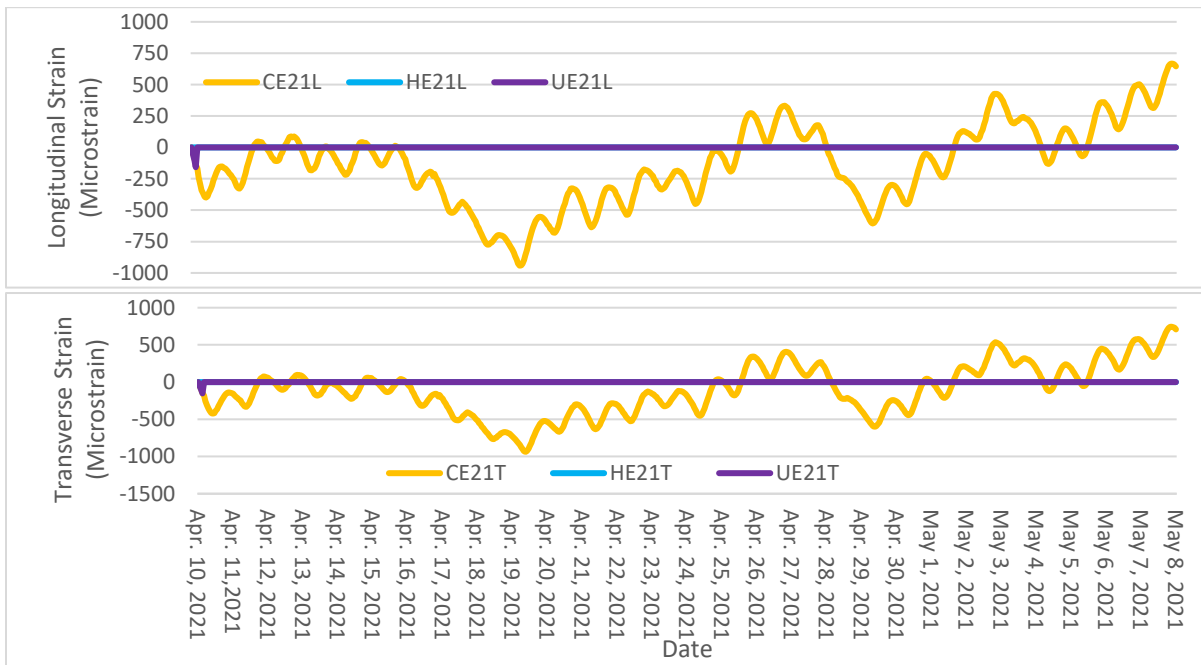


Figure 79. Early-age longitudinal and transverse strain in eastbound lane - bay 1 – position 1.



**Figure 80. Early-age longitudinal and transverse strain in eastbound lane - bay 1 – position 1.**



**Figure 81. Early-age longitudinal and transverse strain in eastbound lane - bay 2 – position 1.**

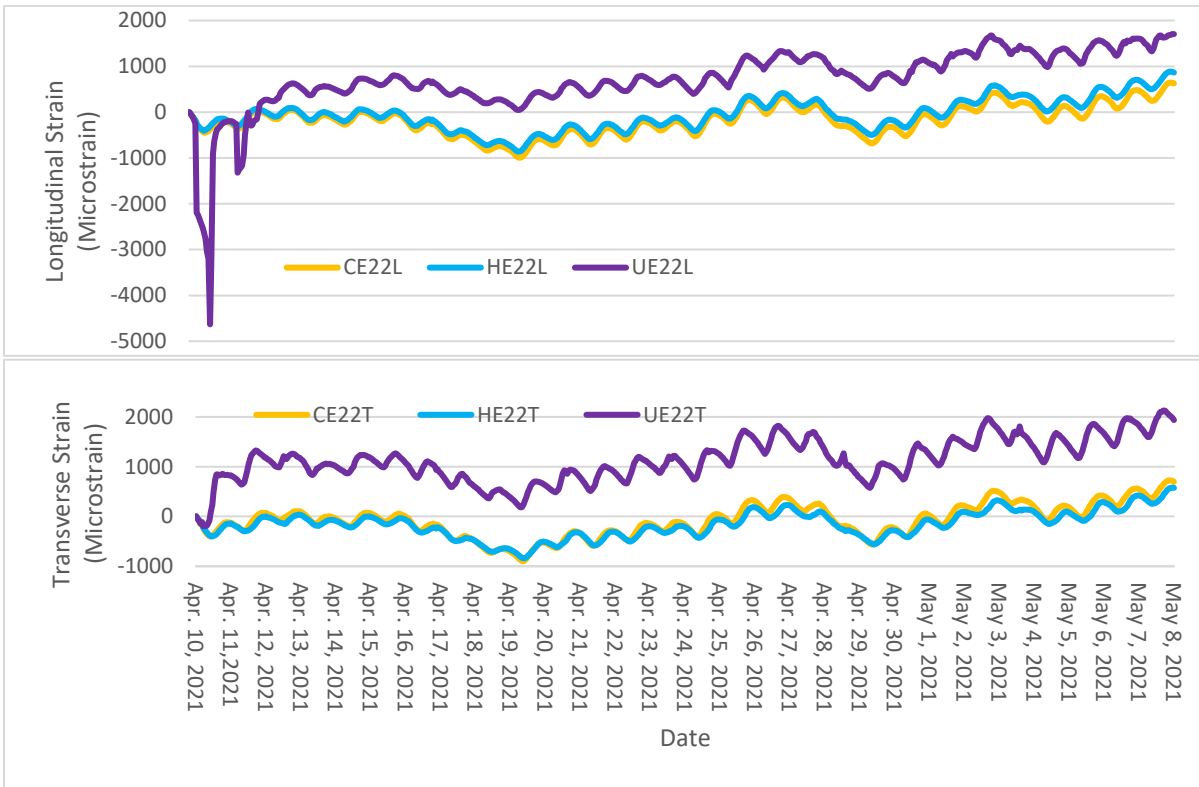


Figure 82. Early-age longitudinal and transverse strain in eastbound lane - bay 2 – position 2.

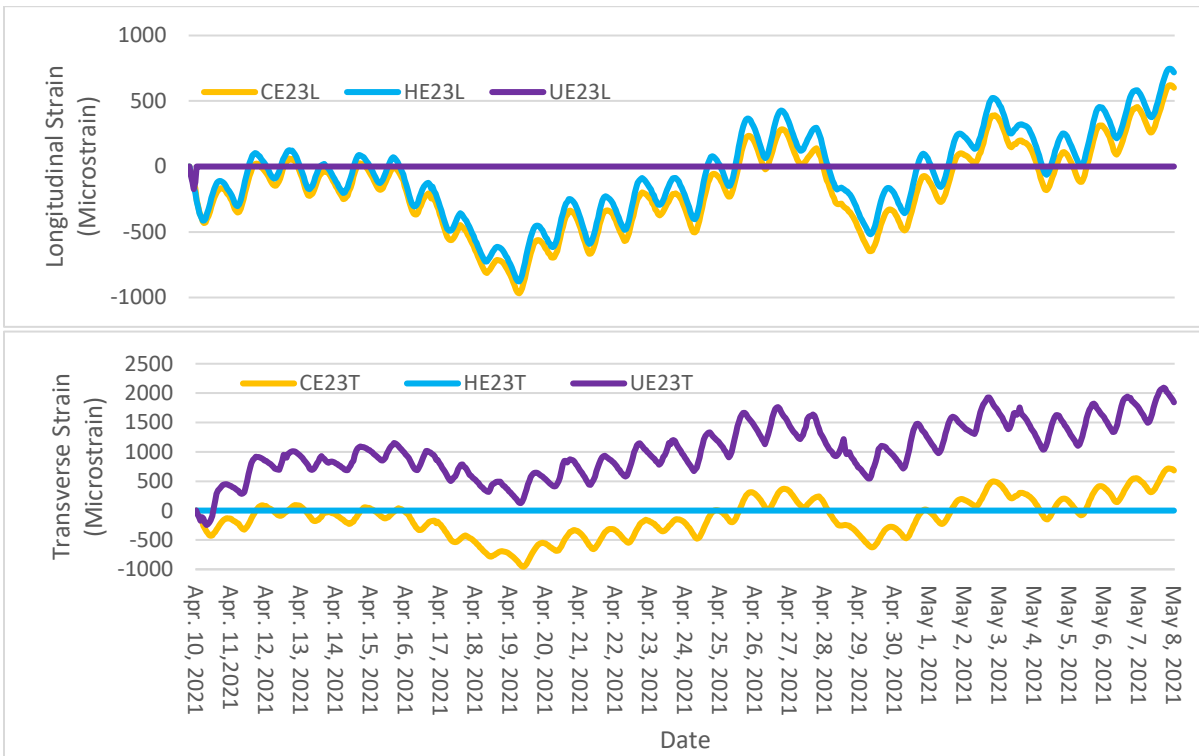
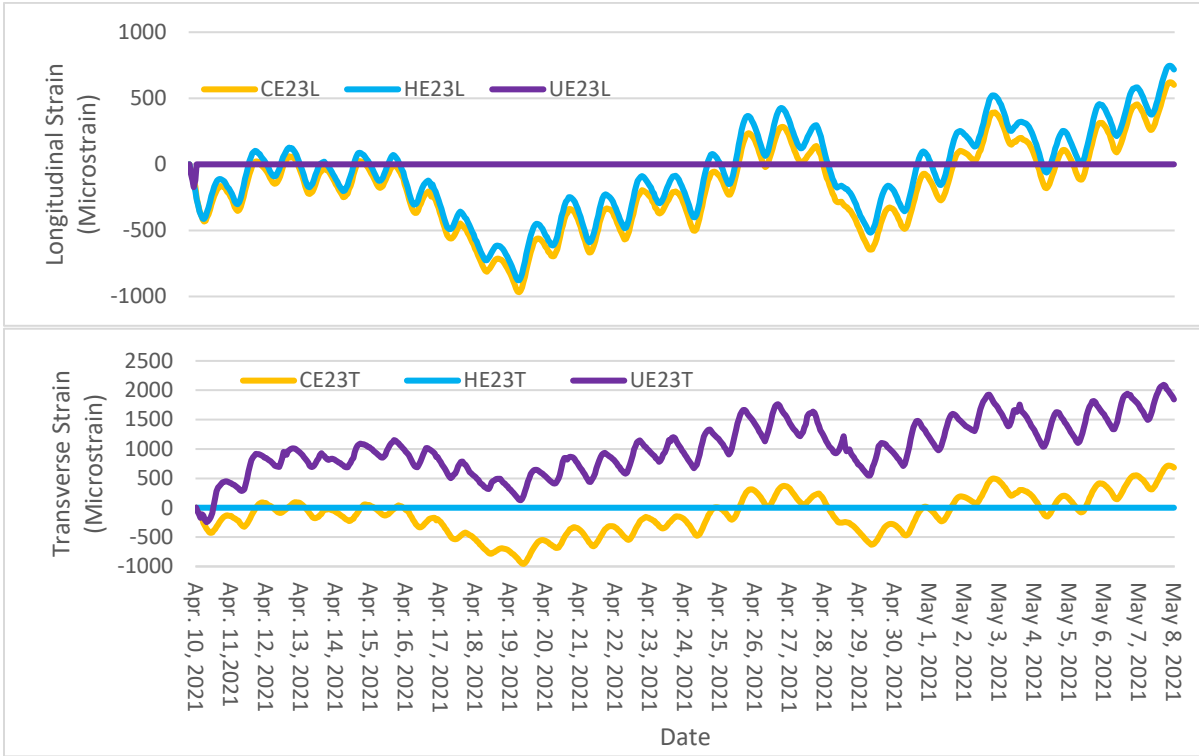
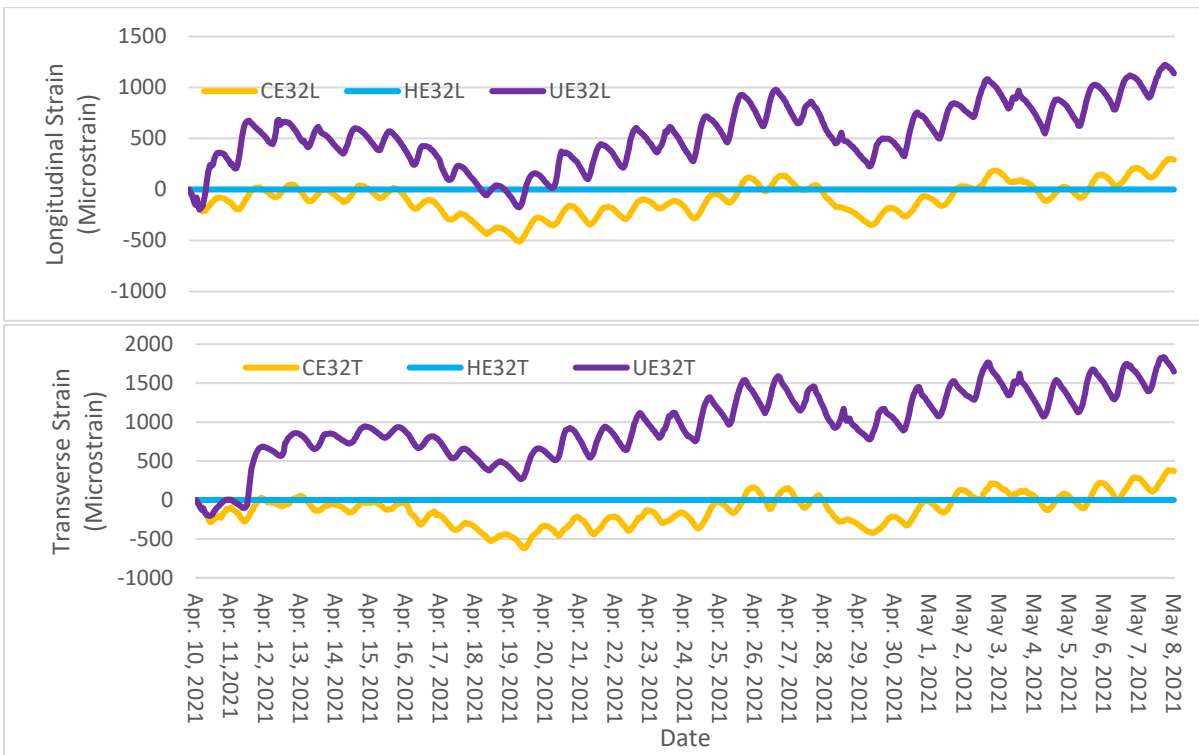


Figure 83. Early-age longitudinal and transverse strain in eastbound lane - bay 2 – position 3.



**Figure 84. Early-age longitudinal and transverse strain in eastbound lane - bay 3 – position 1.**



**Figure 85. Early-age longitudinal and transverse strain in eastbound lane - bay 3 – position 2.**

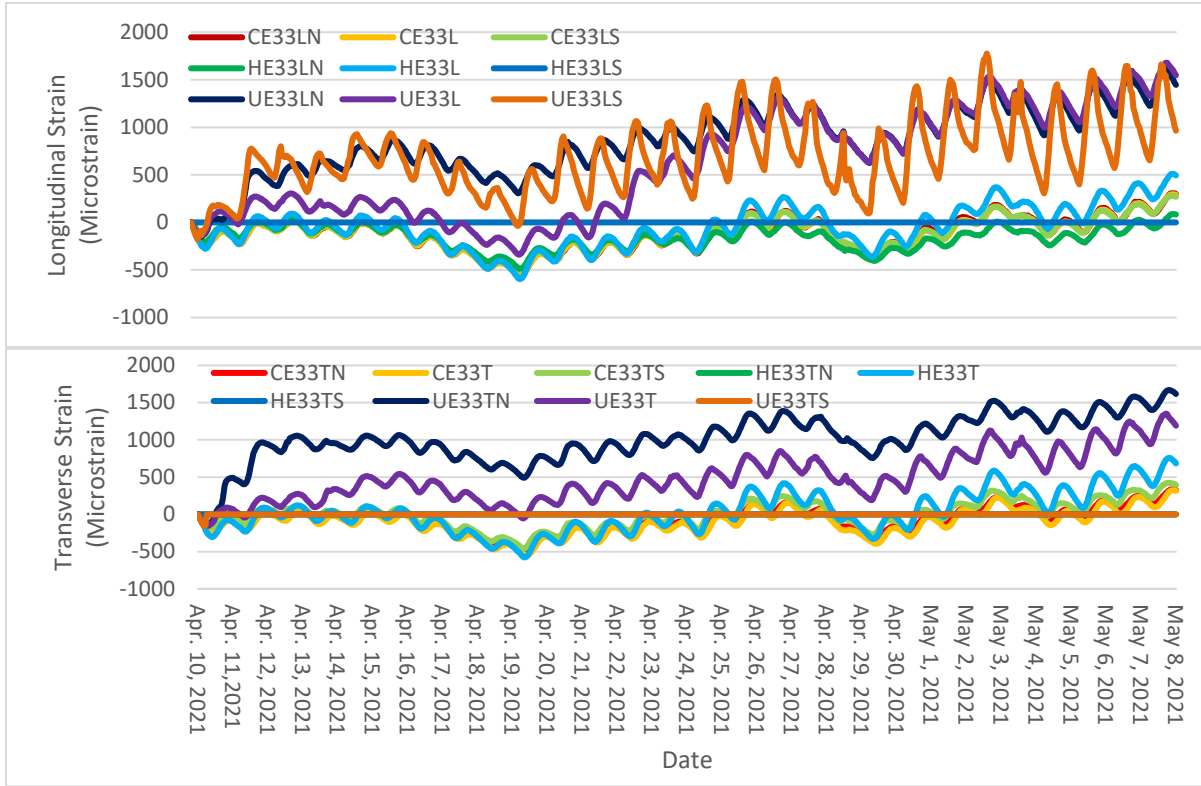


Figure 86. Early-age longitudinal and transverse strain in eastbound lane - bay 3 – position 3.

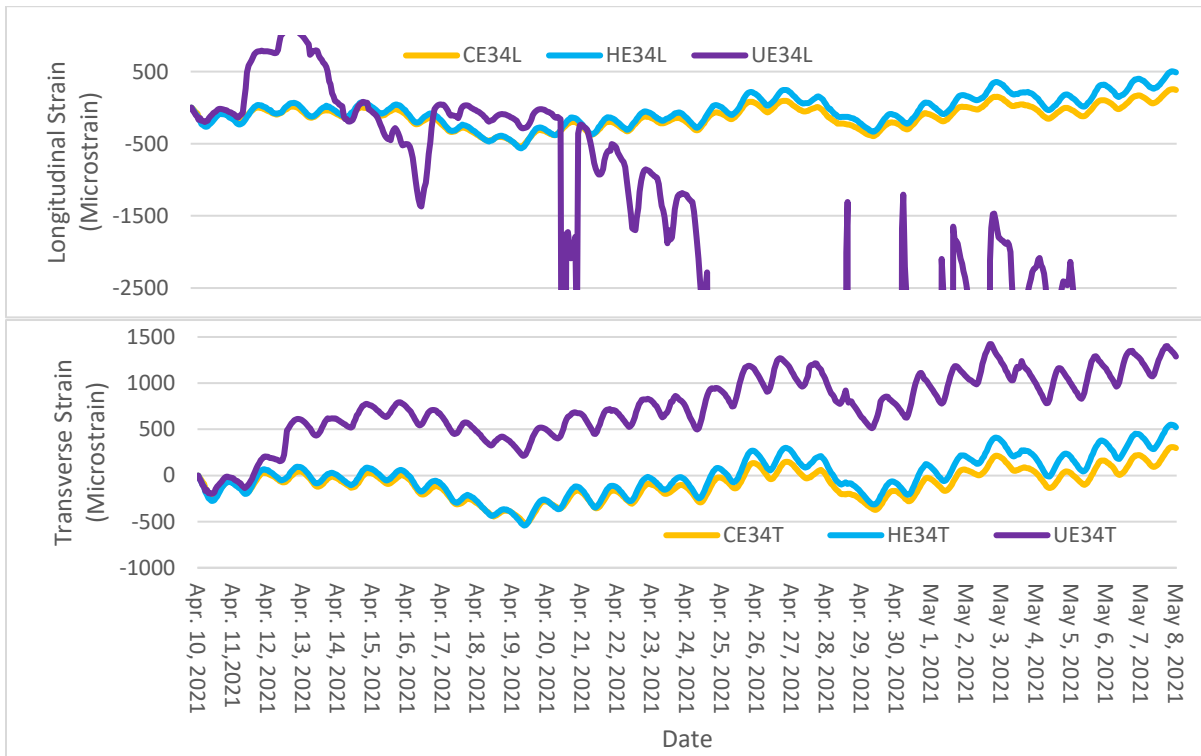


Figure 87. Early-age longitudinal and transverse strain in eastbound lane - bay 3 – position 4.

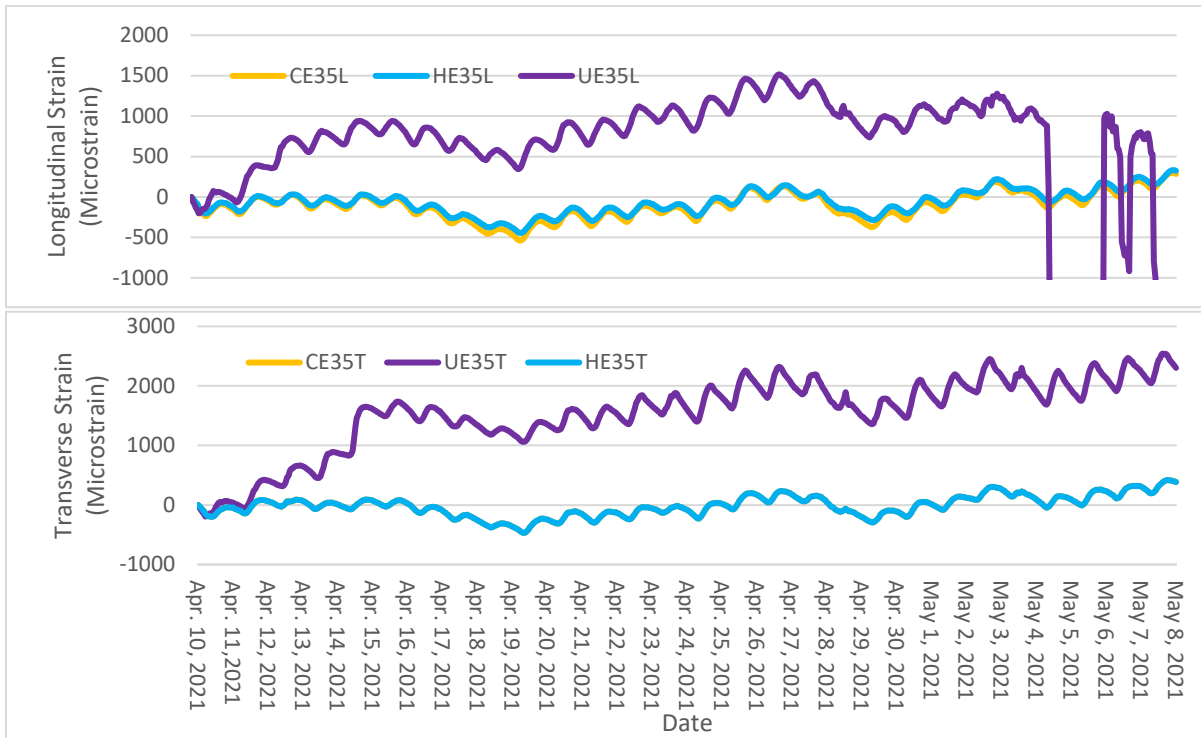


Figure 88. Early-age longitudinal and transverse strain in eastbound lane - bay 3 – position 5.

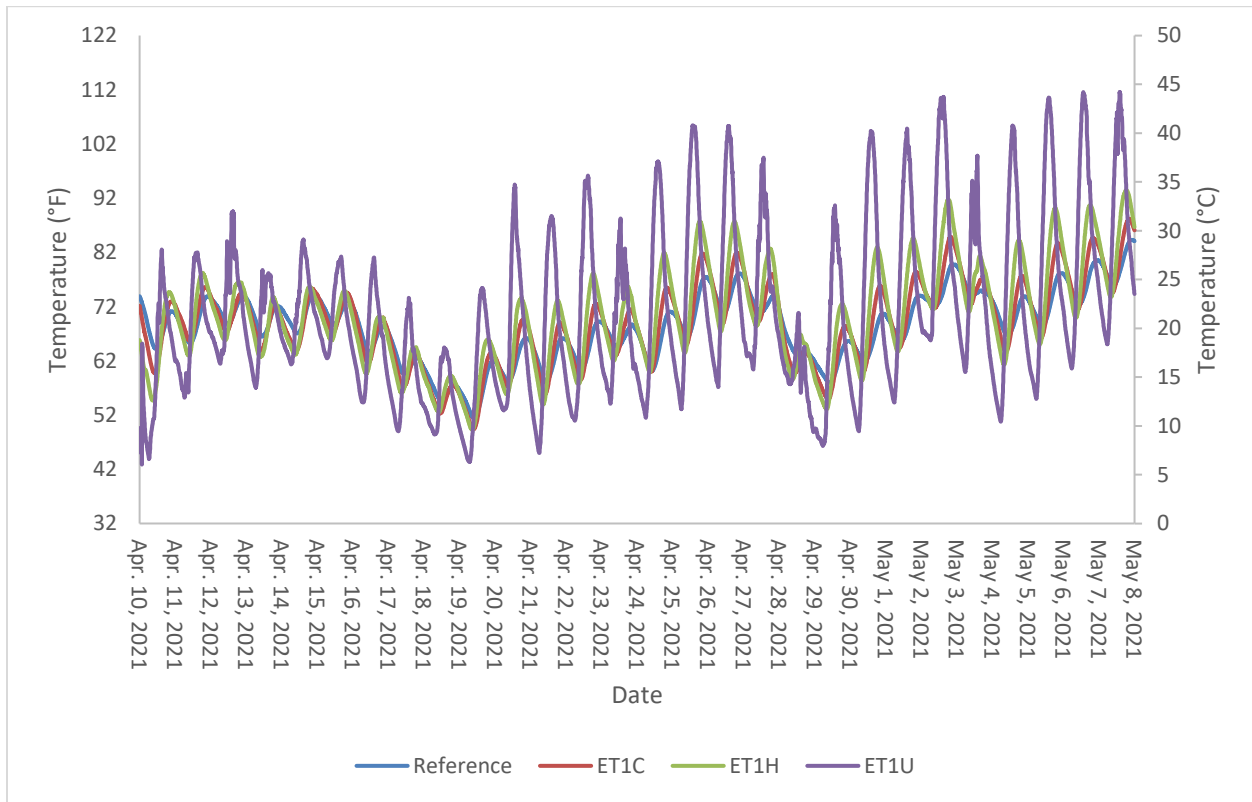
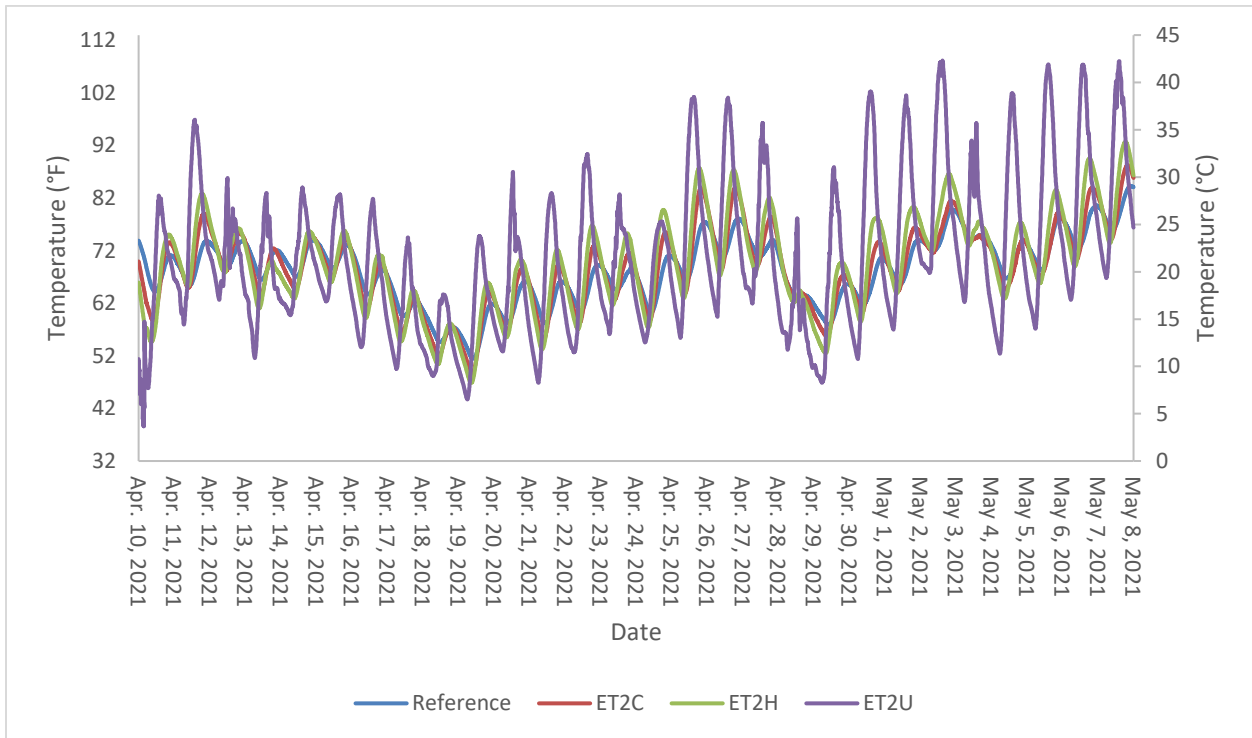
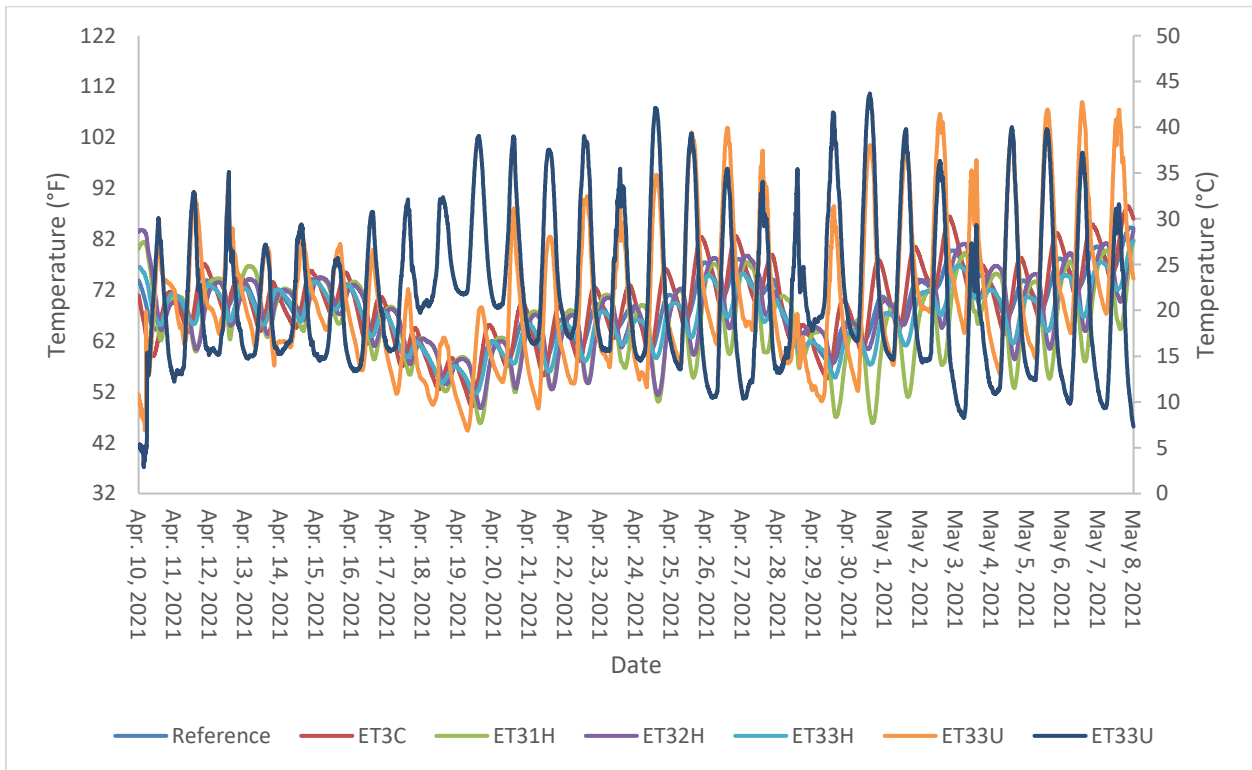


Figure 89. Temperature during UHPC Production Placements 1 and 2 (eastbound lane) – bay 1.



**Figure 90. Temperature during UHPC Production Placements 1 and 2 (eastbound lane) – bay 2.**



**Figure 91. Temperature during UHPC production placements 1 and 2 (eastbound lane) – bay 3.**

Early-age monitoring began with the UHPC overlay placement on the eastbound lane. As can be seen in Figure 78 through Figure 80, five of 18 strain gauges (UE11T, UE12L, UE12T, UE13L, and UE13T) from bay 1 were damaged during overlay placement. For bay 2, three of six strain gauges in the UHPC overlay (UE21L, UE21T, and UE23L) were damaged and did not record any data as can be seen in Figure 81 through Figure 83. Bay 3 only had one of 14 strain gauges (UE33TS) damaged during UHPC placement on the eastbound lane. As seen in Figure 78 through Figure 88, early-age strain was monitored from the day of overlay placement to an overlay age of 28 days (April 10, 2021 through May 8, 2021).

An increase in strain of approximately 1000  $\mu$ strain observed during the first two days in data from gauges UE22T (Figure 82), UE23T (Figure 83), UE32L (Figure 85), UE33LN (Figure 86), and UE33LS (Figure 86) appears to be caused by heat of hydration effects occurring in the UHPC overlay. Daily thermal cycles are clearly seen in the oscillating pattern of the strain responses obtained from properly functioning gauges. The response due to thermal effects of unrestrained UHPC can be as large as 1000  $\mu$ strain based on the thermocouple readings. However, the measured strain responses are generally 200 to 250  $\mu$ strain, this small range (less than 1000  $\mu$ strain) for the daily cycle can be attributed to restraint provided by the concrete superstructure (substrate). Gauges UE33LN and UE33LS in Figure 86 showed different magnitudes for daily cycles. This difference appears to provide an indication that UE33LS is embedded in material that is less restrained by the substrate concrete, which could be evidence of delamination at that location.

Trends in daily temperature also influenced the strain measurements. Specifically, rising daily temperatures caused increasing strain magnitudes and decreasing temperatures cause decreasing daily strain magnitudes. For example, decreasing daily temperatures were observed from April 16, 2021 to April 20, 2021 which coincided with a multi-day trend of decreasing strain for all properly functioning strain gauges. Another example of this behavior occurred between April 19, 2021 and April 27, 2021 where daily temperature and strains increased together. Differential strains observed between strain gauges in the UHPC and in the substrate show the combined effects of temperature and shrinkage for a selected period of time. For instance, in Figure 84, differences in strain measurements between gauges UE31T and CE31T decreased from April 19, 2021 to April 27, 2021, which describes the combined temperature and shrinkage effects between the UHPC overlay and the bottom of the existing deck during this period. Differential strains at each gauge location are being analyzed in this manner using multiple timeframes for the ongoing NMDOT project that continues for another two years.

Thermocouple measurements (Figure 89 through Figure 91) confirm a significant temperature change in the UHPC for all three bays due to the placement of the overlay. The change in temperature was from bay 1 to bay 3 since overlay placement began on the west end of the eastbound lane.

#### ***5.4.3. Westbound Early-age Monitoring***

The UHPC placement on the westbound lane was also divided into two production placements. Early-age monitoring of the westbound production placements include strain and temperature monitoring data for the first 28 days after placing the UHPC overlay. The third production

placement was placed on April 24, 2021 starting from the east end of the westbound lane at around 2:00 am and was completed the same day at around 7:00 am. The fourth production placement began April 27, 2021 at 9:00 pm and was completed the next morning by 5:00 am. All of the strain gauge locations in the westbound lane were covered in the fourth production placement. Strain (Figure 92 through Figure 102) and thermal data (Figure 103 through Figure 105) were collected from UHPC placement to an overlay age of 28 days.

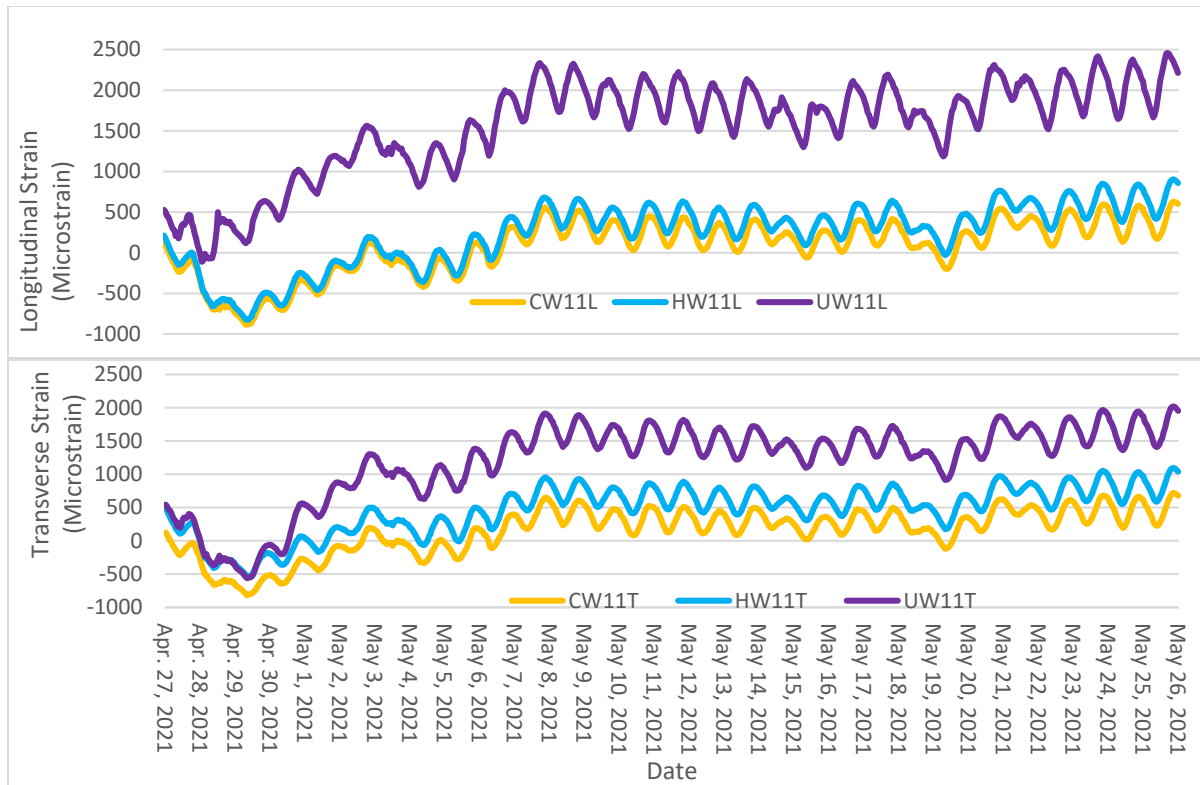


**Figure 92. Early-age longitudinal and transverse strain in westbound lane - bay 1 – position 1.**

The westbound lane only had one of 26 UHPC strain gauges, UW31L (Figure 98), damaged during placement. As with the eastbound lane, early-age monitoring was from the day of overlay placement to an overlay age of 28 days. The 28-day monitoring period for the overlaid westbound lane was from April 27, 2021 through May 26, 2021.

As with the eastbound lane, daily thermal cycles are clearly seen in the oscillating pattern of the strain responses obtained from properly functioning gauges. The response due to thermal effects of unrestrained UHPC can be as large as 600  $\mu$ strain based on the thermocouple readings. However, the measured strain responses are generally less than 600  $\mu$ strain, which can be attributed to restraint provided by the concrete superstructure (substrate).

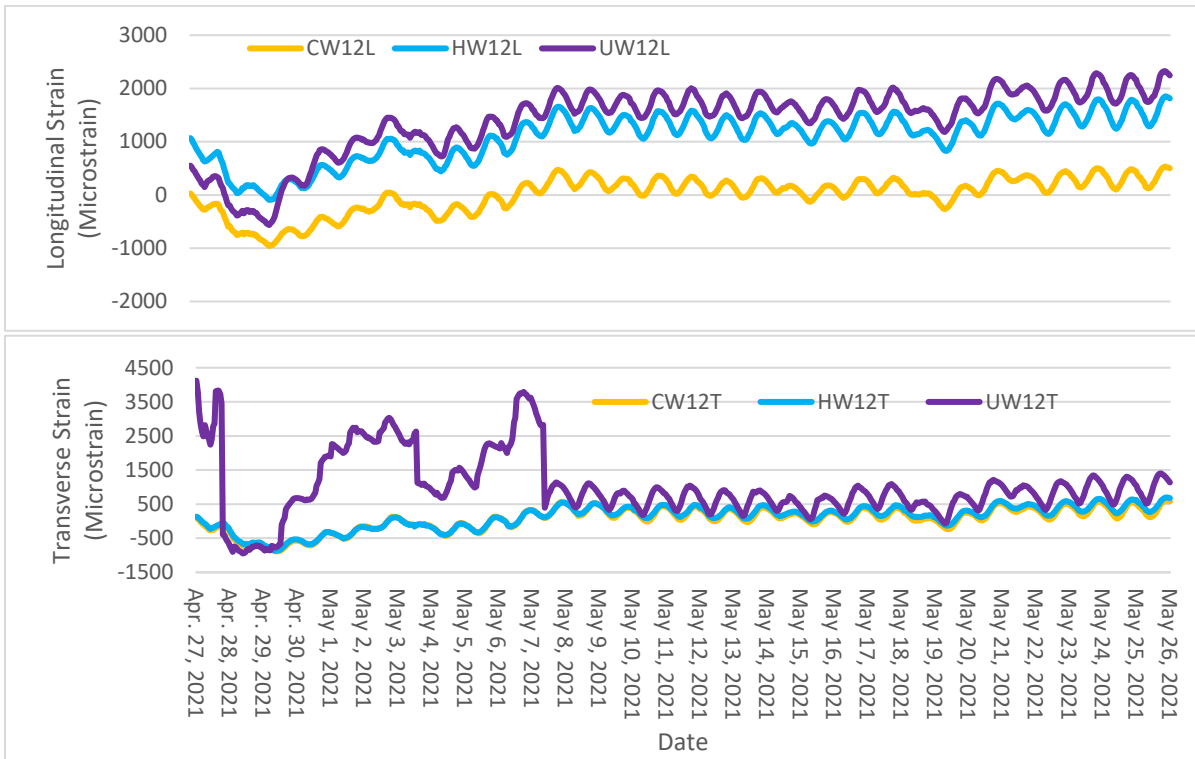


**Figure 93. Early-age longitudinal and transverse strain in westbound lane - bay 1 – position 2.**

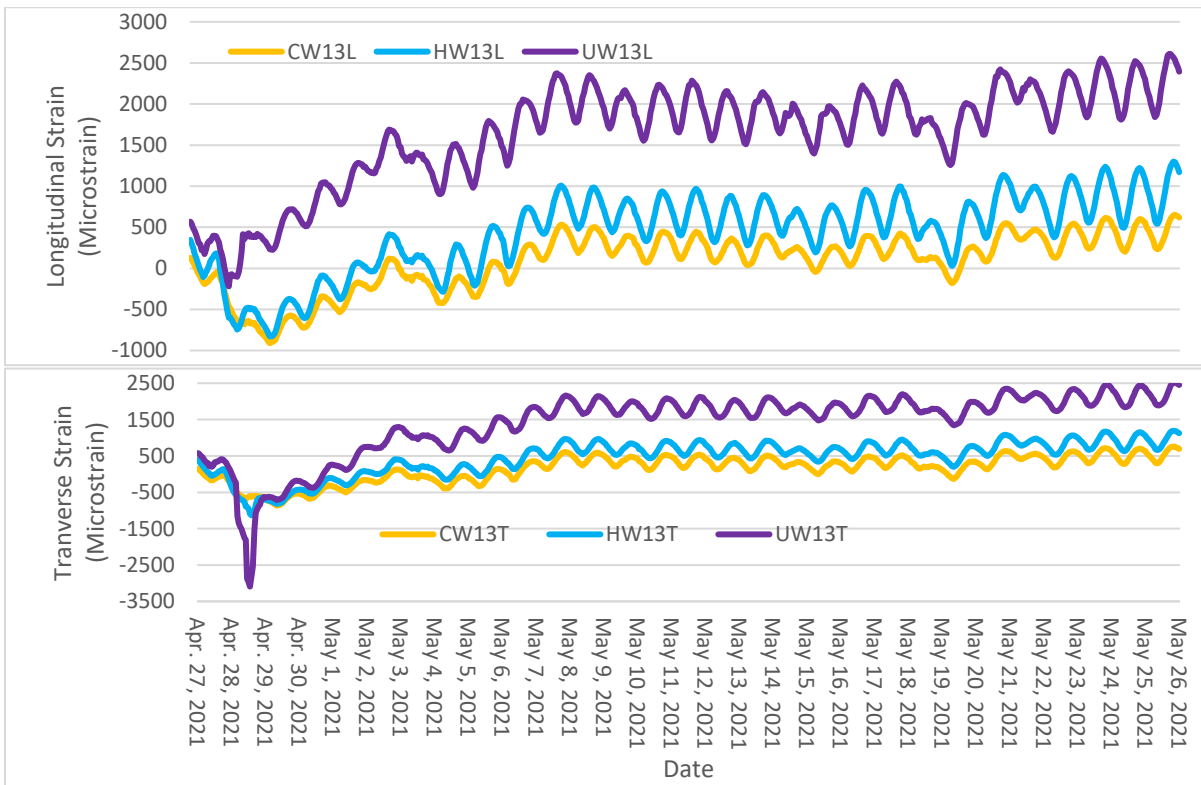


**Figure 94. Early-age longitudinal and transverse strain in westbound lane - bay 1 – position 3.**

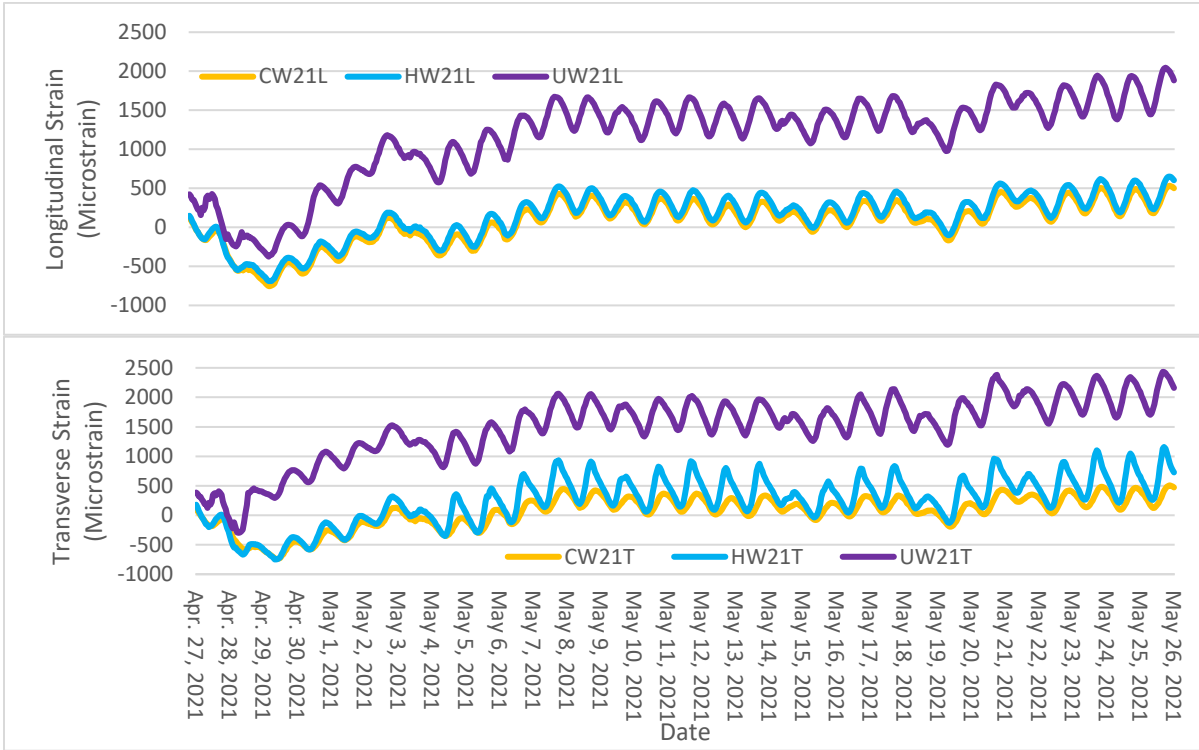


**Figure 95. Early-age longitudinal and transverse strain in westbound lane - bay 2 – position 1.**

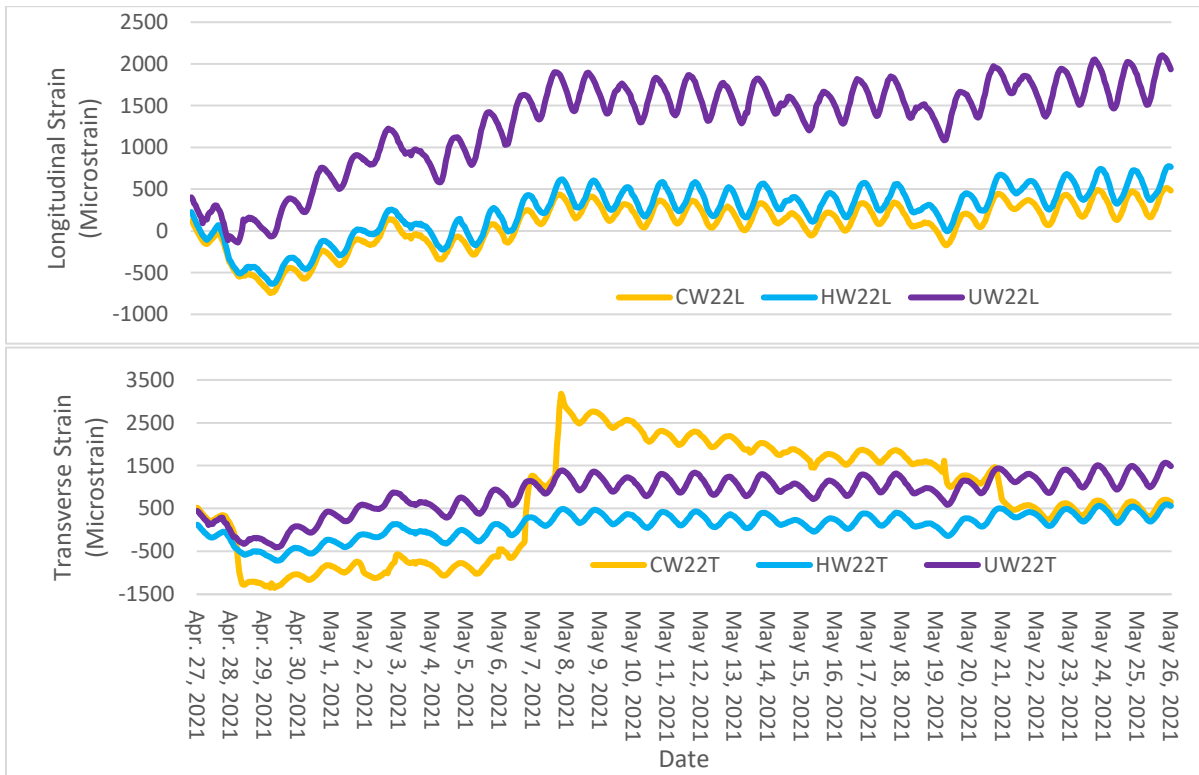


**Figure 96. Early-age longitudinal and transverse strain in westbound lane - bay 2 – position 2.**

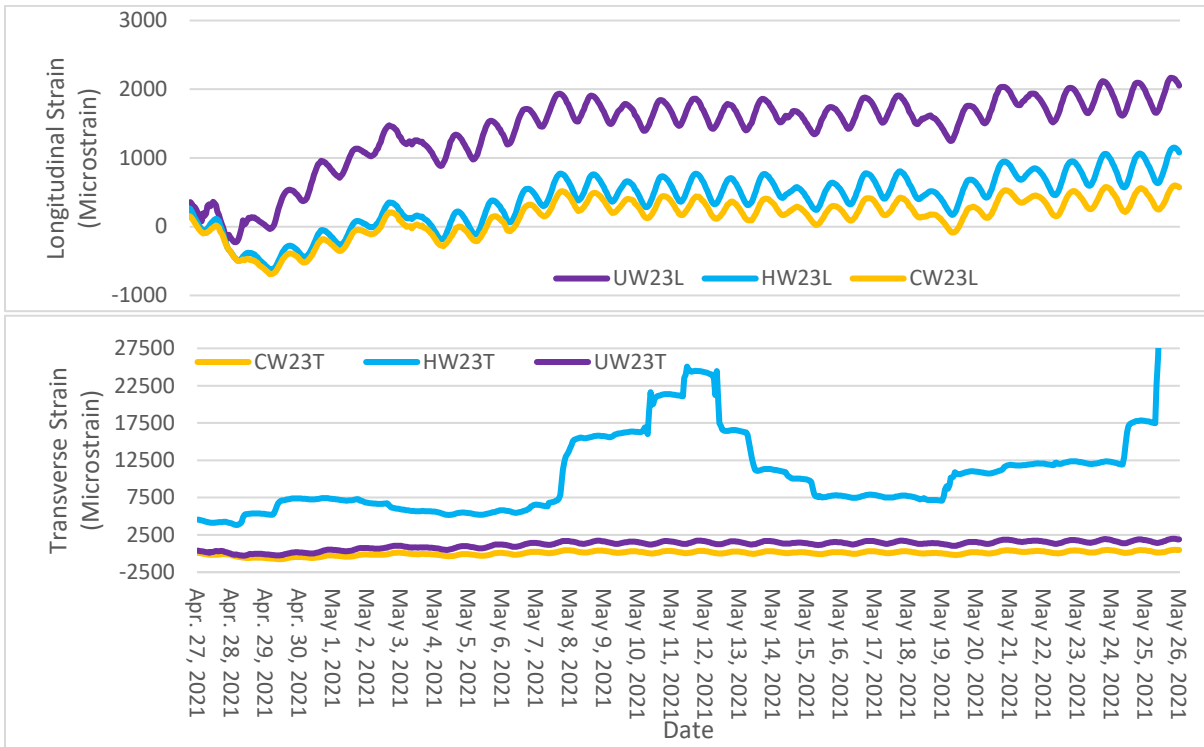


**Figure 97. Early-age longitudinal and transverse strain in westbound lane - bay 2 – position 3.**

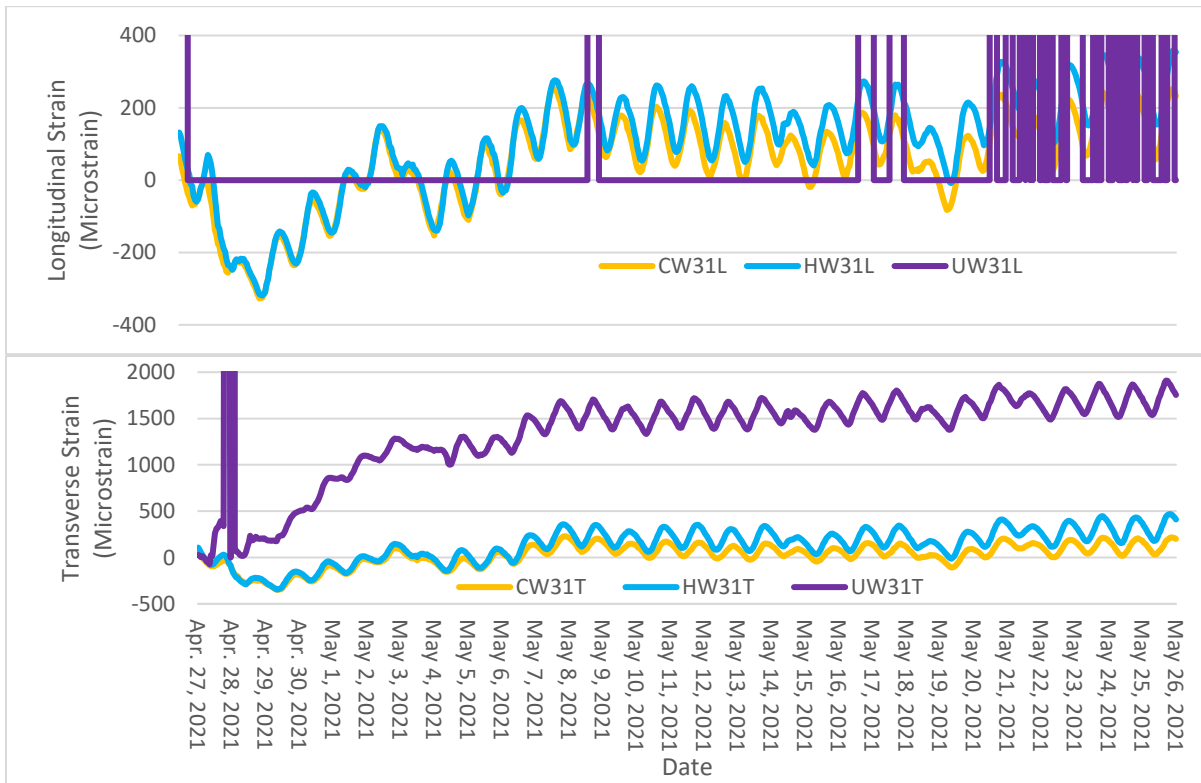


**Figure 98. Early-age longitudinal and transverse strain in westbound lane - bay 3 – position 1.**

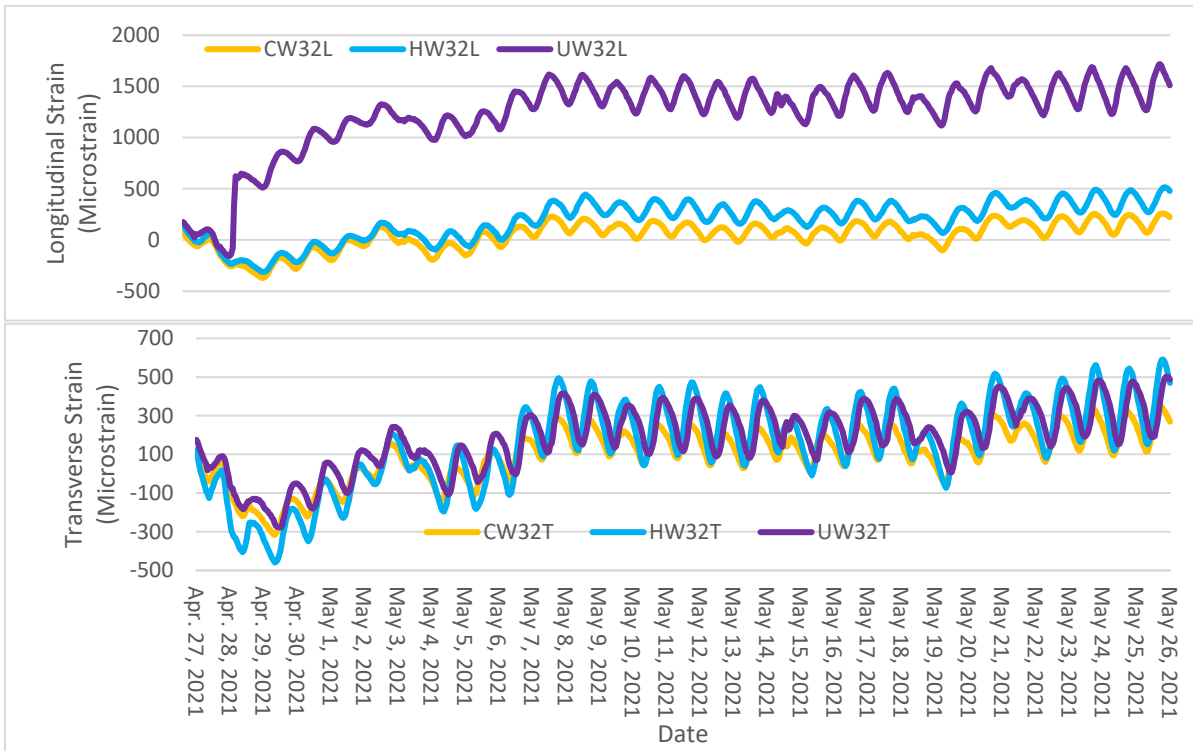


**Figure 99. Early-age longitudinal and transverse strain in westbound lane - bay 3 – position 2.**

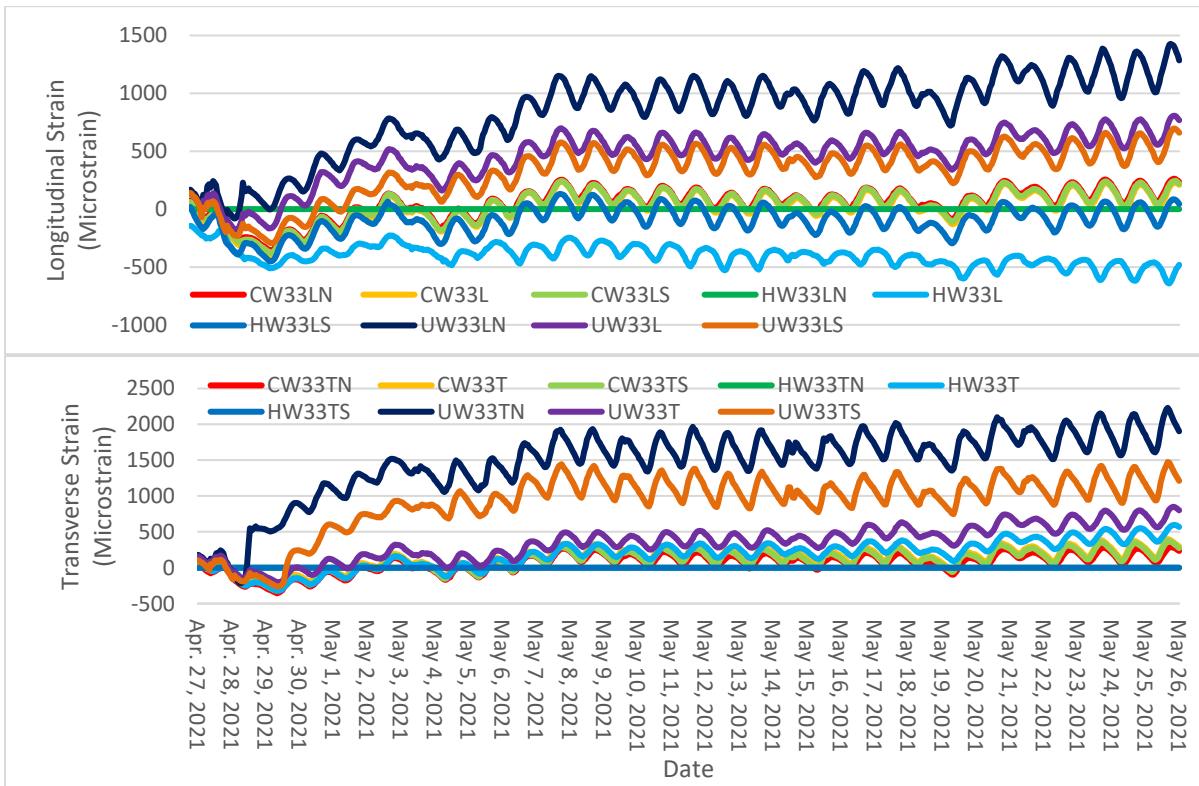


**Figure 100. Early-age longitudinal and transverse strain in westbound lane - bay 3 – position 3.**

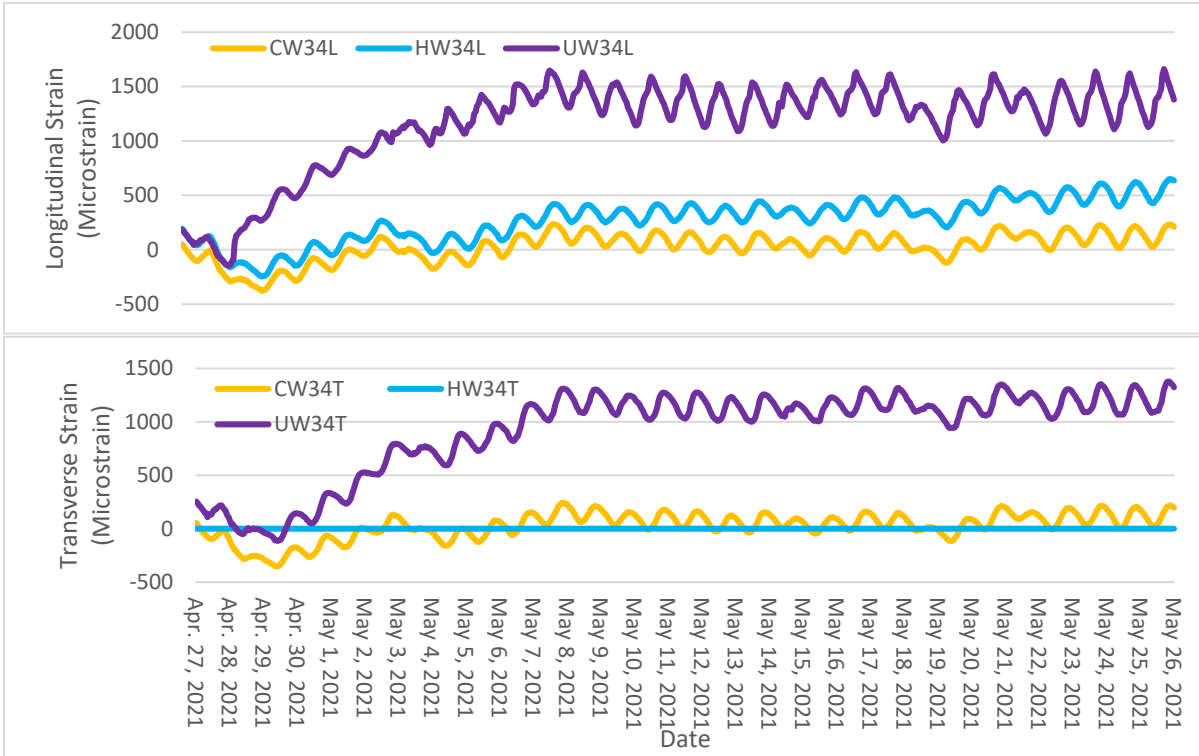


**Figure 101. Early-age longitudinal and transverse strain in westbound lane - bay 3 – position 4.**

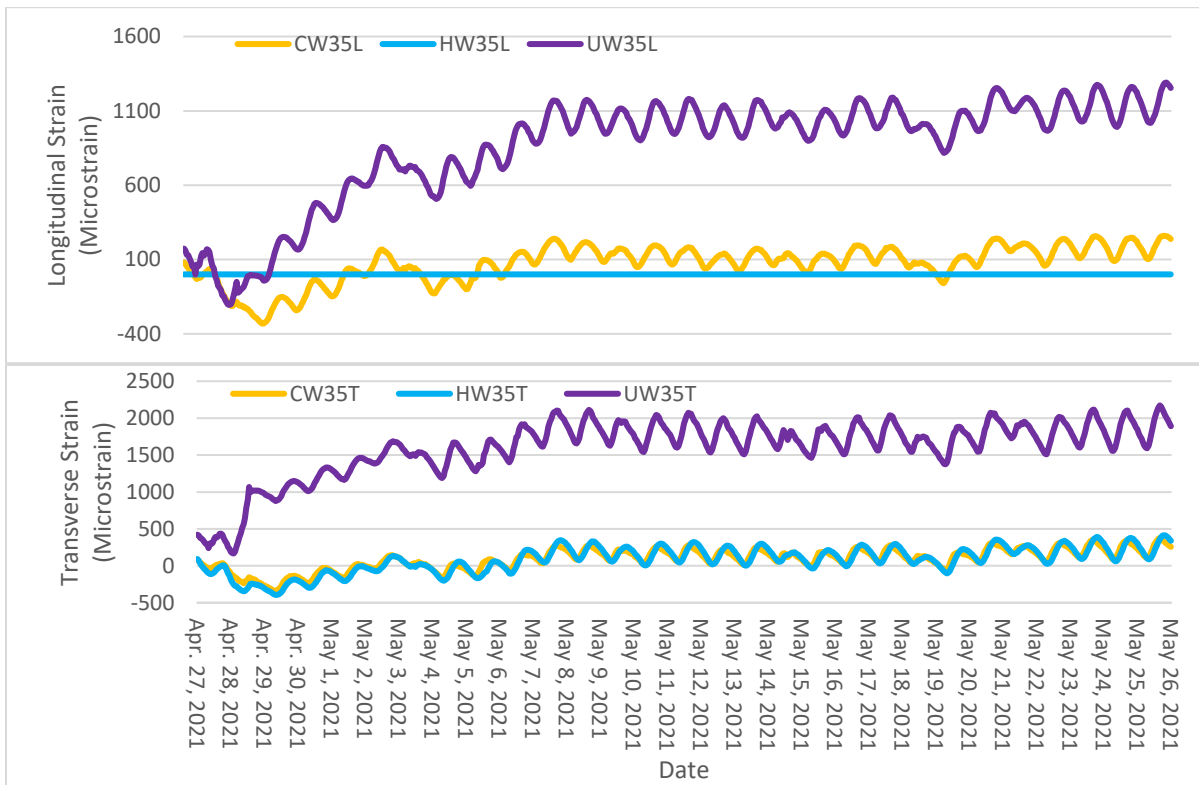


**Figure 102. Early-age longitudinal and transverse strain in westbound lane - bay 3 – position 5.**

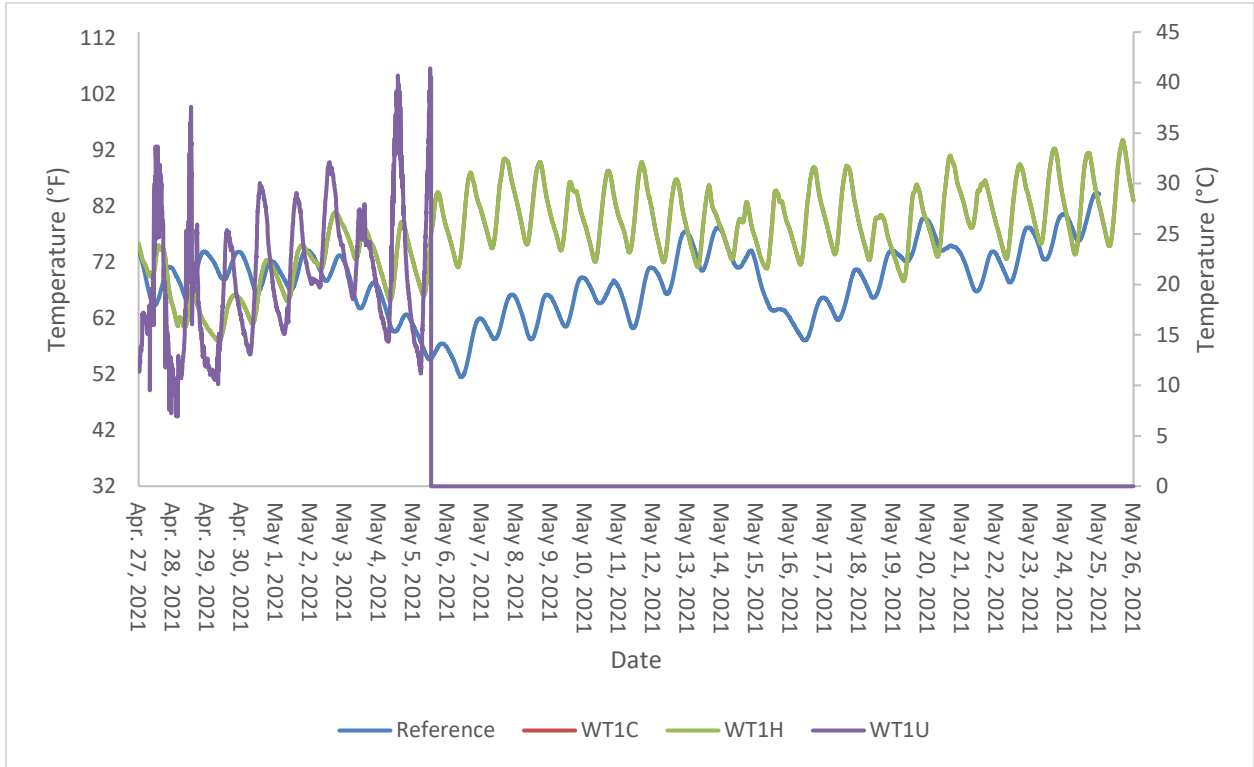


**Figure 103. Temperature during UHPC Production Placements 3 and 4 (westbound lane) – bay 1.**

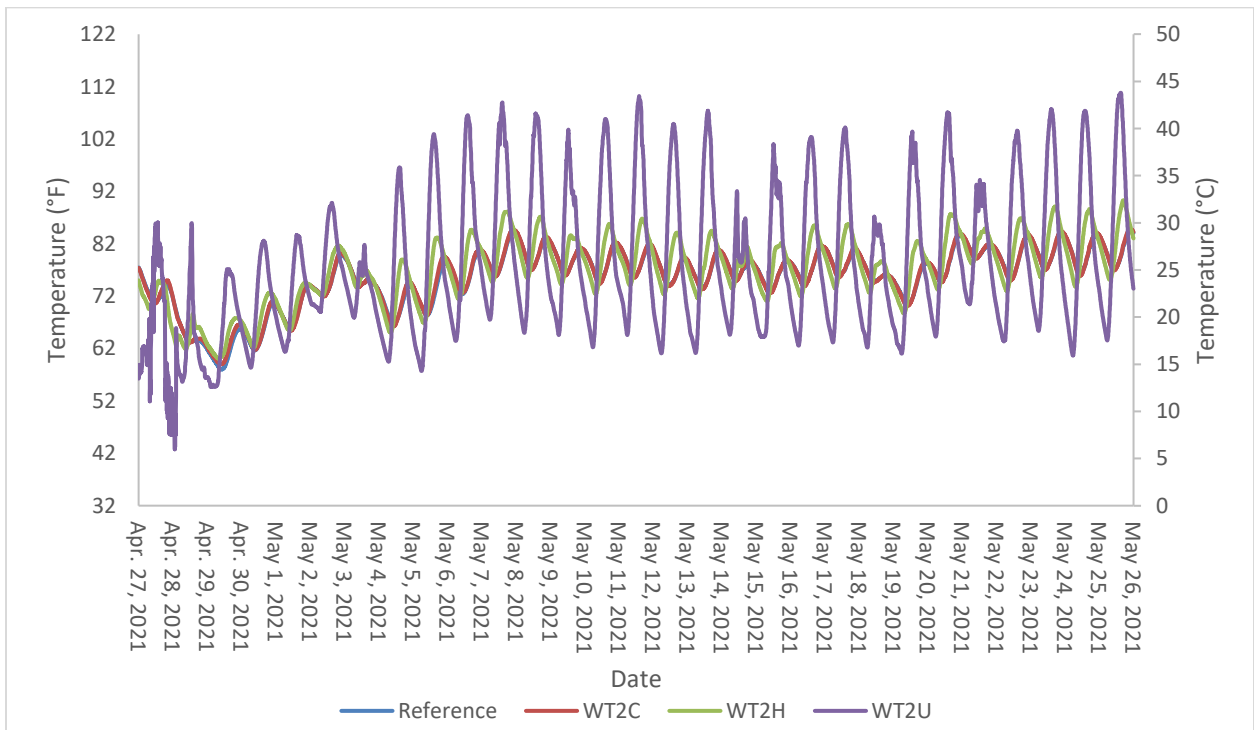


**Figure 104. Temperature during UHPC Production Placements 3 and 4 (westbound lane) – bay 2.**

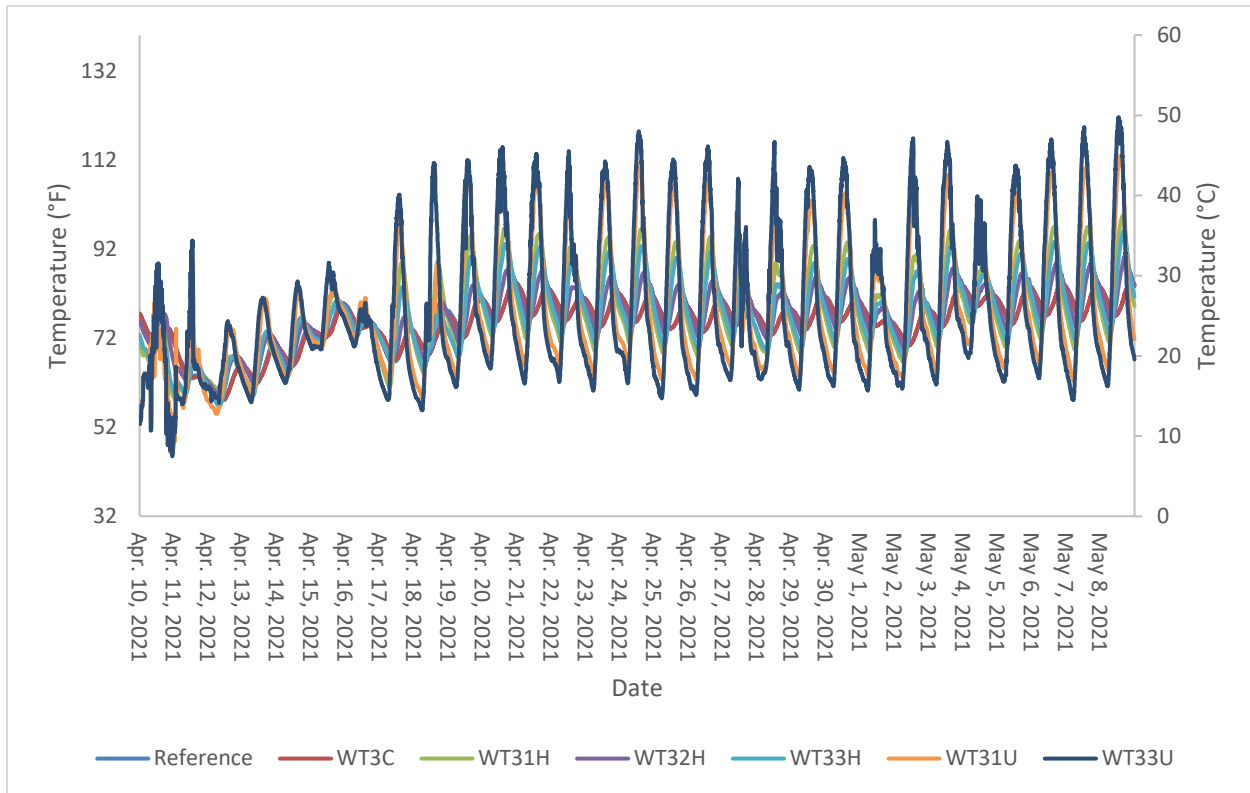


**Figure 105. Temperature during UHPC Production Placements 3 and 4 (westbound lane) – bay 3.**

As with the eastbound lane, trends in daily temperature also influenced the strain measurements. Between May 5, 2021 to May 7, 2021 the plastic was removed from the UHPC which is observed in Figure 100 where the gauges in the UHPC begin to show greater swings in strain from low of day to high of day as can be seen for gauges UW33TN and UW33TS in Figure 100. While UW33TN and UW33TS showed similar magnitudes for their daily cycles, they both experienced greater daily strain swings than UW33T after removal of the plastic sheeting. This may be caused by the overlay being thicker near strain gauge UW33T, which would reduce temperature swings at the depth of the gauge.

The daily highs from May 5, 2021 to May 18, 2021 were generally above 80°F (27°C). On May 19, 2021 the high temperature dropped to 74°F (23°C) causing measured strains to decrease for properly functioning gauges. Strain gauges then recorded greater strains once daily highs reached above 90°F (32°C) beginning on May 20, 2021. As before, differential strains observed between strain gauges in the UHPC and in the substrate show the combined effects of temperature and shrinkage for a selected period of time. For instance, in Figure 102, differences in strain measurements between gauges UW35L and CW35L increased between April 28, 2021 and May 3, 2021, which describes the combined temperature and shrinkage effects between the UHPC overlay and the bottom of the existing deck during this period. This trend can be observed throughout the period from May 7, 2021 to May 26, 2021. As stated in the previous sub-section, the differential strains at each gauge location are being analyzed in this manner, using multiple timeframes, for the ongoing NMDOT project that continues for another two years.

Thermocouple measurements, Figure 103 through Figure 105, confirm a significant increase in temperature swing of the daily cycle in the UHPC for all three bays due to removal of plastic sheeting. As observed in Figure 103 thermocouple WT1U malfunctioned around May 5, 2021 and did not record any data for the remainder of the 28-day monitoring period. It was also observed that thermocouples inside the UHPC overlay fluctuated with greater amplitude than sensors in the box girders or HPD since the overlay has direct exposure to ambient weather.

### **5.5. Longer-term Monitoring**

Longer-term monitoring of the overlaid bridge consisted of monitoring strain and temperature of the UHPC overlaid bridge from an overlay age of 28 days to December 15, 2021. Figure 106 through Figure 116 and Figure 120 through Figure 130 present the strain data from all sensors located in the eastbound and westbound lanes, respectively. Temperature data are presented for the eastbound and westbound lanes in Figure 117 through Figure 119 and Figure 131 through Figure 133, respectively. The data provide a record of the behavior of all three profile locations within the bridge (multi-cell box girder, HPD, and UHPC overlay). A thermal effect in compression resulting in a decrease in strain is clearly observed from June 28, 2021 through June 30, 2021. During these dates, cold and rainy weather were experienced, which was confirmed from the collected temperature data.

There are numerous anomalies in the strain data that must be avoided in the detailed analysis being conducted for the NMDOT project that continues for the next two years. Some of these anomalies were periods of excessive drift that occurred during mid-July through early-October. Two examples of excessive drift are gauge UW33TN (Figure 128) during the first half of July and UW33TS (Figure 128) during late July and again in late August. Additionally, some data reflect sensor malfunctions since readings spiked out of range. Observed data anomalies were thought to be potential indicators of delamination or irregularities in the bridge and were investigated during the chain drag on the entire overlay. However, no delaminated areas were identified near the sensor locations. Although the strain data had irregularities, sensor readings often appeared to be functioning correctly at later ages. Since the anomalies reflect erroneous data, relative strains occurring during windows of time that do not contain anomalies are being used for detailed analysis of the bridge and overlay behaviors for the NMDOT project.

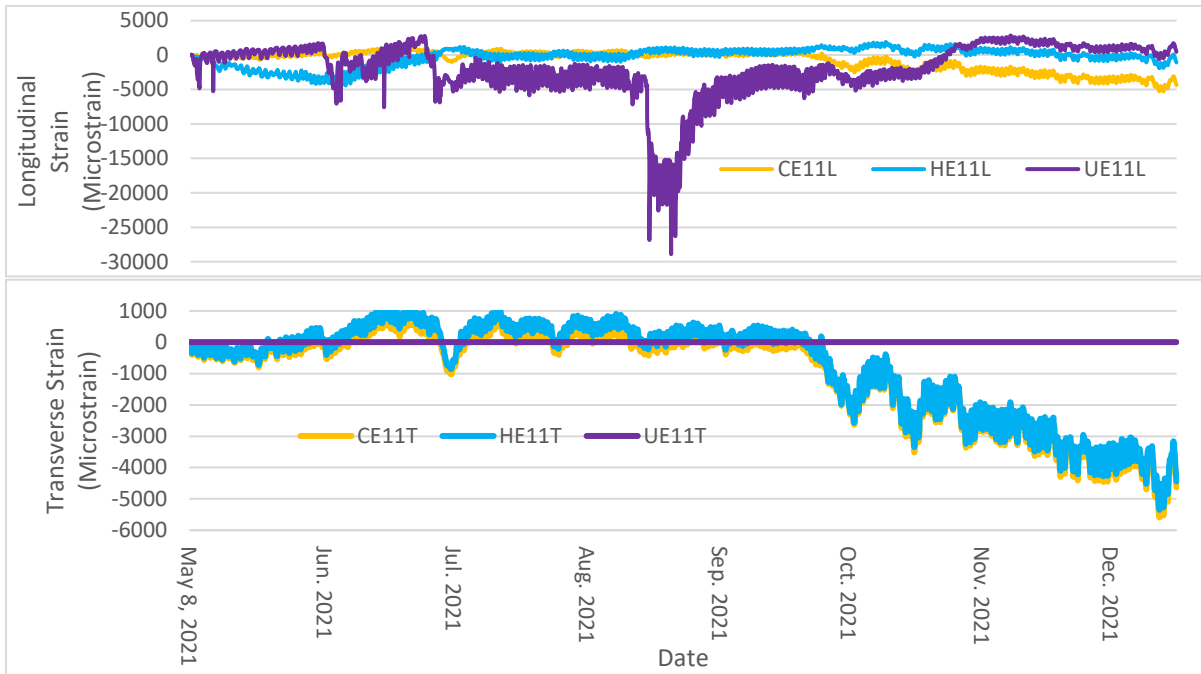


**Figure 106. Longer-term longitudinal and transverse strain in eastbound lane - bay 1 – position 1.**

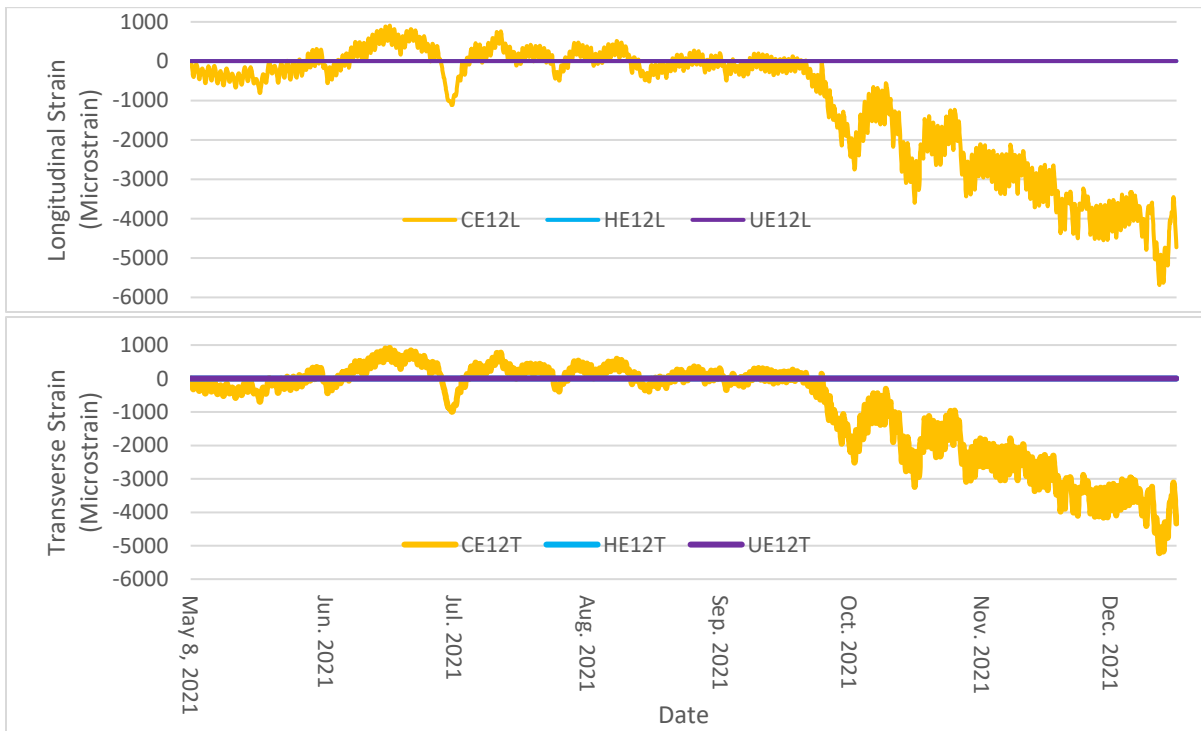


**Figure 107. Longer-term longitudinal and transverse strain in eastbound lane - bay 1 – position 2.**

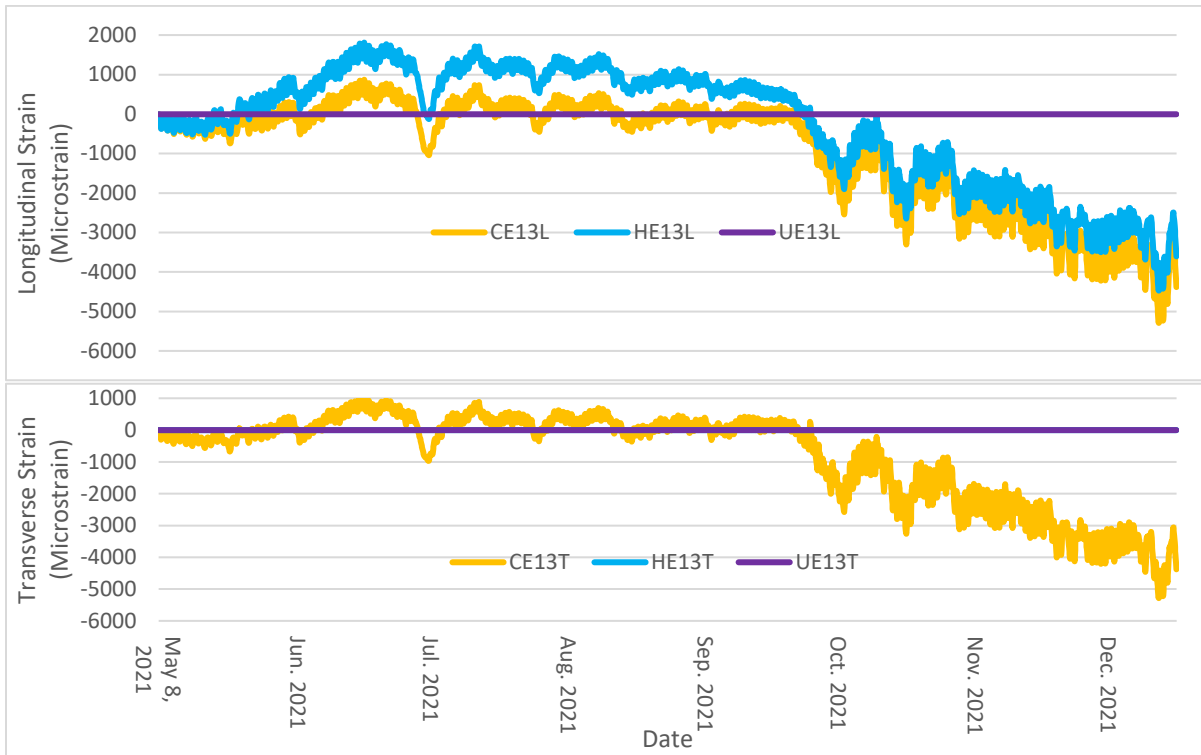


**Figure 108. Longer-term longitudinal and transverse strain in eastbound lane - bay 1 – position 3.**

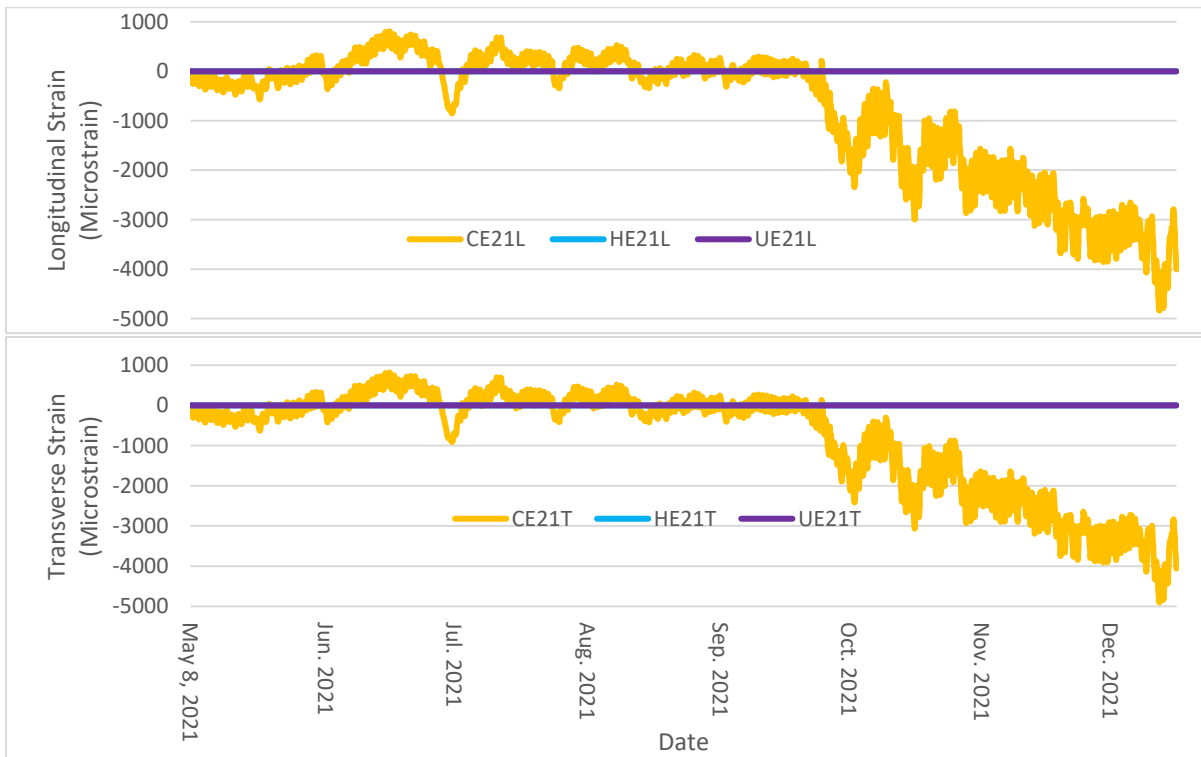


**Figure 109. Longer-term longitudinal and transverse strain in eastbound lane - bay 2 – position 1.**



**Figure 110. Longer-term longitudinal and transverse strain in eastbound lane - bay 2 – position 2.**

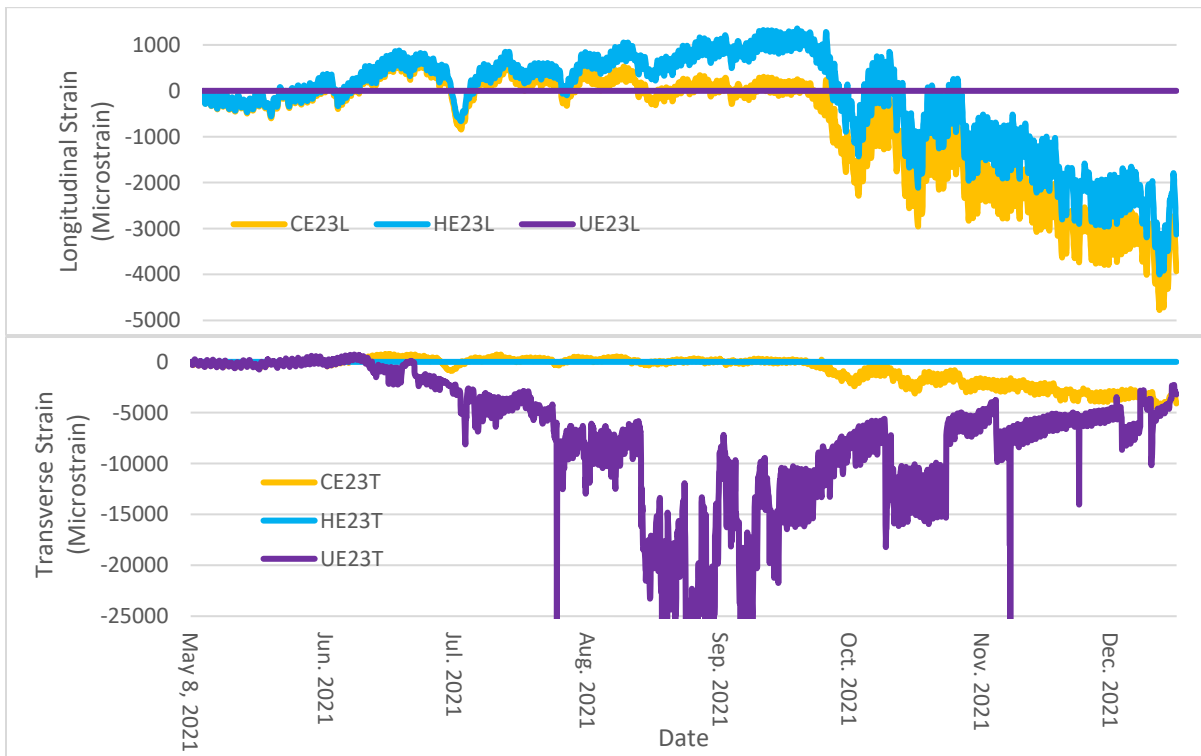


**Figure 111. Longer-term longitudinal and transverse strain in eastbound lane - bay 2 – position 3.**

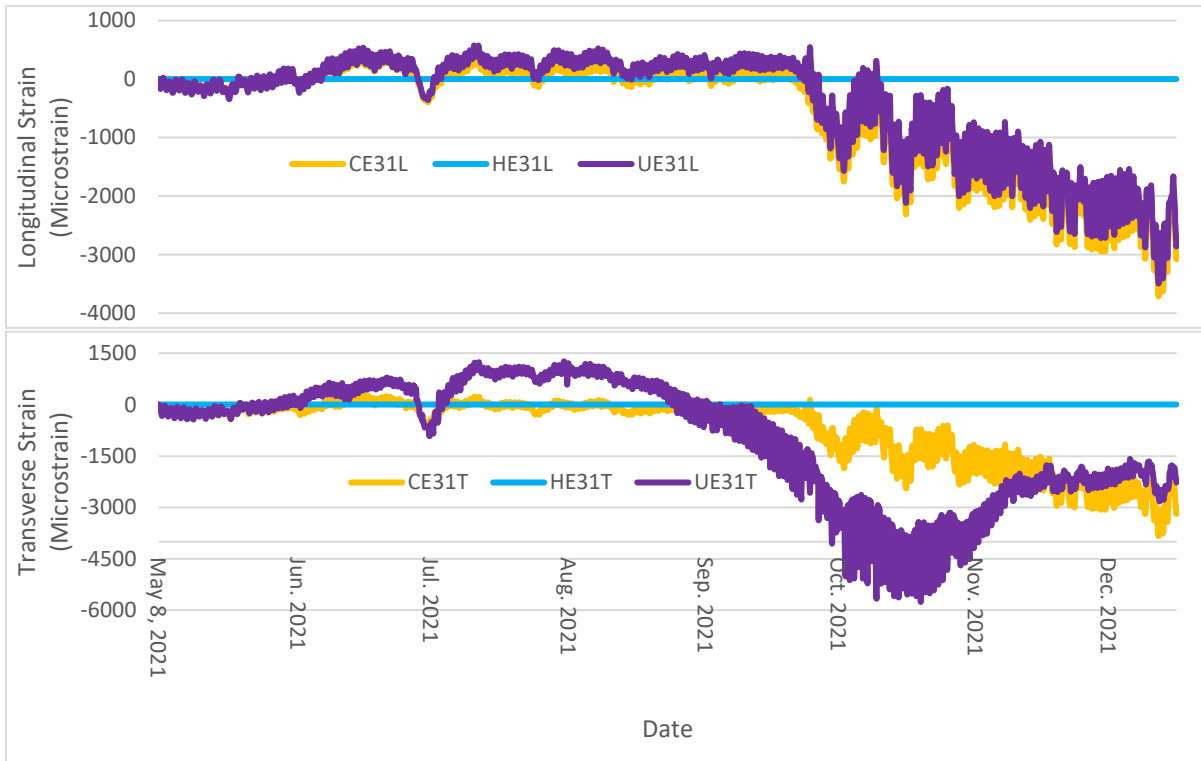


**Figure 112. Longer-term longitudinal and transverse strain in eastbound lane - bay 3 – position 1.**

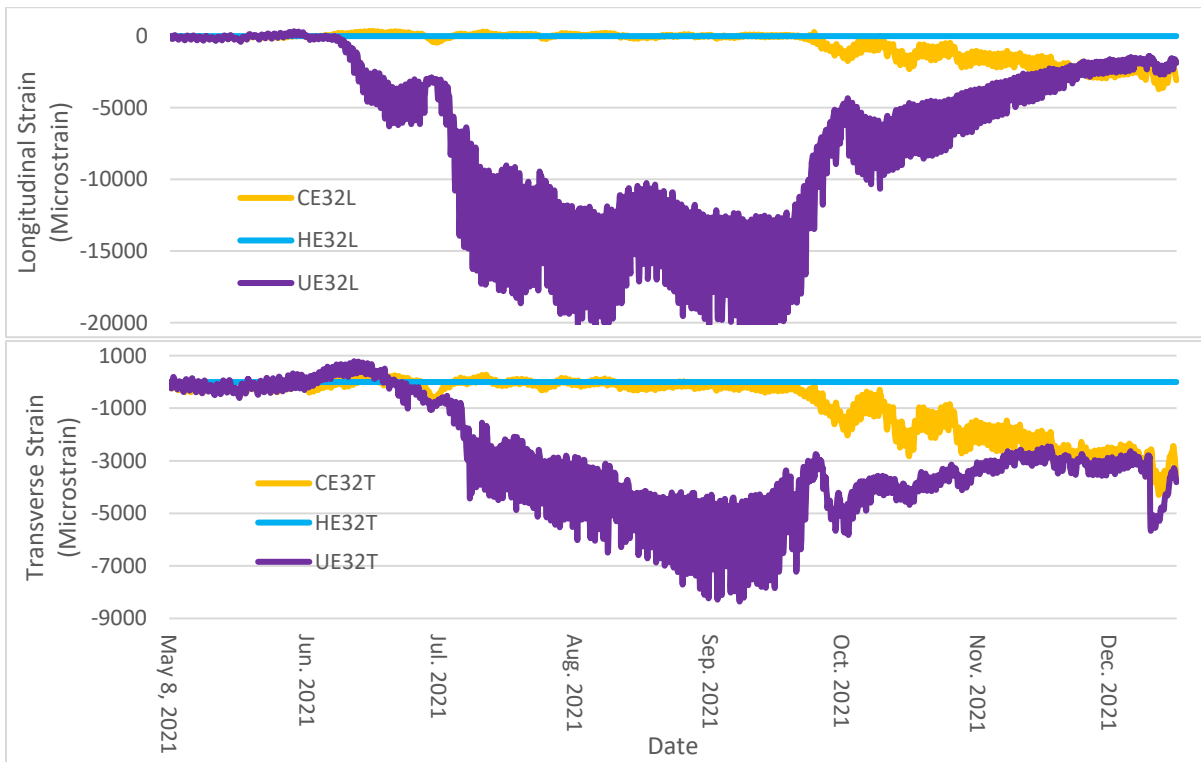


**Figure 113. Longer-term longitudinal and transverse strain in eastbound lane - bay 3 – position 2.**

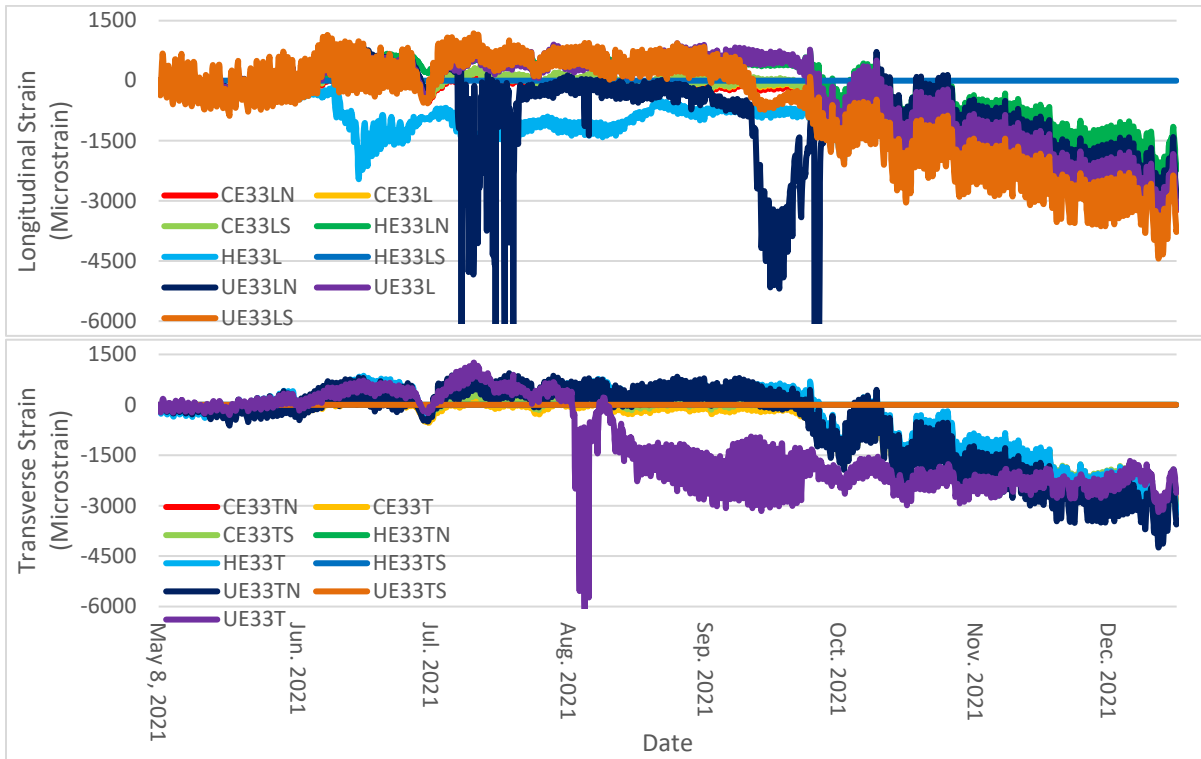


**Figure 114. Longer-term longitudinal and transverse strain in eastbound lane - bay 3 – position 3.**

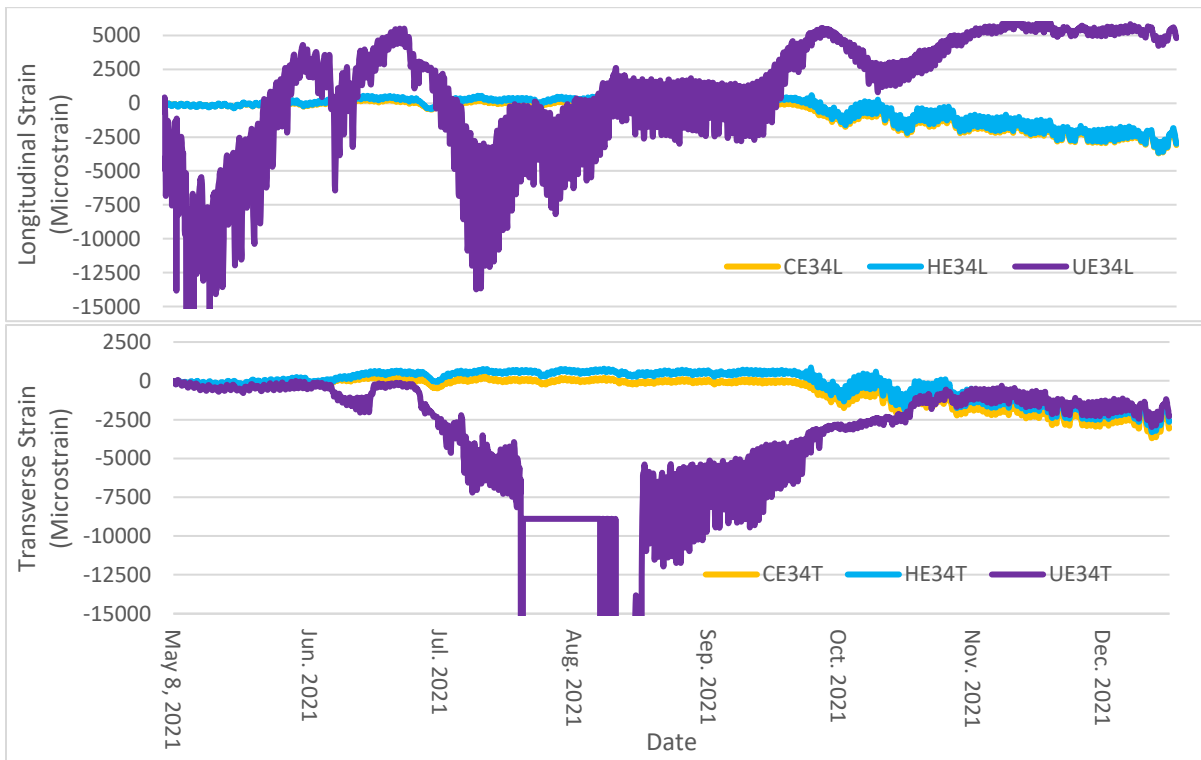


**Figure 115. Longer-term longitudinal and transverse strain in eastbound lane - bay 3 – position 4.**

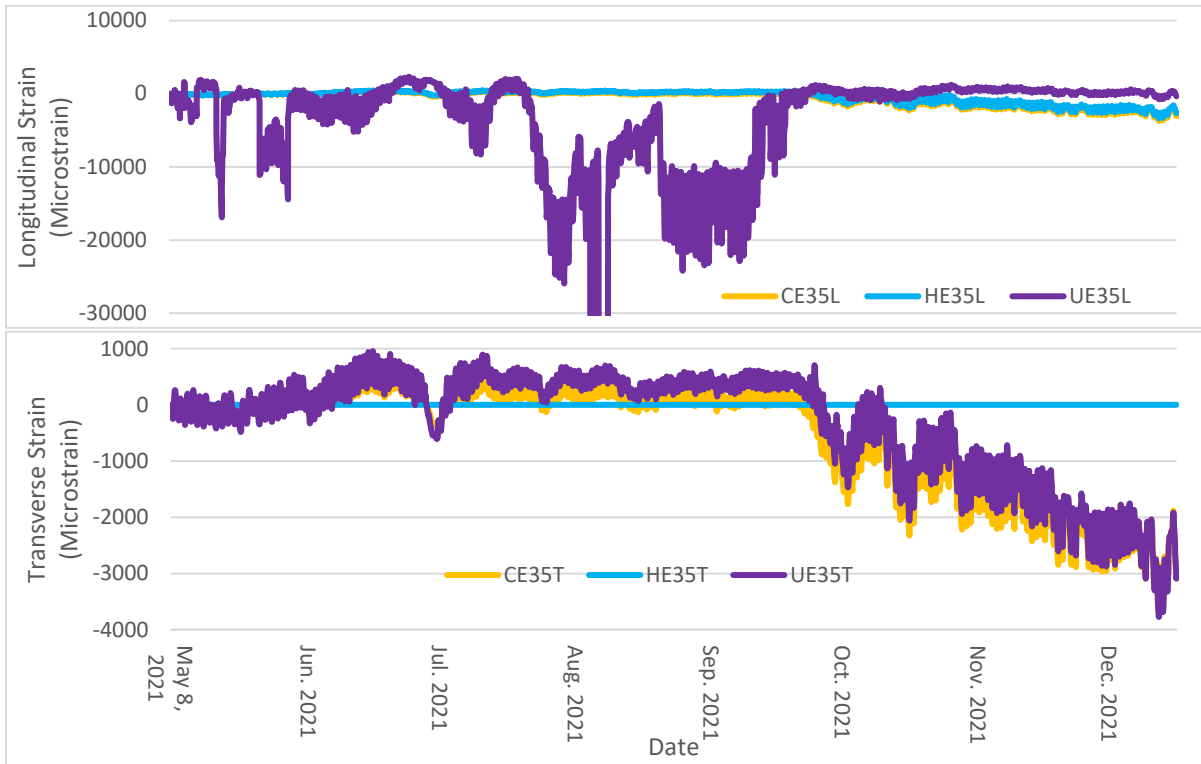


**Figure 116. Longer-term longitudinal and transverse strain in eastbound lane - bay 3 – position 5.**

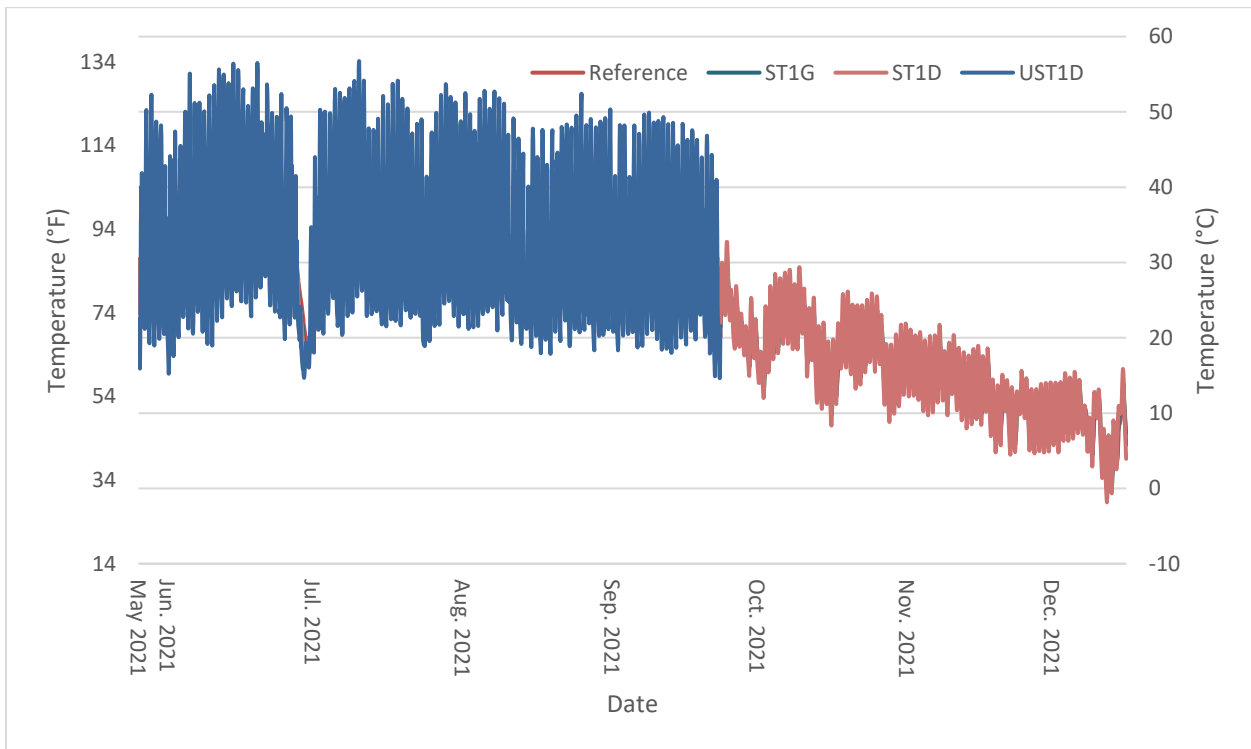


**Figure 117. Temperature during UHPC Production Placements 1 and 2 (eastbound lane) – bay 1.**

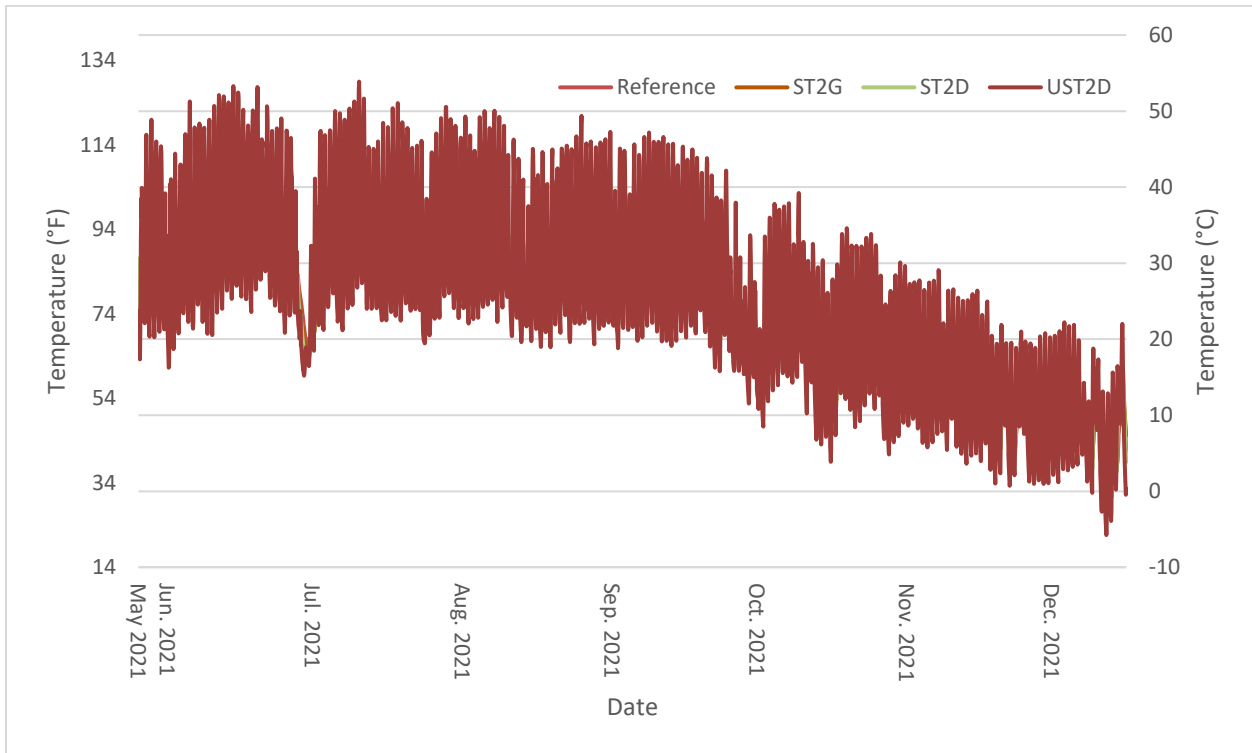


**Figure 118. Temperature during UHPC Production Placements 1 and 2 (eastbound lane) – Bay 2.**

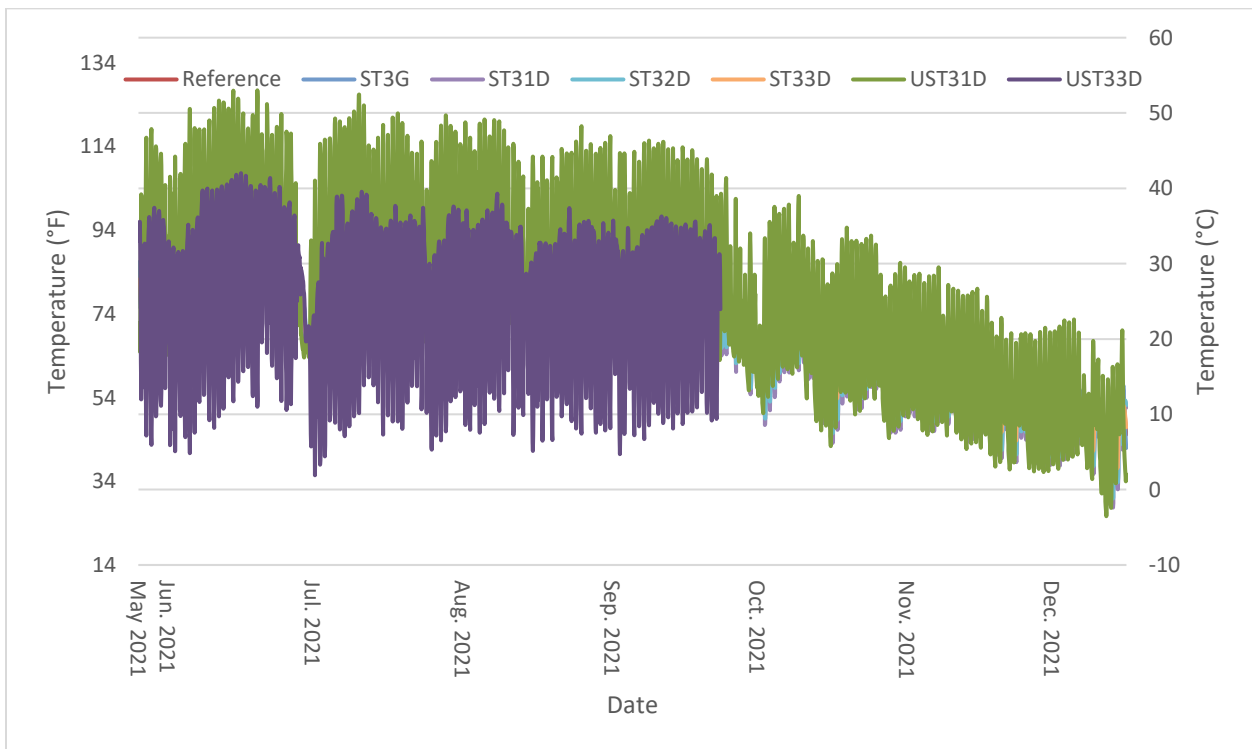


**Figure 119. Temperature during UHPC Production Placements 1 and 2 (eastbound lane) – bay 3.**

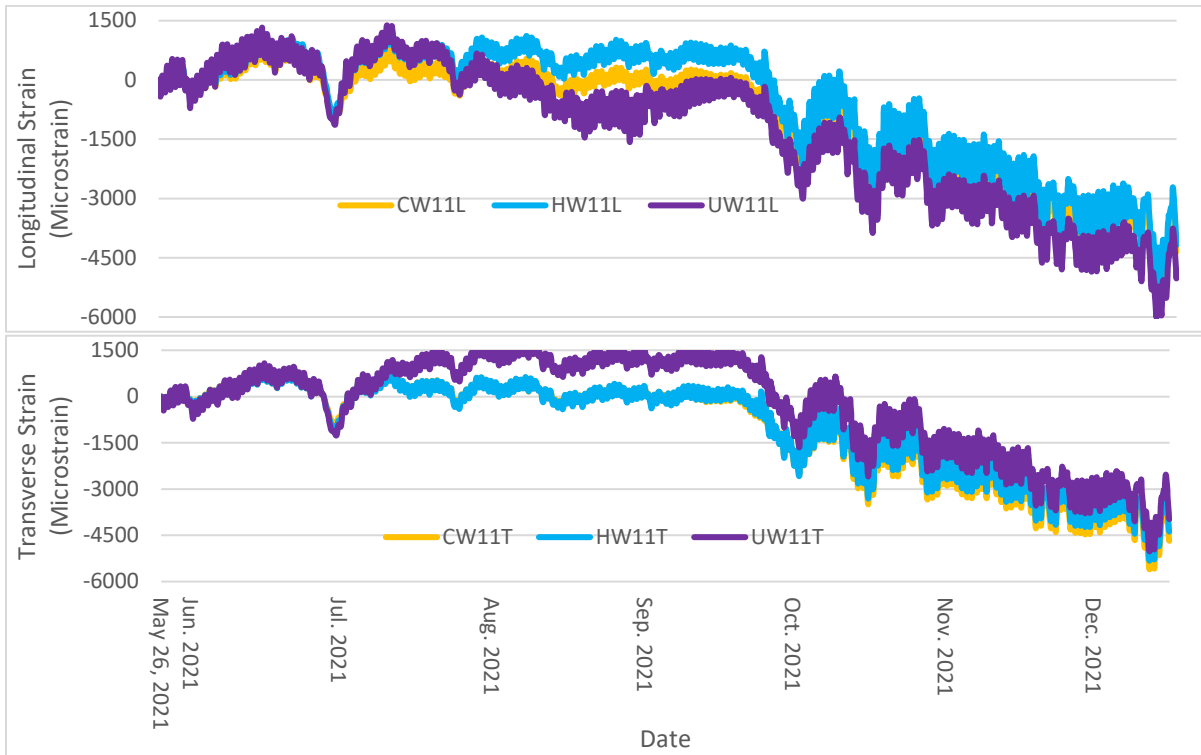


**Figure 120. Longer-term longitudinal and transverse strain in westbound lane - bay 1 – position 1.**

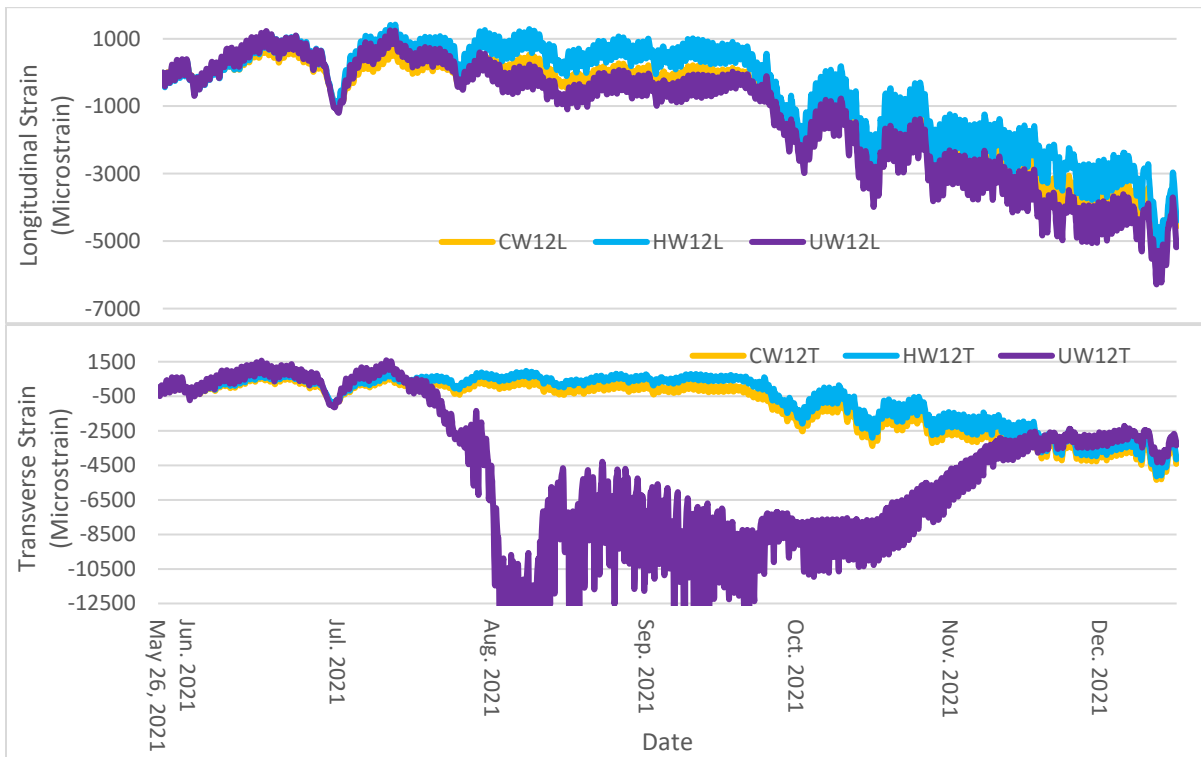


**Figure 121. Longer-term longitudinal and transverse strain in westbound lane - bay 1 – position 2.**

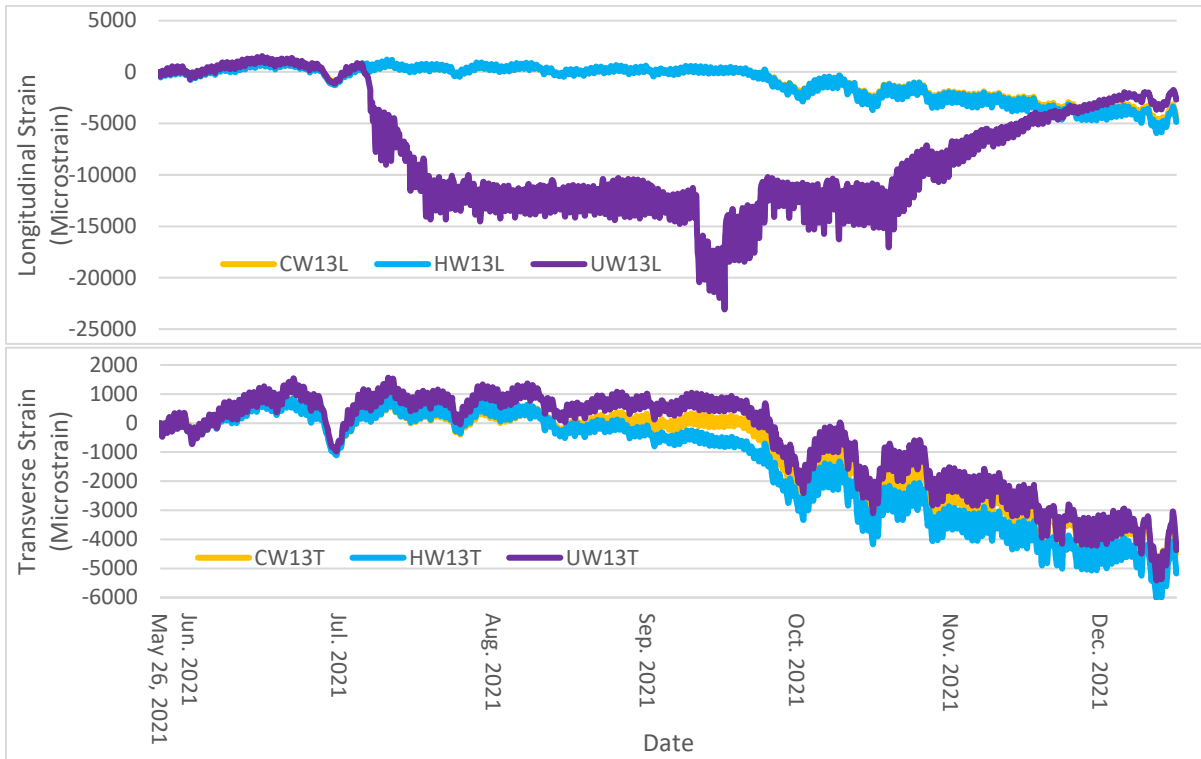


**Figure 122. Longer-term longitudinal and transverse strain in westbound lane - bay 1 – position 3.**

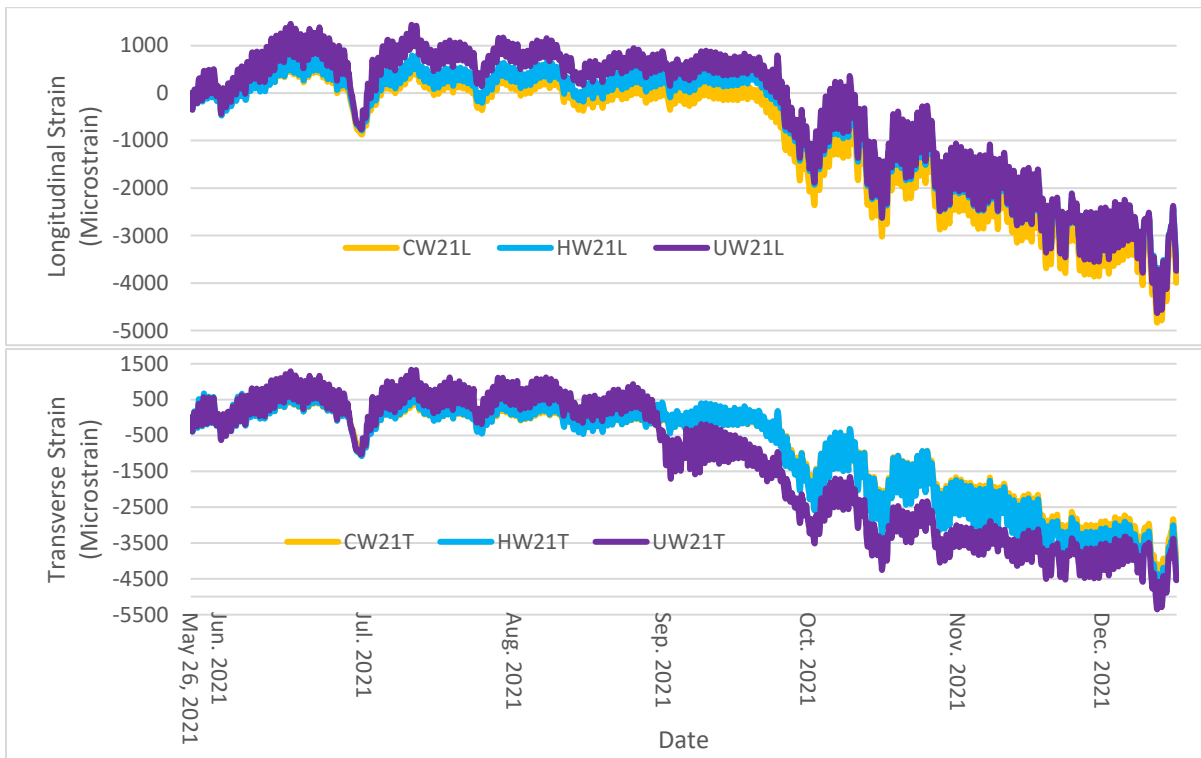


**Figure 123. Longer-term longitudinal and transverse strain in westbound lane - bay 2 – position 1.**

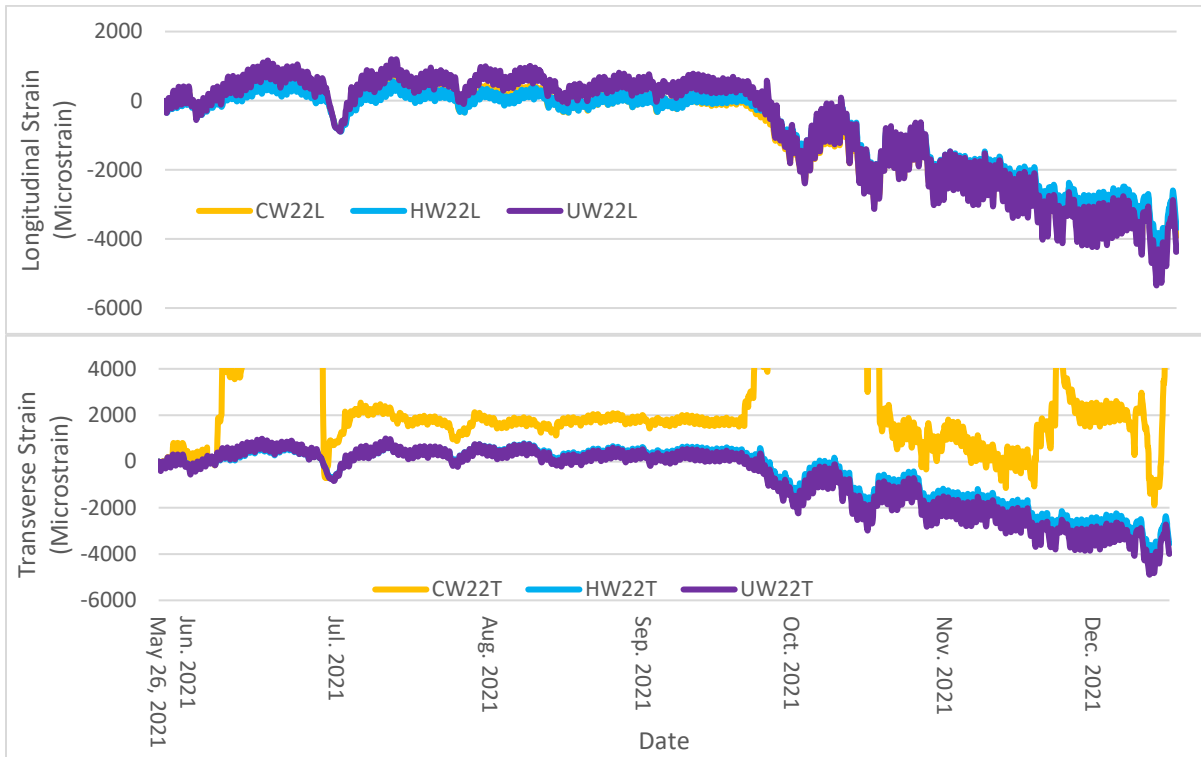


**Figure 124. Longer-term longitudinal and transverse strain in westbound lane - bay 2 – position 2.**

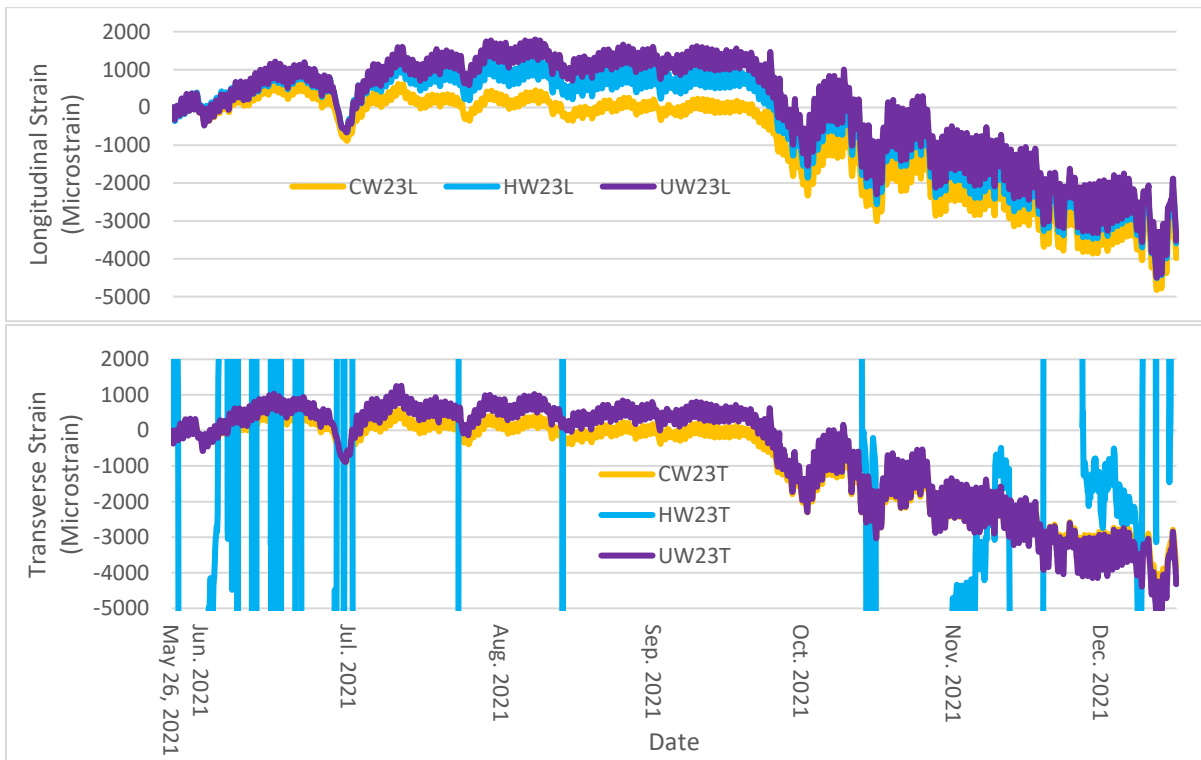


**Figure 125. Longer-term longitudinal and transverse strain in westbound lane - bay 2 – position 3.**

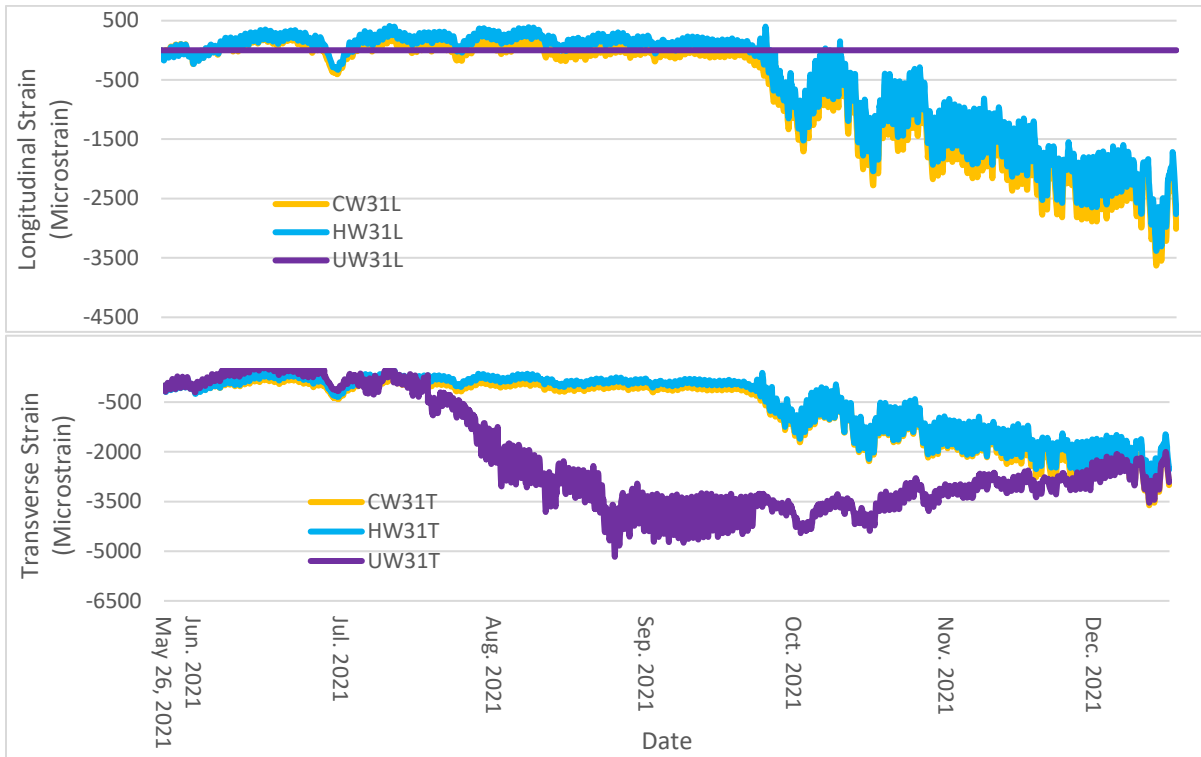


**Figure 126. Longer-term longitudinal and transverse strain in westbound lane - bay 3 – position 1.**

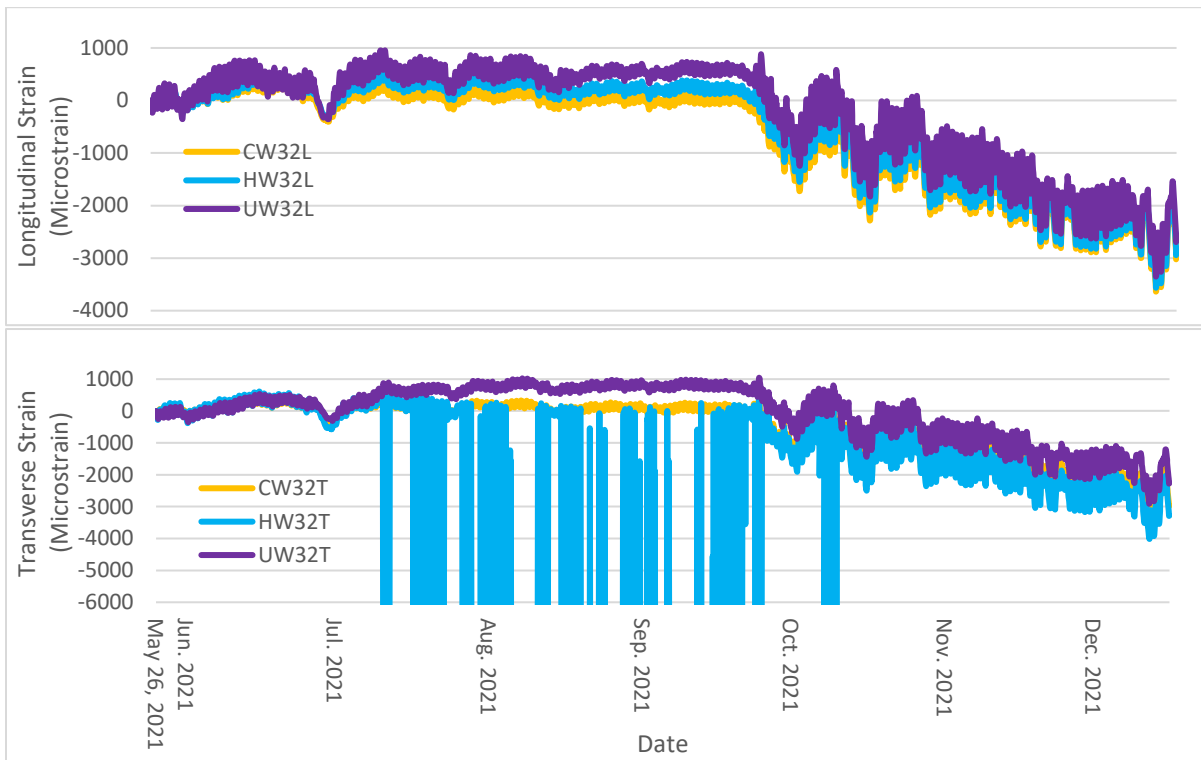


**Figure 127. Longer-term longitudinal and transverse strain in westbound lane - bay 3 – position 2.**

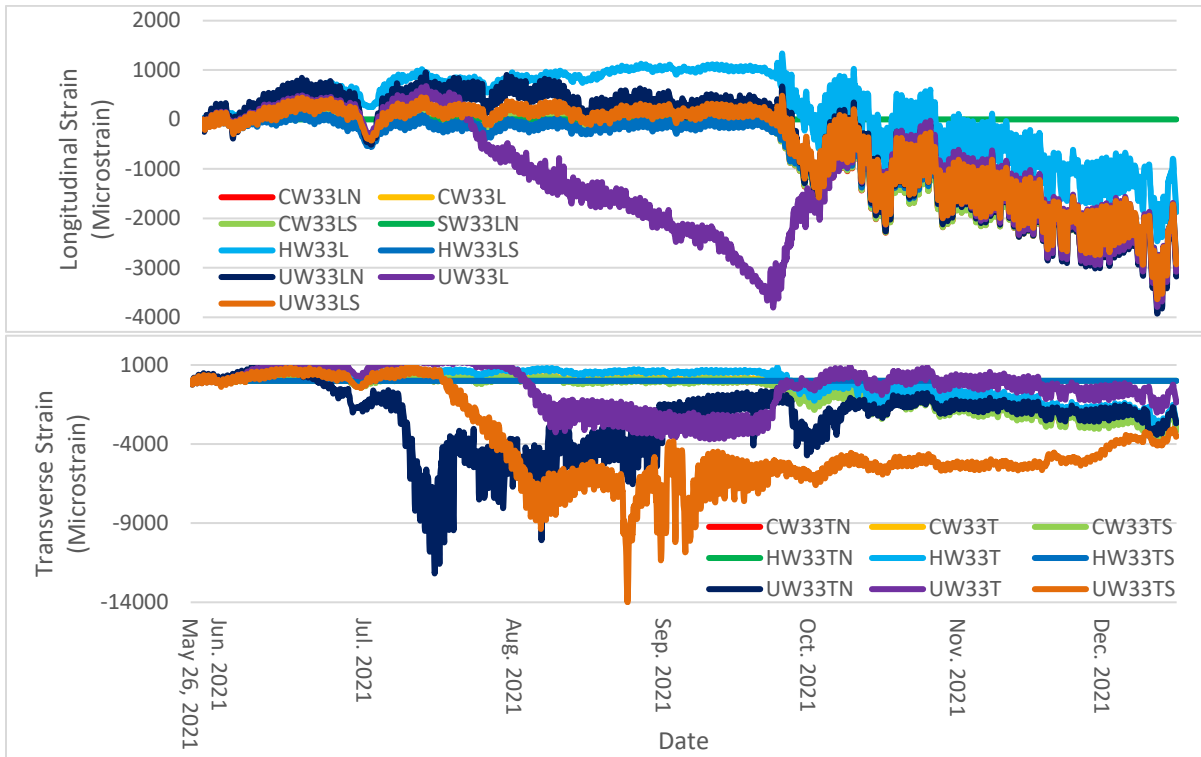


**Figure 128. Longer-term longitudinal and transverse strain in westbound lane - bay 3 – position 3.**

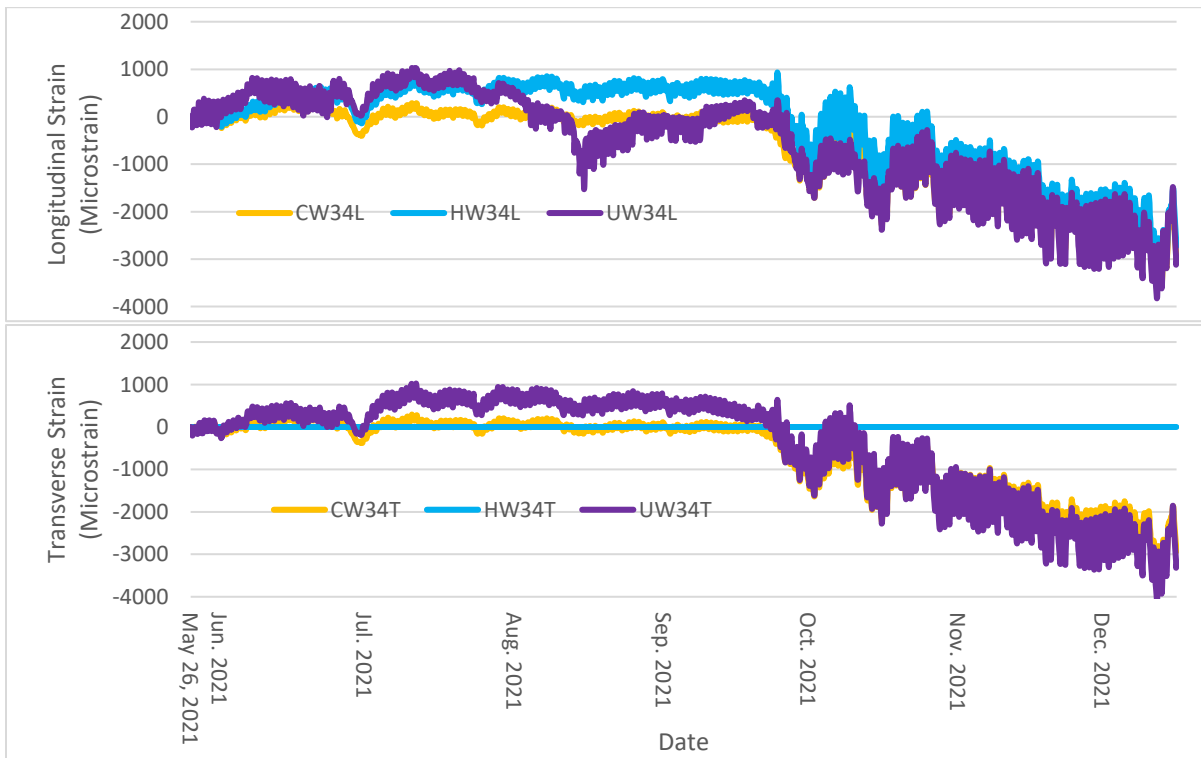


**Figure 129. Longer-term longitudinal and transverse strain in westbound lane - bay 3 – position 4.**

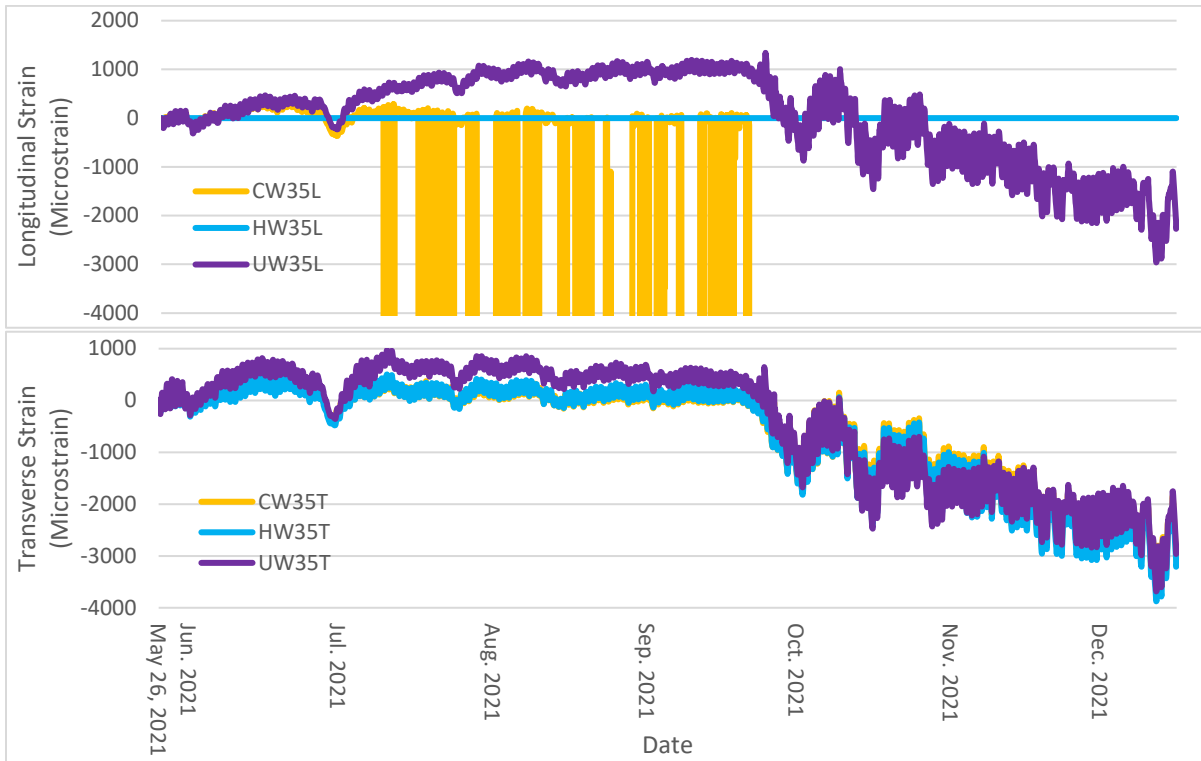


**Figure 130. Longer-term longitudinal and transverse strain in westbound lane - bay 3 – position 4.**

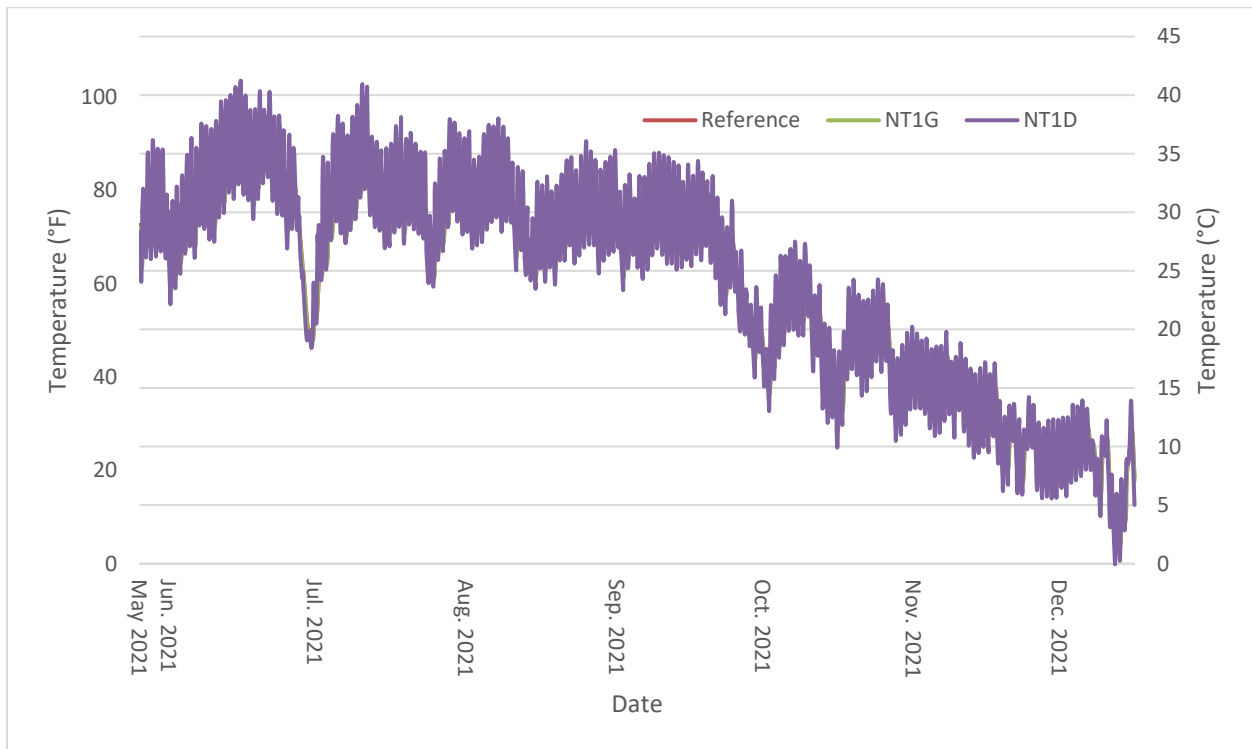


**Figure 131. Temperature during UHPC Production Placements 3 and 4 (westbound lane) – bay 1.**

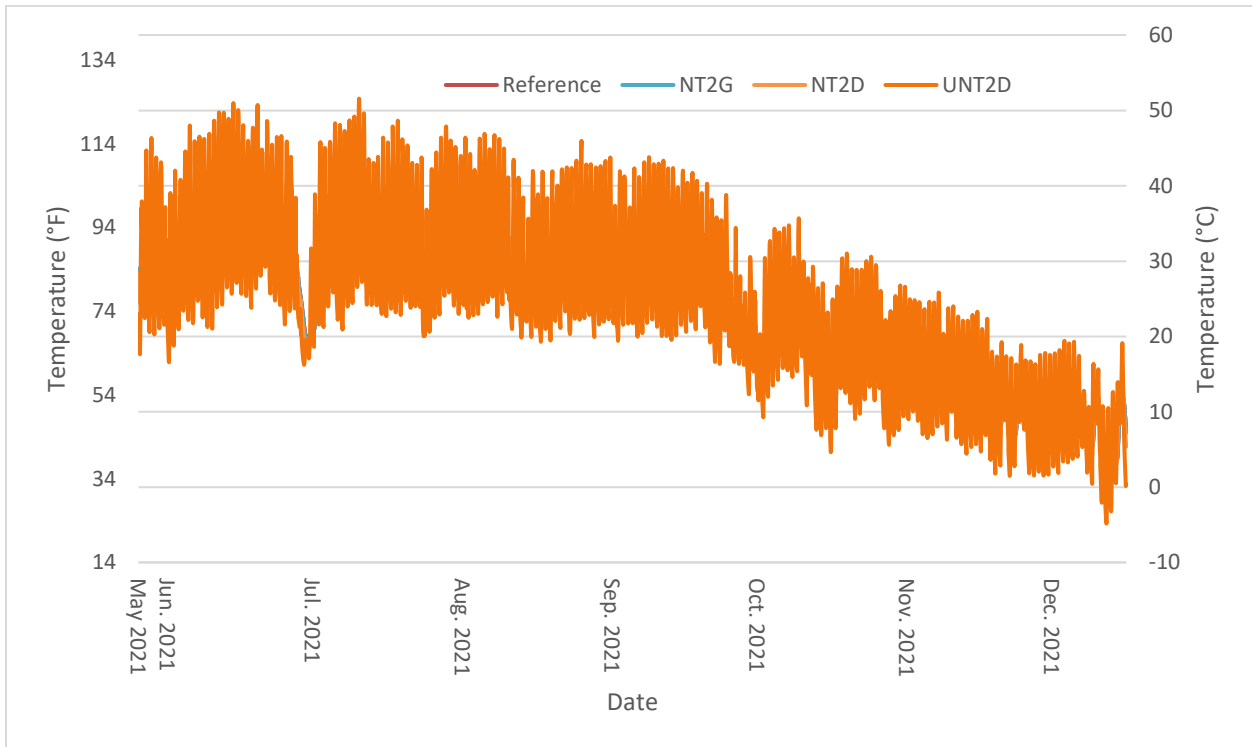


**Figure 132. Temperature during UHPC Production Placements 3 and 4 (westbound lane) – bay 2.**

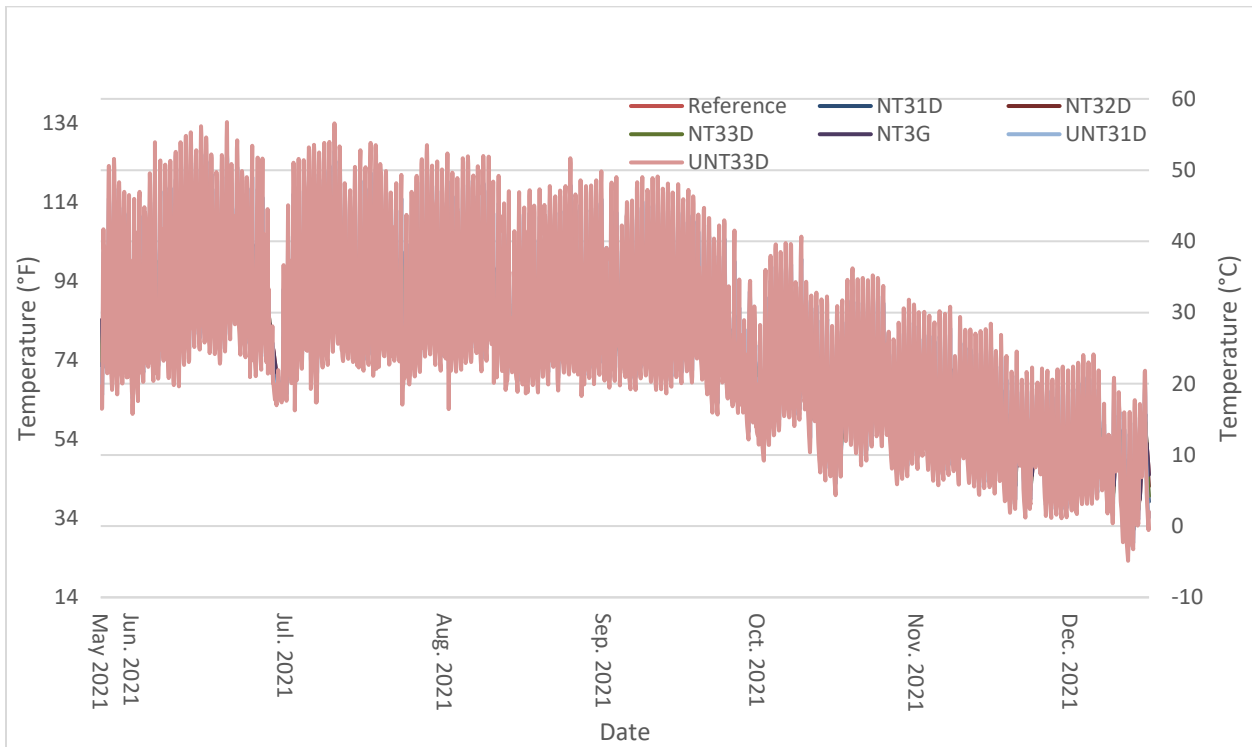


**Figure 133. Temperature during UHPC Production Placements 3 and 4 (westbound lane) – bay 3.**

## CONCLUSIONS

Based on the work conducted during the course of this project, the following conclusions were drawn:

1. Field implementation of the UHPC technology resulted in changes to the mixture proportions (steel fiber product). To accommodate a potential lack of availability of a constituent material, robust or additional UHPC mixture proportions should be available prior to letting a project.
2. Field cast specimens should be cured in a curing chamber. Specimens for this project were not field cured in a curing chamber, which led to low compressive strengths.
3. For this project, four mock placements were required to transfer the technology for batching, mixing, placing, and finishing UHPC to the contractor. Based on this experience, it is important to plan multiple mock placements requiring the contractor to demonstrate the ability to perform all procedures required for the project.
4. Mock placement bond tests revealed the importance of maintaining saturated conditions for 24 hours prior to overlay placement and providing a visibly moist substrate surface during placement of the overlay to achieve adequate bond between the overlay and substrate concrete materials. To achieve adequate bond (greater than 150 psi [1.0 MPa]), the substrate should also have a surface texture that removes surface paste and exposes some aggregate.
5. The approximately 15,350 ft<sup>2</sup> (1430 m<sup>2</sup>) non-proprietary UHPC overlay was successfully placed in four production placements, performed between April 10, 2021 and April 27, 2021.
6. Cracking on the UHPC surface was observed when curing compound and plastic sheeting were not applied as soon as possible to the finished overlay surface.
7. Chain drags, hammer sounding, and thermal imaging were used to identify four areas of possible delamination that were 2 to 3.5 ft<sup>2</sup> (0.19 to 0.33 m<sup>2</sup>).
8. The average direct tensile bond strength between the UHPC overlay and HPD substrate, calculated from nine pull-off tests performed at intact locations on the overlaid deck, was 239 psi (1.65 MPa). This average is considered to be conservative because four of the tests had fractures that occurred at the epoxy-UHPC interface.
9. The strain response of unrestrained UHPC can be as large as 1000  $\mu$ strain due to the thermal effects observed during a daily cycle during early-age monitoring. However, measured strain responses were generally 200 to 250  $\mu$ strain, which is attributed to restraint provided by the concrete superstructure (substrate).
10. Early-age monitoring also showed that multi-day strain trends coincided well with daily temperature trends. The early-age monitoring data are being analyzed in detail for an ongoing NMDOT project that continues for another two years.
11. The longer-term monitoring data contained periods where gauges spiked out of range or experienced excessive drift. Relative strains occurring during windows of time that do not contain such anomalies are being used for detailed analysis of the bridge and overlay behaviors for the NMDOT project.

## REFERENCES

1. Newton, C.M., B.D. Weldon, A.J. Al-Basha, M.P. Manning, W.K. Toledo, and L.D. Davila. Bridge Deck Overlays Using Ultra-High-Performance Concrete. Tran-SET final research report 17CNMS01. Transportation Consortium of South-Central States (Tran-SET), 2018.
2. Haber, Z.B., Graybeal, B.A., and Munoz, J.F. "Field Testing of an Ultra-High Performance Concrete Overlay." FHWA-HRT-17-096, Federal Highway Administration, 2017.
3. Krauss, P., Lawler, J., and Steiner, K. (2009). Guidelines for Selection of Bridge Deck Overlays, Sealers, and Treatments, NCHRP Project 20-07 Report, p. 51, Transportation Research Board, Washington, DC.
4. Chamberlin, W.P. and R. E., Weyers, "Field Performance of Late-Modified and Low-Slump Dense Concrete Bridge Deck Overlays in the United States," *Concrete Bridges in Aggressive Environments*, SP 151, American Concrete Institute, Farmington Hills, Mich., 1994, pp. 1-16.
5. Babaei, K., and Hawkins, N. M. (1987). "Evaluation of Bridge Deck Protective Strategies," NCHRP No. 297, Transportation Research Board, Washington, DC.
6. Sprinkel, M.M. and Ozyldirim, C. "Evaluation of High Performance Concrete Overlays Placed on Route 60 Over Lynnhaven Inlet in Virginia." 2000.
7. Anderson, K. W., Uhlmeyer, J. S., Russel, M., Simonson, C., Littleton, K., McKernan, D., Weston, J. (2013). "Polyester Polymer Concrete Overlay," Washington State Department of Transportation. Report WA-RD-797.1.
8. Graybeal, B. A. (2007). "Material Property Characterization of Ultra-High Performance Concrete." Federal Highway Administration, Report FHWA-HRT-06-103, McLean, VA.
9. Graybeal, B., & Davis, M. (2008). "Cylinder or cube: strength testing of 80–200 MPa (11.6–29 ksi) ultra-high performance fibre-reinforced concrete," *ACI Materials Journal*, 105(6), 603–609.
10. Graybeal, Benjamin & Hartmann, Joseph. (2003). "STRENGTH AND DURABILITY OF ULTRA-HIGH PERFORMANCE CONCRETE," Concrete Bridge Conference.
11. Muro-Villanueva, J., Newton C. M., Weldon, B. D., Jauregui, D. V., and Allena, S. "Freezing and Thawing Durability of Ultra High Strength Concrete," *Journal of Civil Engineering and Architecture*, Aug. 2013, 8(7), pp. 907-915.
12. Montoya, K.F. (2010). "Feasibility of Using Ultra High Performance Concrete in New Mexico Bridge Girders," MS thesis, New Mexico State University.
13. Tahat, M. N., "Creep of Ultra-High Performance Concrete made with Local Materials," Ph.D. dissertation, New Mexico State University, Las Cruces, NM, 2017.
14. ASTM C1856: Fabricating and Testing of Ultra-High Performance Concrete, Annual Book of ASTM Standards, ASTM International, Conshohocken, PA, 2017.

15. Magureanu, C., Sosa, I., Negrutiu, C., and Heghes, B. "Mechanical Properties and Durability of Ultra-High-Performance Concrete." *ACI Materials Journal*, Vol. 109, No. 2, 2012, pp. 177-183.
16. Villanueva, J.M. "Mixture Proportioning and Freezing and Thawing Durability of Ultra High Performance Concrete Using Local Materials." Ph.D. dissertation, New Mexico State University, 2015.
17. Way, R. and Wille, K. "Material Characterization of an Ultra High-Performance-Fibre Reinforced Concrete under Elevated Temperatures." *Third International Symposium on UHPC and Nanotechnology for High Performance Construction Materials*, Kassel, 2012, pp. 565-572.
18. Al-Basha, A.J. "Frost Resistance of Concrete Cladded with Locally Produced Ultra-High Performance Concrete Cured at Elevated Temperatures." Master's Thesis, New Mexico State University, 2017.
19. Xue, J., Briseghella, B., Huang, F., Nuti, C., Tabatabai, H., and Chen, B. (2020). "Review of ultra-high performance concrete and its application in bridge engineering," *Elsevier, Construction and Building Materials* 260(2020).
20. Nault, G. and Samson, E. (2019). "UHPC: a Durable Concrete Overlay Solution for Bridge Decks," 2019 IABSE Congress, New York City.
21. Ju, Y., Shen, T., and Wang, D. (2020). "Bonding behavior between reactive powder concrete and normal strength concrete," *Elsevier, Construction and Building Materials*, 242 (2020).
22. Allena, S. and Newtonson, C.M., "Shrinkage of Fiber-Reinforced Ultrahigh Strength Concrete." *Journal of Materials in Civil Engineering*, Vol. 24, No. 5, 2011, pp. 612-614.
23. Lyelle, E. "Optimization of Ultra High Performance Concrete Mixture Proportions using Locally Available Materials." Master's thesis, New Mexico State University, 2012.
24. Newtonson, C., Weldon, B., Flores, E., Varbel, J., and Toledo, W. K., "UHPC Shear Keys in Concrete Bridge Superstructures," *Tran-SET Final Report 18CNMS01*. Transportation Consortium of South-Central States (Tran-SET), 2019.
25. Al-Basha, A. J., Toledo, W. K., Newtonson, C. M., Weldon, B. D., "Ultra-High Performance Concrete Overlays for Concrete Bridge Decks," *World Multidisciplinary Civil Engineering-Architecture-Urban Planning Symposium (WMCAUS)*, *Materials Science and Engineering* 471, 032007, 2019.
26. Flores, E. Y., Varbel, J., Toledo, W. K., Newtonson, C. M., and Weldon, B. D., "Ultra-High-Performance Concrete Shear Keys in Concrete Bridge Superstructures," *Transportation Research Record*, *Journal of the Transportation Research Board*, 2020.
27. Tayeh, B., Aadi, A. S., Hilal, N. N., Abu Bakar, B. H., Al-Tayeb, M. M., and Mansour, W. N. (2019). "Properties of Ultra-High-Performance Fiber-Reinforced Concrete (UHPRFC) - A Review Paper," *AIP Conference Proceedings* 2157, 020040.
28. Graybeal, B., and Haber, Z. (2018). "Ultra-High Performance Concrete for Bridge Deck Overlays," *FHWA Publication No.: FHWA-HRT-17-097*, Technical Note.

29. Aaleti, S. and Sritharan, S. (2019). "Quantifying Bonding Characteristics between UHPC and Normal-Strength Concrete for Bridge Deck Applications," *ASCE Journal of Bridge Engineering*, 24(6).
30. Valikhani, A., Jahromi, A. J., Mantawy, I. M., and Azizinamini, A. (2019). "Experimental evaluation fo concrete-to-UHPC bond strength with correlation to surface roughness for repair application," *Elsevier, Construction and Building Materials*, 238 (2020).
31. ACI Committee 546R-04: Guide to Materials Selection for Concrete Repair, American Concrete Institute ACI546R-04, 2004.
32. Lee, H.-S.; Jang, H.-O.; Cho, K.-H. Evaluation of Bonding Shear Performance of Ultra-High-Performance Concrete with Increase in Delay in Formation of Cold Joints. *Materials* 2016, 9, 362.
33. Silfwerbrand, J., and Beushausen, H. "Bonded Concrete Overlays – Bond Strength Issues." *Proceedings of the International Conference on Conference Repair, Rehabilitation and Retrofitting*, M.G. Alexander, H.-D. Beushausen, F. Dehn, and P. Moyo, eds., Cape Town, South Africa, Vol. 512, Nov. 2005.
34. Muñoz, M. Á. C., Harris, D. K., Ahlborn, T. M., and Froster, D. C. (2014). "Bond Performance between Ultra high-Performance Concrete and Normal-strength Concrete," *Journal of Materials in Civil Engineering*, ASCE, 26(8).
35. Simonsen, J. E. "Low-slump High-density Concrete Bridge Deck Overlay. "Report 75-B-93, Michigan Transportation Commission, 1988.
36. Zhu, Y. "Effect of Surface Moisture Condition on Bond Strength between New and Old Concrete." *Bulletin No. 159, Dept. of Structural Mechanics and Engineering, Royal Institute of Technology, Stockholm*, Vol. 27, 1992.
37. ICRI 310. "Committee 310: Selecting and Specifying Concrete Surface Preparation for Sealers, Coatings, Polymer Overlays, and Concrete Repair." ICRI310.2R-2013, International Concrete Repair Institute, ICRI, 2013.
38. Valipour, M., and Khayat, K.H. Debonding test method to evaluate bond strength between UHPC and concrete substrate. *Mater Struct* 53, 15 (2020). <https://doi.org/10.1617/s11527-020-1446-6>
39. Silfwerbrand, J., and Paulsson, J. (1998). "Better Bonding of Bridge Deck Overlays," *Concrete International*, Vol. 20, No. 10, pp. 56–61.
40. Momayez, A., Ehsani, M. R., Ramezani pour, A. A., Rajaie, H., "Comparison fo Methods for Evaluating Bond Strength between Concrete Substrate and Repair Materials," *Cement and Concrete Research*, 34(4), 2005, pp. 748-757.
41. Clímaco, J. C. T. S., and Regan, P. E. "Evaluation of bond strength between old and new concrete in structural repairs." *Magazine of Concrete Research*, Vol. 53, 2001, pp.377-390
42. Farzad, M., Fancy, S. F., Lau, K., and Azizinamini, A., "Chloride Penetration at Cold Joints of Stuctural Members with Dissimilar Concrete Incorporating UHPC," *Multidisciplinary Digital Publishing Institute, Infrastructures*, 4(18), 2019.

43. Nursyamsi, N., Tarigan, J., Abu Bakar, B.H., Hardjasaputra, H. (2020). "Ultra-High-Performance Fiber-Reinforced Concrete an Alternative Material for Rehabilitation and Strengthening of Concrete Structures: A Review," *Journal of Physics: Conference Series* 1529 052010.
44. Delatte, N. J., Williamson, M. S., and Fowler, D. W. "Bond Strength Development with Maturity of High-Early-Strength Bonded Concrete Overlays." *ACI Materials Journal*, ACI, Vol. 97, No. 2, 2000, pp. 201-207
45. ASTM C882: Bond Strength of Epoxy-Resin Systems Used with Concrete by Slant-Shear, Annual Book of ASTM Standards, ASTM International, Conshohocken, PA, 2013.
46. Espeche, A. D., and Leon, J. "Estimation of Bond Strength Envelopes for Old-to-new concrete Interface Based on a Cylinder Splitting Test." *Construction Building Materials*, Vol. 25, 2011, pp.1222-1235.
47. TXDOT. "Test Procedure for Determining the Coefficient of Thermal Expansion of Concrete." Tex-428-A, 2011.
48. Chilwesa, M., Facconi, L., Minelli, F., Reggia, A., and Plizzari, G., "Shrinkage Induced Edge Curling and Debonding in Slab Elements Reinforced with Bonded Overlays: Influence of Fibers and SRA," *Cement and Concrete Composites*, 2019.
49. Hong, T., "Edge Curling Effect on Interface Delamination of Concrete Overlays for Bridge Decks," *West Virginia University*, MS Thesis, 2006.
50. ASTM A820: Standard Specification for Steel Fibers for Fiber-Reinforced Concrete, Annual Book of ASTM Standards, ASTM International, Conshohocken, PA, 2016.
51. Visage, E. T. 2013. "Experimental Analysis of the Flexural Behavior of Ultra-High Performance Concrete Beams Using Local Materials." MS thesis, New Mexico State University, Las Cruces, NM.
52. ASTM C143: Standard Specification for Slump of Hydraulic-Cement Concrete, Annual Book of ASTM Standards, ASTM International, Conshohocken, PA, 2020.
53. ASTM C1611: Standard Specification for Slump Flow of Self-Consolidating Concrete, Annual Book of ASTM Standards, ASTM International, Conshohocken, PA, 2018.
54. BS 1881 Part 116: British Standard Testing concrete, British Standards Institution, London, UK, 1983.
55. ASTM C1609: Standard Test Method for Flexural Performance of Fiber-Reinforced Concrete (Using Beam With Third-Point Loading), Annual Book of ASTM Standards, ASTM International, Conshohocken, PA, 2019.
56. Diaz, D. E., "Ground Penetrating Radar," MS Thesis, New Mexico State University, Las Cruces, NM, 2018.

## **APPENDIX**

### **A.1. Best Practices**

The following sub-sections provide a detailed list of best practices that should be followed for field implementation of a non-proprietary UHPC overlay. This list provides best practices for preparatory work that includes recommendations for mixture proportioning, preparation for placement, materials handling, and mixing. These best practices also include recommendations regarding overlay placement, curing practices, and quality assurance testing. Lastly, recommendations are provided for contracts related to UHPC overlay projects.

#### ***A.1.1. Materials Selection***

1. Materials should be selected for the UHPC overlay mixture proportions such that alternative materials can be used to produce acceptable mixtures in case any given material is unavailable. For example, if the mixture proportion called for a steel fiber produced internationally, an alternative steel fiber produced domestically should be verified as acceptable for use in case the Buy-America requirement on steel products is enforced. This is important because there is little time to adjust a UHPC mixture if changes are required just prior to letting a project or after the project is let. Providing a robust mix design can provide an assurance that the final product will perform as proposed.
2. When using a developed UHPC mixture, contractors should only use specified admixtures. Admixtures should be referenced by product name and producer so that the contractor uses only admixtures that have been verified through laboratory testing to produce acceptable mixtures.

#### ***A.1.2 Preparation for Placement***

3. Adequate surface texture should be provided during surface preparation of the substrate concrete. Preparing the substrate surface should begin by cleaning the surface of any debris and then using hydro-demolition, sandblasting, or shotblasting to produce an acceptable surface texture. An adequate surface texture is one that removes surface paste and exposes fine aggregate. Steel shotblasting should be used to provide an exposed fine aggregate surface texture that exposes at least as much aggregate as the light sandblasted texture defined by ACI 303. Traffic should not be permitted on surface textured areas prior to placement of the overlay material.
4. The substrate surface should be maintained at saturated conditions for 24 hours prior to overlay placement. Providing a visibly moist substrate surface prior to overlay placement is critical to achieve bond for any cementitious overlay material. Therefore, the substrate should be monitored and maintained saturated up to placement of the overlay.

5. Contractors should be familiar with the overlay material in terms of mixing time, workability, and placement. The contractor's familiarity with the overlay material will allow the contractor to select a number and size of mixers to produce UHPC at a rate that ensures there is no more than 15 minutes between consecutive overlay batch placements. Careful planning of the UHPC production can reduce instances of cold joint formation during placement.
6. Weather forecasts for time of overlay placement should be monitored prior to placement. This is important since the substrate is to be maintained saturated and be visibly moist when the overlay is placed. Therefore, weather should be monitored, and appropriate actions should be taken to ensure substrate surface conditions are adequate at placement of the overlay.
7. UHPC is susceptible to plastic shrinkage that can be exacerbated by evaporation. Moisture losses are particularly problematic for UHPC due to its low water content and low water-to-cementitious materials ratio. If the evaporation rate exceeds 0.04 lbs/ft<sup>2</sup>/hr (0.20 kg/m<sup>2</sup>/hr), either the overlay placement should be postponed or a plan to prevent evaporation from the freshly placed UHPC should be implemented.

#### ***A.1.3. Materials Handling***

8. If aggregates are to be weighed-out more than two hours prior to mixing, the aggregates should be stored in containers capable of maintaining the stock-piled moisture content so that an accurate water content can be achieved. This is important because the moisture content of the aggregate can influence the water-to-cementitious materials ratio, which can significantly change the workability and compressive strength of the UHPC.
9. The contractors should store cementitious materials and aggregate separately. Pre-batching cementitious materials and moist aggregates must be avoided to prevent initiation of hydration between moisture in the aggregate and the cementitious materials.

#### ***A.1.4. Mixing***

10. Contractors must have a basic understanding of moisture adjustments to address the influence of the aggregate moisture content on the water-to-cementitious materials ratio of the resulting UHPC mixture. This will allow the contractors to make adjustments on short notice if the sand moisture content changes from one batch to another or if pre-batched aggregate containers have inconsistent moisture contents.
11. The contractor needs to verify the maximum UHPC volume that can be mixed using a selected mixer. During mixing, the UHPC is extremely stiff and the rated capacity of the mixer is unlikely to be achievable. To ensure efficient mixing, the contractor needs to have identified batch volumes that can be confidently mixed in a reasonable amount of time.

12. The ability of the mixer to mix UHPC that is homogeneous should be verified prior to using the mixer for construction.

#### ***A.1.5. Placement***

13. Areas on the substrate surface with excess moisture should be swept prior to placement of the overlay material. It is important to maintain a saturated substrate surface prior to placement of the overlay. However, excessive moisture can influence the w/cm ratio of the overlay material which is not recommended. Therefore, areas with excess moisture (ponding) should be swept or sponged.
14. To prepare for events where overlay construction needs to be stopped in a manner that will form a cold joint, a pre-determined plan for cold joint practices should be followed. This plan should be developed and agreed upon by the engineers, project manager, and contractor prior to starting construction.

#### ***A.1.6. Curing***

15. Curing compound should be applied after finishing is complete for the overlay. Curing compound can be detrimental if mixed in with the concrete. Therefore, curing compound should be applied only after finishing is complete.
16. The UHPC overlay should be coated with a curing compound and then covered with plastic sheets immediately after finishing is complete. Quick application of these curing methods reduces evaporation and related cracking.

#### ***A.1.7. Quality Assurance***

17. Multiple mock placements should be planned that require the contractor to properly perform procedures needed to place the UHPC overlay. The mock placement should not be accepted until the contractor demonstrates proper performance on all procedures needed to place the UHPC overlay under field conditions. As the construction industry gains experience placing UHPC overlays, the requirement for mock placements may be reduced or eliminated.
18. Quality assurance testing is required for acceptance of each batch of UHPC prior to the batch being placed for the overlay. To ensure results are immediately available, the testing area should be located as close as possible to the mixing area.
19. Slump and spread tests should be conducted for each UHPC batch. The slump and spread tests allow the consistency of the UHPC mixture to be monitored and can be used to accept or reject each batch of UHPC.

20. Specimens for strength testing produced at the jobsite should be stored in curing chambers to protect the specimens from environmental conditions that may hinder strength development. In accordance with ASTM C1856, field specimens should be covered with a plastic sheet within one minute after finishing the top surface. Additionally, field specimens should be cured in accordance with ASTM C31 by storing them in a temperature-controlled chamber at 68°F to 78°F (20°C to 26°C) for 48 hours. After 48 hours, specimens should be removed from molds and cured in a moist room, with free water on specimen surfaces, at a temperature of 73.5°F ± 3.5°F (23°C ± 2.0°C).

#### ***A.1.8. General Contracts***

21. When specifying non-proprietary UHPC, a transportation agency should try to minimize liability associated with prescriptive specifications. The ability of the contractor to develop an UHPC overlay material should be included in the bid for the project. A performance-based specification for the UHPC overlay with workability and strength gain requirements should be stipulated as part of the contract. Requiring the contractor to develop an UHPC mixture that meets performance specifications mitigates the need for prescriptive specifications that may shift liability to the agency.